REGULATIONS OF ZINC HOMEOSTASIS AND GENETIC PROGRAM DURING EARLY B CELL DEVELOPMENT

B 細胞初期分化における亜鉛恒常性および遺伝子プログラムの制御

by

Tomohiro MIYAI

A Thesis Submitted for

DOCTOR OF PHILOSOPHY

in

GRADUATE SCHOOL OF FRONTIER BIOSCIENCE

OSAKA UNIVERSITY

(Osaka, Japan)

Supervisor: Ichiro TANIUCHI

March 2016

SUMMARY

B cells play essential roles in acquired immune system by producing the antigen-specific antibodies. The B cells are generated from hematopoietic stem cells (HSCs) in bone marrow (BM). During the developmental process, external stimuli from microenvironment alter the physiological status in progenitor cells, and lineage-appropriate genetic program is induced. In this study, I focused on these intrinsic regulatory mechanisms in early B lymphopoiesis.

Zinc (Zn) is the second abundant trace element in our body, and bone tissue is one of the largest pools of Zn. Zn deficiency leads to various diseases including lymphopenia. Cellular Zn homeostasis is tightly regulated by various Zn transporters (14 ZIP and 8 ZnT family genes as importers and exporters, respectively). ZIP10 is a cellular membrane-bound Zn importer highly expressed in B cells. However, its function and molecular target in B cells were largely unknown. Therefore, I investigated the role of ZIP10-mediated Zn influx for early B cell development. B cell-specific ZIP10 knockout mice showed drastic reduction of B cells at the earliest developmental stage in BM. The impaired B cell production was caused by an abnormal activation of caspase-dependent apoptotic pathway in Zn^{2+} dependent manner. I also found that JAK-STAT signaling pathway which mediates an intracellular signal upon various cytokines induced the transcription of *Zip10* in B cells. Therefore, I concluded that JAK-STAT-ZIP10-Zn^{2+}-caspase axis is essential for anti-apoptosis during early B lymphopoiesis.

In Chapter 2, I investigated the sequential transcriptional events during B cell commitment process using a novel inducible culture system. B cell lineage commitment can be induced and completed within a week in this system. Multiple time course samples were harvested and performed RNA-sequencing (RNA-seq) and chromatin immunoprecipitation-sequencing (ChIP-seq) analysis. Of note, sequential and transient up-regulations of transcription factors (TFs) were found. The activation of the early responding TFs, such as *Nfil3*, *Nr4a* and *Egr1* preceded the induction of B cell specific TFs, suggesting the critical roles of the early TFs at the initiation of B cell lineage commitment. To validate the contribution of the early TFs in B cell development, I performed the loss- or gain-of-function experiments and showed their essential roles in B cell commitment. I also constructed the TF networks by combining the time course RNA-seq dataset in this study and deposited ChIP-seq database of multiple TFs. Tight relationship of each TFs was disclosed and polycomb-mediated gene suppression is suggested as the terminator of multi-lineage program in B cell commitment process.

Collectively, this study demonstrated the contribution of Zn transporter in early B cell development. The dynamic and sequential TF networks during B cell lineage commitment were also determined. I thus believe that these two studies would contribute to a better understanding of molecular mechanisms during B cell commitment and developmental process.

TABLE OF CONTENTS

GENERAL INTRODUCTION

The immune system is essential for protection against diseases in our body. There are many kinds of immune cells, including T cells, B cells, NK cells, monocytes and granulocytes. Among them, B lymphocyte is the key player for antigen-specific adaptive immune system. **Fig G-1** illustrates the process of normal B cell development. The early developmental process takes place in bone marrow (BM) in adult, or in fetal liver (FL) before birth. Hematopoietic stem cells (HSCs) maintain both long-term self-renewal activity and multipotency generating all blood cells[1]. Multipontent progenitors (MPPs), which are following population of HSCs, still maintain multipotency, but they have lost the self-renewal activity[1]. First step to lymphoid pathway is to generate lymphoid-primed multipotent progenitors (LMPPs) which lost megakaryocyte/erythrocyte potential, but still maintain the potential to give rise to lymphoid and myeloid lineage cells[2]. LMPPs differentiate into common lymphoid progenitors (CLPs), which do not have any myeloid potential but maintain lymphoid repopulating capacity[3]. After the CLP stage, cells are specified to the B cell lineage (pre-pro-B cells)[4]. Pre-pro-B cells are finally determined to the B cell lineage in pro-B cells, which start to express the pan-B cell marker CD19 on their surface[5,6].

During the developmental process, the cells gradually lose their multipotency and obtain the cell type specific features affected by extrinsic and intrinsic factors (**Fig G2**)[7]. So far, the requisite environmental niches and factors for B cell development have been vigorously discussed[8–10]. BM environment consists of many different

non-hematopoietic cells, such as endothelial cells, mesenchymal cells and osteoblasts. Early lymphoid progenitors are mainly localized in endosteal niche[11], and osteoblast supports B lymphopoiesis[12,13]. Thus, bone-associated cells are thought to be essential for B cell development. The involvement of cytokines that include interleukin-7 (IL-7)[14,15], Flt3 ligand (Flt3L)[16] stem cell factor (SCF)[17], receptor activator of nuclear factor-κb ligand (RANKL)[18,19], and of chemokines such as CXC-chemokine ligand 12 (CXCL12)[8,20], has been implicated as the important extrinsic signal inputs that supports the B lymphocyte developmental process. Once the cells receive these external signals, intracellular signaling pathways are triggered and the expressions of multiple transcription factors (TFs) are activated. In B cell commitment, combinational activity of E2A, Forkhead box protein O1 (FoxO1) and Runt-related transcription factor (Runx)/Core-binding factor-beta (Cbfβ) triggers activation of B cell-specific transcriptional program which is subsequently governed by Early B cell factor-1 (Ebf1) and Paired box protein-5 (Pax5)[21–26]. An orchestrated activity of such a wide variety of TFs guarantees the proper fate decision into B cell lineage.

In this study, I investigated the cellular intrinsic controls during early B cell development. In the first chapter, I focused on intracellular zinc (Zn) homeostasis in early B cell developmental process. Zn is one of pivotal micronutrient, and bone is the second largest store pool of Zn in our body (**Fig G-3A**)[27]. Cellular homeostasis of Zn is tightly controlled by various Zn transporters (**Fig G-3B**). There are two types of Zn transporters, ZIPs (Zrt-. Irt-like Protein, Slc39) and ZnTs (Zinc Transporter, Slc30). ZIP family proteins transport Zn^{2+} from extracellular space or organelle into cytoplasm, and

vice versa in the case of ZnT families. Their cellular localization and expression pattern among organs are varied from each transporter[28]. Zn transporter Slc39a10/ZIP10 is localized on the cell surface, and its mRNA expression was observed in multiple lymphoid organs such as thymus, spleen and lymph nodes (LNs) (**Fig G-3C**). The RefDIC database (http://refdic.rcai.riken.jp) indicated the high expression of *Zip10* in various B lineage subsets[29]. To determine the role of ZIP10 in B cell development, I analyzed B cell-specific *Zip10* conditional knockout (*Zip10*$^{flox/flox}$*:mb1-cre*, thereafter '*Zip10*^{mb1}') mice. I found the drastic impairment of early B cell development at pro-B cells. Detailed investigation of molecular mechanism clearly demonstrated that Zn^{2+} fluxed from *Zip10* is essential for anti-apoptosis by suppression of the enzymatic activity of various caspases. *Zip10* expression was regulated by cytokine-mediated Janus kinase (JAK)-signal transducer and activator of transcription (STAT) signaling pathway, and the involvement of ZIP10 in human B cell lymphoma in which STAT3/5 was highly activated was also implicated. Therefore, I concluded that JAK-STAT-ZIP10-Zn^{2+}-Caspase axis is essential for survival of B cell progenitors[29].

In the second part of this paper, I will show the whole picture of intrinsic transcriptional regulation in B cell commitment. A number of TFs that orchestrate early B cell development have been identified[25]. However, it remains to be elucidated how the TFs interact with each other or what triggers the B cell commitment[30]. Moreover, the heterogeneity of hematopoietic stem and progenitor cells (HSPCs) hampered our understanding of the precise molecular events during commitment[31,32]. To overcome this issue, I established novel *in vitro* culture system that

is able to homogeneously induce B lineage cells from multipotent progenitors.

Our group has recently shown that block of transcriptional activity of E2A by overexpression of Id3 is sufficient to induce and maintain the stemness in hematopoietic progenitors[33]. Id3 is one of the Inhibitor of DNA binding (Id) proteins that heterodimerize with E2A and suppress the transcriptional activity. It was shown that the differentiation of Id3-transduced HSCs was arrested at the multipotent progenitor stage under the B cell culture condition. This culture was modified to the 4-hydroxytamoxifen (4-OHT) inducible system by transducing the Id3-estrogen receptor (Id3-ER^{T2}) fusion construct instead of Id3. We termed the Id3-ER^{T2} transduced cells as 'induced leukocyte stem (iLS)' cells, since they maintain the self-renewal activity in vitro for a long time and are capable of generating lymphoid and myeloid lineage cells[33]. In this study, I decided to use this system to clarify a dynamic transcriptional cascade and its epigenetic status during B cell commitment (**Fig G-4**).

I investigated the sequential alteration of transcriptome in multiple time points during B cell commitment process. The dynamic and transient inductions of various TFs were observed before the initiation of B cell specific transcriptional program. The transient expression of TFs as a cluster was termed as 'TF wave'. Loss- and gain-of-function studies supported the importance of the 'early waves' for proper B cell commitment. I finally constructed the TF networks by combining the time course dataset obtained here and publicly deposited ChIP-seq database of multiple TFs. The time phase was divided into 3 clusters (early, mid and late) based on the expression variance of TFs. The TFs and epigenetic factors among the gene regulatory circuits in

each cluster were closely connected each other. Of note, the data suggested that the polycomb repressive complex (PRC)-mediated gene suppression was a terminator of lineage-inappropriate gene program. This study will give us an insight of “true” gene regulatory networks in B cell fate determination.

CHAPTER 1

Zinc homeostasis regulated by ZIP10 transporter is essential for anti-apoptosis during early B cell development

INTRODUCTION

Zinc (Zn) is one of the essential trace elements for maintaining our life[34,35]. In immune system, dramatic effects of Zn have been observed in several leukocytes including B cells[36–39]. Although the perturbation of Zn homeostasis causes splenic atrophy associated with lymphocyte reduction[40], and compromises cellular and humoral immune responses[39], the mechanisms underlying how Zn controls immune cell function, and in particular, how Zn contribute to the early B cell development, have been largely unknown.

In molecular level, Zn is a structural component in numerous proteins, such as enzymes and TFs[41,42]. Recent proteomic analysis has shown that about 10% of whole genes possessed sequence(s) of Zn-binding motif[43] which suggests the general importance of Zn. Cellular Zn^{2+} homeostasis is tightly regulated by zinc transporters[34,44]. Zinc transporters have two families, importers (SLC39/ZIP) and exporters (SLC30/ZnT) (see **Fig G-3B** for their cellular localization)[35,45]. Various reports have been shown the involvement of these transporters in physiological and pathogenic events. Zn transporter ZIP4 is important for the initial absorption of dietary Zn in intestine, and mutations in the *SLC39A4/ZIP4* gene causes the inherited disorder acrodermatitis enteropathica (AE)[46]. ZIP13 controls the formation of bone, teeth, and

connective tissues by modulating BMP/TGF-β signaling[47], and its loss-of-function mutation causes spondylocheiro dysplastic Ehlers-Danlos syndrome in humans[47–49]. ZIP14 controls systemic growth by regulating G protein-coupled receptor (GPCR) signaling[50]. ZIP8 is involved in osteoarthritis by targeting metal-regulatory transcription factor 1 (MTF1)[51] and negatively manipulates nuclear factor-kappa B (NF-κB) activation in host defense[52]. Thus, Zn homeostasis mediated by Zn transporters is linked to a wide variety of biological and regulatory functions. Moreover, these reports clearly indicate the target and functional specificity of Zn^{2+} influx among various Zn transporters, and the disruption of a Zn transporter-Zn^{2+} axis can lead to various symptoms in the absence of redundant machinery[53].

Here I demonstrate a definitive role of ZIP10 in early B cell development. I found that a loss of ZIP10 during an early B cell differentiation stage specifically abrogated pro-B cell survival. The inducible deletion of *Zip10* in pro-B cells increased the caspase activity due to the reduced intracellular Zn^{2+} level, leading to a cell death. This phenomenon was mimicked by the intracellular chelation of Zn^{2+}. These findings indicated that Zn homeostasis via ZIP10 played an indispensable role in the survival of early B cell progenitors. I also demonstrated that the ZIP10 expression level was regulated by STAT3/STAT5 activation, and that ZIP10 was highly expressed in human B cell lymphoma samples in which both STAT3 and STAT5 proteins were activated, indicating that the JAK-STAT-ZIP10-Zn^{2+} signaling axis is important for maintenance of B lymphopoiesis. These results establish a functional link between ZIP10 and the survival of early stages of B cells differentiation, revealing an aspect of molecular

mechanism underlying the requirement of Zn for maintenance of the immune system.

RESULTS

Zip10^{mb1} mice showed severe developmental defects in B cell lineage.

It is well established that Zn deficiency causes severe lymphopenia resulting in immune deficiency, which is mainly due to a significant reduction in the developmental stages of B cells in the BM[40]. However, how Zn homeostasis helps to maintain early B cell development has remained elusive. I first asked whether ZIP10 plays a role in B cell development by analyzing *Zip10*^{mb1} mice, in which the *mb1-Cre* transgene mediates constitutive Cre recombination at the pro-B cell stage in the B lineage cells. *Zip10*^{mb1} mice exhibited severe splenoatrophy compared to control mice (**Fig 1-1A**) accompanied by reduction of B cell number (**Fig 1-1B**). These data indicated that an ablation of *Zip10* impaired normal B cell generation and/or proliferation. To examine the developmental abnormality of B cells in *Zip10*^{mb1} mice, B cell populations in BM and spleen were analyzed by flow cytometer. In *Zip10*^{mb1} mice, the number of pro-B cells, the earliest B cell progenitor, was strikingly reduced (**Fig 1-1C**). The intracellular Zn^{2+} levels in pro-B cells were also decreased by the loss of ZIP10 (**Fig 1-1D, E**). These data indicated that Zn^{2+} influx from Zn transporter ZIP10 is essential for early B cell development.

ZIP10 regulates cell death by suppressing the caspase activity.

To investigate the molecular function of ZIP10 in early B cells, *Zip10*^{flox} mice were crossed with *Rosa26-Cre-ER*^{T2} mice (*Zip10*$^{R26\text{-}ERT2}$) to delete ZIP10 in a tamoxifen-inducible manner. First, pro-B and pre-B cells were isolated and

co-cultured with TSt-4 stromal cells, which support the proliferation and differentiation of B cells, followed by 4-OHT treatment. Surface ZIP10 and intracellular Zn^{2+} levels were diminished in both pro-B and pre-B cells upon 4-OHT treatment (**Fig 1-2A, B**). According to this, *Zip10*-ablated B cell progenitors were immediately disappeared (**Fig 1-2C**). Annexin-V^{+} apoptotic cells were increased (**Fig 1-2D**) with activation of caspase-3 (**Fig 1-2E**). To assess the function of ZIP10 in B cell survival, I performed knockdown (KD) of *Zip10* gene by short-interference RNA (siRNA) using BM-derived cell line, BAF-B03. By siRNA transduction, surface ZIP10 protein and intracellular Zn^{2+} levels were significantly decreased (**Fig 1-3A,B**). Furthermore, Annexin-V^{+}7-$AAD^{-/+}$ apoptotic cells were increased (**Fig 1-3C**) with activation of various caspases involving multiple apoptotic cascades (**Fig 1-3D**, caspase-8 for Fas-dependent pathway; caspase-9 for mitochondrial stress-mediated pathway; caspase-12 for endoplasmic reticulum stress-mediated pathway and caspase-3 functions as an 'effector' in down-stream of each pathway). To determine whether this caspase-dependent apoptosis is caused by insufficiency of Zn^{2+} influx from extracellular space, Zn chelator *N*,*N*,*N*',*N*'-Tetrakis(2-pyridylmethyl)ethylenediamine) (TPEN) was treated with BAF-B03 cells. As a result, activation of caspase-dependent apoptosis was observed similar to the case of ZIP10 deficient conditions (**Fig 1-3E,F**). In addition, this caspase-dependent apoptosis was rescued by Zn^{2+} supplement into the culture (**Fig 1-3E,F**). These results indicate that loss of Zn^{2+} influx by ZIP10 triggers hyperactivation of a wide variety of caspases and results in abnormal apoptosis.

Cytokine signaling controls ZIP10-mediated intracellular zinc homeostasis.

In zebrafish, expression of LIV1 (homologue of mammalian ZIP10) is regulated by STAT3[54]. On the other hand, STAT signal from IL-7 is known to be essential for proliferation of early B lymphocytes[14]. SCF is also a STAT activator[55], and exerts the predominant effect on early B cell development in vitro by enhancing the IL-7-mediated proliferative response[56]. Therefore, I hypothesized that cytokine signaling induces expression of *Zip10*. To examine this possibility, the pro-B cells from wild type mice were isolated and treated with IL-7 and SCF for 3 hours *in vitro,* thereby mRNA levels of *Zip10* and *Socs3* were strikingly up-regulated (**Fig 1-4A**). Similarly, ZIP10 expression and intracellular Zn^{2+} level were also increased in cytokine stimulated BAF-B03 G133 cells (**Fig 1-4B**, STAT5 signal from IL-3, STAT3 signal from G-CSF, respectively). In addition, *Zip10* was also induced by stimulating pre-B cell line 2E8 with IL-7 (**Fig 1-4C**). Notably, BAF-B03 $G133^{STAT3F}$ cells[57], which express dominant negative form of STAT3 (**Fig 1-4D**), or STAT5 KD (**Fig 1-4E**) markedly repressed *Zip10* transcription upon cytokine stimulations. These data indicate that the transcription of *Zip10* is induced by STAT from cytokine signaling. Together with this, ChIP assay showed STAT3 and STAT5 proteins both bound to potential transcriptional regulatory site of *Zip10* locus in BAF-B03 cells (**Fig 1-4F**). These results clearly indicate that cytokine signaling induces *Zip10* expression, which leads to the elevation of intracellular Zn^{2+} concentration. Taken together, JAK-STAT-ZIP10-Zn^{2+} signaling axis is essential for survival of B cell progenitors by suppressing the enzymatic activity of caspases.

Hyper-activated STAT and ZIP10 in human B cell lymphoma

It is known that STAT proteins are highly activated under oncogenic condition [58,59]. To investigate the involvement of ZIP10 in lymphoma, I analyzed the phosphorylation of STAT3 and STAT5 (pSTAT3, pSTAT5) and ZIP10 expression in B cell lymphoma in salivary gland from human patients by immunohistochemistry. In all cases of follicular lymphoma (FL) and diffuse large B-cell lymphoma (DLBCL), pSTAT3, pSTAT5 and ZIP10 proteins were highly detected (**Fig 1-5A**) and the signals of pSTAT and ZIP10 were co-localized in fluorescent immunostaining assay (**Fig 1-5B**). These results suggest that ZIP10 expression is at least partly induced with the activated STAT3 and STAT5 proteins in B cell lymphoma, and it may impair the resistance for programmed cell death in oncogenic status.

DISCUSSION

Connection between Zn homeostasis and immune system

In this study, I demonstrated that ZIP10 promotes pro-B cell survival by inhibiting the activation of caspases, and that ZIP10 expression and Zn homeostasis are regulated in a STAT-dependent manner. Thus, ZIP10-mediated Zn signaling is a novel regulator of early B cell development, which establishes a functional link between Zn homeostasis and B cell development **(Fig. 1-6)**. So far, numerous reports have emphasized physiological importance of Zn in the immune system[60–63]. Aberrant Zn homeostasis leads to a regression of lymphoid tissue and compromises both B and T cell development[40]. In particular, early B cell development is severely affected by Zn deprivation *in vivo*[40,62]. Similar immunological disturbance was demonstrated in the present study. The ablation of ZIP10 caused decreasing intracellular Zn levels, leading to a substantial reduction in the total B cell populations **(Fig. 1-1,2)**. In addition, these dramatic reduction of B cell number was not observed when ZIP10 is ablated in mature B cell population (*invariant chain(Ii)-Cre* or *Cd21-Cre*::*Zip10*$^{flox/flox}$)[64]. Our results clearly demonstrated an essential role for cellular Zn homeostasis in early B cell development, providing a molecular basis for the immunodeficiency that results from Zn deficiency.

Zn influx regulates apoptotic cell death

I showed that ZIP10 negatively regulates the activity of caspases by inducible gene knockout, RNA interference, and Zn chelation experiments **(Fig. 1-2,3)**. Thus,

ZIP10 is a novel survival factor for B cell progenitors and has a suppressive effect on caspase activity through Zn uptake. Caspases (**c**ystein-**asp**ertic-acid-prote**ase**) are series of cystein proteases, and they possess a cystein residue in their catalytic site[65]. So far, enzymatic activity of caspase-3 is inhibited by binding of Zn^{2+} in the cysteine residue[66–69], and similar inhibition is also reported in other caspase family proteins[69–71]. These studies indicate the physiological significance of Zn-mediated regulation of caspases in immune system. There are many kinds of enzymes that possess cystein residue in catalytic site, such as protein tyrosine phosphatases (PTPs) and matrix metalloproteases (MMPs). PTPs have a reducing cystein residue in their active center, and they lost the activity by Zn^{2+} binding to that residue or under the oxidative condition[72–75]. Series of MMPs, which involve in the motility and cellular attachment in cancer cells, conserve the 'cystein switch' motif (PRCGVP) in their catalytic regulatory region[76]. It has previously reported that a wide variety of TFs possess Zn-binding motif such as Zn finger[77]. Of note, several Zn-finger TFs, Ikaros (*Ikzf1*), Helios (*Ikzf2*) and Aiolos (*Ikzf3*) are shown to be important for early lymphopoiesis[78]. Furthermore, it has recently reported that Ikaros plays a pivotal role for integrin-dependent survival and its potential to involve in leukemic pathogenesis[79]. These reports suggest that ZIP10-Zn^{2+} axis could regulate the activities of the Zn-finger TFs to promote the B cell differentiation ("Factor X" in **Figure 1-6**). Further investigations, like identification of ZIP10-binding proteins and clarification of transcriptional alteration under Zn-deficient conditions in early B cell development, will help us to understand the impact of Zn transporter-Zn^{2+} axis on maintaining immune homeostasis in more detail.

Significance of ZIP10-Zn-mediated anti-apoptosis in early B cell development

It has been shown that STAT is important for inhibition of cell death and progression of cell cycle in cytokine-mediated cell proliferation[80,81]. To evade from cell death, anti-apoptotic factors B-cell lymphoma (Bcl)-2 and Bcl-xL are also induced by STAT[57,82–84]. In this study, I showed a novel cell survival mechanism mediated by STAT signal. During early B cell development, there are several checkpoints to select functional B cell clone[85,86]. In pre-B cell stage, a clone is eliminated when they failed to rearrange the immunoglobulin (Ig) heavy chain locus in both maternal and paternal allelles[87]. In addition, auto-reactive B cell clones are also negatively selected in immature B cells[88,89]. During that process, Bcl-2 expression is maintained at low level from late-pro-B to immature B cell stage, suggesting the enhancement of apoptosis for efficient selection in these stages[40,90]. However, functional B cell clones are threatened to be eliminated without other anti-apoptotic mechanism(s); thus it is inferred that ZIP10-Zn^{2+} axis-mediated caspase inhibition is essential for guaranteeing cellular survival in the process. Not only early B cell progenitors, but also T cell progenitors and some other cell types may have similar 'back-up system' to stably maintain the cell survival.

Potential roles of ZIP10 in blood cancer

As mentioned above, activated STAT proteins regulated both Bcl famly genes and ZIP10 expression upon cytokine stimulations. Given that STAT signaling is highly

activated in multiple oncogenic cases[59], and that ZIP10 is involved in the migration of breast cancer[91], ZIP10 might play a role in wide variety of human blood cancers. This notion is consistent with the results of an *in silico* search, which showed high ZIP10 expression in various types of cancers including acute myeloid leukemia (AML) and acute lymphoid leukemia (ALL)[29,92]. I have shown that the ZIP10 expression was highly correlated with STAT3/STAT5 activation in lymphoma cells **(Fig. 1-5)**. Since most follicular lymphoma cells also overexpress Bcl-2[93] , the highly expressed ZIP10 via JAK-STAT signaling, at least in part, may exacerbate malignancy by eliciting anti-apoptotic effects in coordination with Bcl-2. STAT family members are activated not only by cytokines but also by growth factor receptors and oncogenic tyrosine kinases[59]. Therefore ZIP10 may be involved in various disease conditions associated with abnormal STAT activation.

Taken together, this study uncovered an essential role of ZIP10 in early B cell development, and revealed that ZIP10-mediated intracellular Zn homeostasis contributes to B cell survival by inhibiting the activity of caspases. Notably, our group also reported that ZIP10 modulates the strength of BCR signaling for optimal humoral immune respose[64], indicating that ZIP10 has unique functions in both early and mature B cell populations by regulating different molecular targets and cellular events. These studies on ZIP10 in B cells provide new insights into the relevance of Zn signaling in immuno-physiological events. Further exploration of the functions of Zn transporter-Zn signaling axis will shed light on the involvement of Zn in various aspects of the immune system.

CHAPTER 2

Transcriptional regulatory network during B cell lineage commitment

INTRODUCTION

In the previous chapter, I described the importance of Zn for controlling the enzymatic activity of caspases. It is also known that Zn contribute to the stabilities and activities of TFs which contain Zn-finger motifs. It has previously reported that multiple Zn-finger TFs such as Ikaros and Aiolos play essential roles in B cell development[94]. Cell fate determination in many developmental processes requires an acquisition of appropriate cell type-specific gene expression signature governed by TF networks[25]. So far, numerous TFs have been shown to be involved in B cell commitment and development (**Fig G-4**)[7,23,95–97]. Prominent regulators among them are E proteins E2A, E2-2 and HeLa E-box binding protein (HEB), which contain basic helix-loop-helix motif as a DNA binding domain[98]. The E2A proteins have two splicing isoforms, E12 and E47 (both are encoded by *Tcf3* gene). In contrast, Id proteins act as dominant-negative regulators of E proteins. Activities of E and Id proteins regulate the cell fate at distinct checkpoints during lymphoid developmental process[99]. Once the B cell program is initiated, E2A up-regulates the expression of FoxO1 and creates feed-forward loops[100,101]. Runx1/Cbfβ is also shown to be required for the induction of Ebf1[23,102]. Once Ebf1 is upregulated, it cooperates with E2A to induce multiple early B cell genes[22,103,104]. Another master regulator of B cells, Pax5 is also

up-regulated by cooperation of Ebf1 and PU.1[105]. For additional regulatory inputs, Ikaros[106], Bcl11a[107,108], Myeloblastosis oncogene (Myb)[109,110] and Growth factor independent-1 (Gfi1)[111,112] also contribute to the initiation of B cell program in concert with Ebf1 and Pax5. Although these reports indicated the essential roles of each TFs, the whole picture of transcriptional networks is still elusive mainly because of a lack of a suitable experimental system.

I established the in vitro B cell induction culture system using iLS cells as described above (General Introduction, see **Fig G-4**). Virtually all iLS cells were homogeneously induced into B cells within a week by simply removing 4-OHT from culture. I collected 16 time course samples during the B cell induction, and performed transcriptome analysis. Gene expression profiles dynamically altered in the several hours' intervals, and many undefined factors in B cell developmental process were strongly induced before the expression of B cell specific genes. TFs were classified into 7 clusters based on their expression patterns. Interestingly, transient and sequential 'TF waves' were dynamically induced at the beginning of B cell induction. Several epigenetic factors, *Cbx2*, *Uhrf1* and *Mysm1* were unexpectedly upregulated in harmony with B cell-specific TFs and short hairpin RNA (shRNA)-mediated KD of these factors perturbed B cell commitment. Of note, immediate early genes *Klf4* and *Egr1* were transiently activated at early phase, and their essential roles are confirmed by KD experiments. *Nfil3* gene expression is also transiently induced at immediate early phase. Nuclear factor, interleukin-3 regulated (Nfil3) has been reported as an essential factor for the function of helper T cells[113] and development of innate lymphoid cells

(ILCs)[114,115]. However, there are no reports about the role of Nfil3 in B cells; I thus validated their roles in the B cell commitment. *Nfil3*$^{-/-}$ mice exhibited mild increase in number of B cell progenitors in BM. On the other hand, clear reduction of early pre-B (Fr. C') and subsequent populations was found in the Eμ-driven Nfil3 transgenic (Eμ-Nfil3 Tg) mice. Finally, I established a TF networks by combining the time course expression profiling and genome-wide TF occupancy from deposited ChIP-seq data, and found that TFs could be separated into three groups, early, middle and late according to their expression peaks. Each group had the complex regulatory circuits and mutually connected each other. The TF networks identified here will not only facilitate the mechanistic analysis of B cell commitment but give us new insights into the general genomic control circuits that underlie the development, inflammatory disorders and tumorigenic transformation.

RESULTS

Establishment and characterization of iLS cells

First, I generated multipotent iLS cells that can be induced to differentiate into B cells. HSPCs (Lin^- $Sca\text{-}1^+c\text{-}kit^+$: LSK) were isolated from FL or BM and were transduced with a retroviral vector containing Id3-ER^{T2}. The transduced cells were cultured under optimal conditions for B cell differentiation in the presence of 4-OHT (**Figure 2-1A**). After 2 months cultivation, the surface phenotype of the transduced cells showed similar pattern with LMPPs ($c\text{-}Kit^{low}Sca\text{-}1^+Flk2^+$ $CD34^+IL\text{-}7Ra^{-/low}$, **Figure 2-1B**). These cells were maintained as lineage marker (Lin) negative (negative for CD19, Mac-1 and NK1.1) for at least several months, whereas LSK cells transduced with control vector rapidly differentiated into Lin^+ cells (**Figure 2-1C,D**). To assess the multipotency of Id3-ER^{T2} transduced cells, these cells were cultured under myeloid- and T/NK cell-differentiation condition. They gave rise to $Mac\text{-}1^+$ myeloid cells at day 10 of the culture and $CD3\varepsilon^+$ T and cells and $NK1.1^+$ NK cells at day 21 of the culture (**Fig 2-1E,F**). To determine the developmental potential of the progenitor cells *in vivo*, a total of 5×10^6 of Id3-ER^{T2} transduced cells were transferred intravenously into sublethally irradiated NOD/Shi-scid, IL-$2R\gamma^{null}$ (NOG) mice (**Fig. 2-1G**). After 4 weeks, the mice were dissected and thymus, spleen and BM were analyzed. B ($CD19^+$) cells and NK ($NK1.1^+$) were detected in BM, and T cells ($CD4^+CD8^+$) were observed in thymus of the recipient mice (**Fig. 2-1G,H**). IgD-expressing mature B cells and CD4 single positive (SP) or CD8 SP T cells were also detected in spleen after 6 weeks of transplantation (**Fig. 2-1I**). Compared to

lymphoid cells, only a small proportion of myeloid cells (Mac-1^+) were detected in BM at 6 weeks of injection (**Fig. 2-1J**), suggesting that the cells were biased to lymphoid lineage during the culture. Since these data, confirmed the multipotency of the progenitor cells both *in vivo* and *in vitro*, the cells were regarded as 'induced leukocyte stem (iLS) cells' which were previously reported[33].

Induction of iLS cells into B lineage

Next, I induced iLS cells differentiating into B lineage cells *in vitro*. By simply removing 4-OHT, Id3-ER^{T2} fusion protein was released from nuclei of the iLS cells within 1-2 days (**Fig. 2-2A**) and the cells were synchronously differentiated into $B220^+CD19^+$ committed B lineage cells in 6 days (**Fig. 2-2B**). Quantitative reverse transcription-polymerase chain reaction (qRT-PCR) analysis demonstrated that the B cell-associated genes (*E2A, Ebf1, Pax5, Cd79a* and *Igll1*) were gradually up-regulated but instead, stem/progenitor cell-associated genes (*Flt3* and *Cd34*) were suppressed (**Fig 2-2C**). In accordance with disappearance of Id3-ER^{T2} protein in the nuclei, occupancy of E2A in various target loci was increased (**Fig 2-2D**). The rearrangement of D_H-J_H was detected before the induction similar to $E2A^{-/-}$ cells[116]. On the other hand, V_H-DJ_H and IgL (Vκ-Lκ) rearrangements was clearly observed from approximal to distal segments according to the differentiation into B lineage (**Fig 2-2E**).

Histone modifications were also examined by ChIP-seq analysis at each time point. Transcriptional regulatory regions of B cell-associated genes (Ebf1, Pax5 or Vpreb1) were initially occupied by suppressive histone marks, trimethylation

(me3) in lysine (K)9 or K27 residue of histone 3 (H3) (H3K9me3 or H3K27me3, respectively). During the B cell differentiation, these modifications were gradually replaced by the transcriptional activation mark H3K4me3 (**Fig 2-3A**). In contrast, H3K4me3 mark was disappeared and H3K27me3 was increased in stem/progenitor cell-associated loci (Flt3 and Cd34, **Fig 2-3B**). Lineage-inappropriate gene loci such as Csf2ra (GM-CSF receptor) and Epor (Erythropoietin receptor) were strongly suppressed by high occupancy of H3K9me3 or H3K27me3 (**Fig 2-3C**). The coordination between gene expression and histone modification (H3K4me3 and H3K27me3) was also confirmed in genome-wide (**Fig 2-3D**). These data indicated that histone modification is totally correlated with the mRNA expression during B lineage commitment.

Dynamic alteration of gene expression patterns during B cell commitment

To reveal the variation of genome-wide gene expressions during the B cell commitment process, I collected the 16 time course samples in iLS system and performed RNA-seq analysis (**Fig 2-4A**). To understand the initial transcriptional regulation during B lineage commitment, the samples at the early time points (0.5 - 12 hr) were added. The gene expression profiles among 3 replicates confirmed the high correlations of the each data during B cell induction (**Fig 2-4B**). I next identified the 1182 differentially expressing genes between time points, selected by ANOVA ($p<0.01$ with Bonferroni correction). (**Fig 2-4C**). Using these datasets, I performed the principal component analysis (PCA) to clarify the characteristics of the gene expression patterns. PCA is a statistical method to simply visualize the complex characteristics composed of

multivariate datasets by reducing their dimensionality. Of note, the sequential changes of gene expression were aligned in an arc (**Fig 2-4D,** loading scores of each axis are shown in **Supplemental table 1**). These results suggest that the characteristics of gene expression in initial (0 hr), intermediate (around 10-24 hr) and late (96-168 hr) stages are totally different, and its transition is consecutive. Together, the transcriptome datasets represent dynamic and continuous transition of gene expression status during B cell commitment process with high reproducibility.

TF waves during B cell commitment

To investigate the transcriptional control of B cell fate determination, I performed *k*-means clustering in 1,144 TF gene sets. The results showed that TFs could be divided into 7 clusters by their expression patterns (**Fig 2-5A,** gene lists of each cluster are shown in **Supplemental table 2**). Representative TFs in respective clusters exhibit the wave-like structure of characteristic expression patterns during the specification into B lineage (**Fig 2-5B**). This sequential and transient induction of various TFs was termed as 'TF waves'. I first focused on Cluster VI, which contains up-regulated TFs at the late stage of B cell commitment (e.g. *Ebf1*, *Pax5* and *FoxO1*, **Fig 2-6A**). Among them, not only B cell-related TFs but also various epigenetic factors, such as PRC1 component *Cbx2*, DNA methyltransferase *Dnmt1* and the related gene *Uhrf1*, and histone H2A deubiquitinase *Mysm1* were found. They showed high expression levels in early B cell progenitor populations similar to *Ebf1* and *Bach2* (**Fig 2-6B**). To assess whether these factors are essential for normal B cell generation,

shRNA of these genes were retrovirally transduced with iLS cells and the cells were induced to differentiate into B cell lineage. I found that B cell numbers were decreased in *Cbx2*, *Uhrf1* and *Mysm1*-KD cells similar to *Pax5*-KD (**Fig 2-6C,D**). These results suggested that the epigenetic regulations by these factors act in concert with B cell-specific TF program to promote the B cell differentiation.

Early responding factors are essential for proper B cell commitment

Next, I focused on Cluster II, which contained early responding factors. The immediate early genes such as *Jun*, *Fos*, *Nr4a* and *Egr*, and Krüppel-like factors *Klf2,4* and *7* were found in this cluster (**Fig 2-7A**). I hypothesized that these factors are essential 'trigger' of lineage determination. To examine this possibility, I investigated the function of these factors in more detail. qRT-PCR analysis showed that *Jun, Nr4a1* and *Klf4* were markedly expressed in the earliest B cell progenitor fraction A (**Fig 2-7B**). Moreover, KD of *Nr4a2, Klf4* and *Egr1* inhibited the generation of B cells from iLS cells (**Fig 2-7C,D**), suggesting the functional importance of these general factors in B cell commitment.

Among the Cluster II, I also found *Nfil3* (**Fig 2-7A and 8A**), which previously reported their importance in the development of NK cells, ILCs and CD8α^+ conventional dendritic cells[114,115,117]. However, there are no descriptions about the involvement of Nfil3 in B lymphopoiesis. Therefore, I investigated the involvement of *Nfil3* in B cell commitment. The mRNA expression of *Nfil3* was high in LMPP stage but decreased thereafter (**Fig 2-8B**). Given that the expression of Nfil3 was rapidly

suppressed at the initiation of B cell commitment (**Fig 2-8A**), it could be that the suppression of *Nfil3* is essential for proper B cell commitment. To test this hypothesis, I first examined the *Nfil3*$^{-/-}$ mice. B cell progenitor populations such as fraction A and immature B cells were mildly increased in *Nfil3*$^{-/-}$ mice (**Fig 2-8C,D**). Similar increase of B cell number was also observed in shRNA-mediated *Nfil3* KD in normal BM progenitors differentiating into B cells (**Fig 2-8E**). On the other hand, significant reduction of fraction C', pre-B and immature B cells was observed in Eμ-Nfil3 Tg mice (**Fig 2-8F,G**). I compared the gene expression profiles of CD43^{+} pro-B and CD43^{-} pre-B cells between wild type and Eμ-Nfil3 mice, and found the reduced expression of several B cell-specific TFs such as *Bach2*, *Irf7*, *Spib* and *Ikzf3* in pro-B cells. In contrast, the expressions of *Jun* and *Id3* were continuously high in both pro-B and pre-B cells (**Fig 2-8H**). These results suggested that suppression of *Nfil3* expression at appropriate timing is essential for proper B cell fate determination.

TF networks during the B cell commitment process

Finally, I constructed the TF network using time course gene expression profiling. I selected the wave component and constantly expressed genes from transcriptome datasets by the expression level and variance (detailed gene names and log fold change values are shown in **Supplemental table 3** and **4**). The regulatory relationships between factors and their targets were inferred by the database integrated by the multiple ChIP-seq records deposited in gene expression omnibus (GEO) and ChEA2 database (The program was made by Dr Eiryo Kawakami in RIKEN IMS). The

protein-protein interactions between TFs were also taken into account (**Fig 2-9A**). The time phase was divided into 3 clusters (early, mid and late) based on the expression variance of TFs (**Fig 2-9B**). The TFs and epigenetic factors among the gene regulatory circuits in each cluster were closely connected each other (**Fig 2-9C**). The sequential changes of the transcriptional activities were also disclosed. For example, PRC2 component *Ezh2* and *Suz12* was suggested to be a strong negative regulator in the later stages of differentiation (**Fig 2-9C**). Of note, the activities of constantly expressed TFs such as *Myc* and *Ikaros* (*Ikzf1*) were dramatically activated during differentiation and they (factors in Constant cluster) continuously affected the regulatory networks at all three phases (**Fig 2-9C**). Collectively, orchestrated regulations of TFs and epigenetic factors are essential for initiation of B cell specific transcriptional program, and the disruption of the balance of the networks impairs normal B cell development (**Fig. 2-7C,D**).

DISCUSSION

TF networks highlighted the candidates to terminate programs for the differentiation into other lineages

In this study, I have shown the dynamic and sequential TF waves during B cell lineage commitment. I also constructed the TF networks during B cell commitment process based on hour-scale transcriptome profiles (**Fig 2-9**). The complex relationships between TFs were indicated. At the late stage, PRC2 components *Ezh2* and *Suz12* were suggested to be the strong negative regulator. It is possible that PRC2-mediated gene suppression can be the 'terminator' of lineage-inappropriate genetic programs. Consistent with this possibility, it is reported that crosstalk of PRC2 and its cofactor Jarid2 are essential for deposition of H3K27me3 during ES cell differentiation into embryoid bodies[118]. Moreover, Ezh2 deficiency lead to the arrest of B cell development at pro-B cell stage[119]. Genome-wide deposition of H3K27me3 during B cell fate determination was also observed in this study (**Fig 2-3D**). Therefore, similar mechanisms may regulate the B cell commitment.

On the other hand, the biological meaning of mid wave of TFs is still elusive. It is intriguing that Yap and Tead, which are the transcriptional effector of Hippo signaling, was induced at this phase. The transcriptional activity of these factors are affected by the physical or energetic stress and involved in various cellular responses such as proliferation, motility and differentiation. The requirement of Tead1 in human B cell development has been reported, indicating that the TFs in mid wave may have some essential roles for B cell commitment process.

Strong connection between TF networks and epigenetic regulation during B lineage commitment

Among the components in TF waves, many genes were already reported their essential functions in early B cell commitment and development. In Cluster VI, most of the major B cell-associated TFs, such as *Pax5, Irf4, Tcf3, Bach2, Ebf1, Foxo1* and *Lef1* were contained (**Fig 2-6**). These results clearly certify the validity of this system as a suitable model for B cell fate decision. Moreover, several factors in this cluster have recently characterized as novel regulators for proper B cell specification or commitment. The essential roles of the histone H2A deubiquitinase Mysm1[120] and the chromatin remodeler Smarca4 (Brg1)[121] in early B cell development have been shown. Ctcf is shown to be essential for normal VDJ recombination by binding intergenic control region between V_H and D clusters[122]. These results suggest that there are still 'unknown' essential players for epigenetic regulation in this cluster. Of note, I found the perturbation of PRC1 component *Cbx2* and co-factor of DNA methyltransferase *Uhrf1* lead to defects in B lymphopoiesis (**Fig 2-6C,D**). Together with PRC2 as discussed above, identification of other epigenetic regulators will facilitate the understanding of the mechanisms orchestrating the B lineage commitment.

Who first triggers the lineage commitment process?

I performed the clustering analysis in TFs and found 7 representative expression patterns (**Fig 2-5**). Among the TF waves, I focused on rapidly (0.5-2 hr) and

dramatically up-regulated TFs, *Jun, Fos* and *Egr1* (**Fig 2-7,8**). These genes are generally referred to as immediate early genes (IEGs). The importance of IEGs were first described in virology research[123]. When viruses infect with the host cells, several viral genes are rapidly transcribed. This process requires only pre-existing TFs of the host cell and occurs in the absence of de novo protein synthesis[124]. In mammals, it has become evident that various stimuli, such as growth/differentiation factors, hormones or cytokines, induce rapid and transient mRNA synthesis even in the presence of protein synthesis inhibitor[125–127]. Transcriptional start sites of IEGs are occupied with poised RNA polymerase II (Pol II), and the productive elongation by Pol II is stalled by the negative elongation factor (NELF) in neuronal system. Similar Pol II stalling for rapid induction is also documented in the case of response to environmental and developmental stimuli in *Drosophila*[128,129]. Therefore such regulatory mechanism is thought to be observed in general for developmental process[130,131]. This IEG induction is essential for regulation of secondary response genes to proceed the changes of cell behavior[132] and its abnormal expression causes the defects in cellular homeostasis. In fact, striking reduction of B cells with bone formation defects was shown in c-Fos knockout mice[133]. Conversely, overexpression of Fos and Jun in hematopoietic cells also perturbed B cell development at pro- or pre-B cell stage[134,135]. The number of B cell precursors was increased in Egr1 knockout mice[136], and sustained expression of Egr2 caused severe developmental block in pro-B cells[137]. In the present study, I revealed the essential role of the 1st wave factors (*Egr1, Nr4a2, Klf4* and *Nfil3*) in B cell generation (**Fig 2-7C,D** and **Fig 2-8**). Given that IEGs are sensitively induced by environmental

changes, it is possible that the 1st wave factors including IEGs would be the 'first trigger' of B cell fate determination. However, it remains to be determined which environmental signal activates the early responding TFs in normal B cell development.

Comparison of network construction between this study and previous report

To date, several gene regulatory networks among the immune system were proposed. For example, the complex genomic networks including TFs that control the generation of T_H17 cells were shown[138]. The authors prepared the detailed time course samples during the transition from naïve $CD4^+$ to T_H17 cells similar to this study (**Fig 2-4C**), and constructed the gene regulatory network. They proposed the 'positive' and 'negative' module factors that induce or suppress the expression of T_H17 signature genes. They performed a lot of careful validation experiments, however, the induction efficiency of T_H17 cells in their system is around 30%. Compared to this, since iLS cells could be induced into the B cells with high efficiency (>95%), the networks obtained by this study seem to be more accurate. Moreover, the TF networks identified here were constructed by combining the expression profiles of TFs, activities of each TF and information of the protein interactions among the TFs. It is particularly notable that the networks in this study (**Fig 2-9**) were drawn at three developmental stages separated by the expression patterns during B lineage commitment. Further improvements and validations of networks should contribute to better understandings for transcriptional regulation in the cell fate determination of multipotent progenitors into B cells.

Further applications of iLS cells for basic research and regenerative medicine

In this study, I established the transcriptional networks in B lineage commitment using highly reproducible iLS system. This method could be applied for both basic and clinical studies. For examples, during B cell developmental process, not only TFs, but also the involvement of non-coding RNAs such as microRNAs (miR)[139–141] and long non-coding RNAs (lncRNAs)[142,143] have been suggested. miR-126 was shown to control cell fate determination into B lineage as alternative to B cell-specific TFs[139]. miR-212/132 cluster contributes to B cell development by regulating Sox4 activity[140]. Identification and characterization of lncRNAs are now extensively investigated[144], whereas the roles in B cell development is still elusive. The iLS system will become a powerful tool to investigate how these non-coding RNAs connect with the TF networks during the cell fate decision.

Recently, a novel concept 'super-enhancers' have been proposed; the definition is groups of putative enhancers in close genomic proximity with unusually high levels of Mediator binding[145]. Warren et al. demonstrated that these super-enhancers play essential roles in cellular identity by regulating cell-type specific master TFs (Oct4, Sox2 and Nanog in ES cells, and PU.1, Ebf1 and Foxo1 in pro-B cells)[146]. Recently, it is proposed that super-enhancers are involved in the commitment and plasticity of stem cells[147]. Thus, the iLS system will be useful for in-depth investigation for these molecular regulation in B cell development.

For clinical application, iLS cells have a potential to be able to use for transplantation therapies. Currently, a number of studies of induced pluripotent stem

cell (iPSC)-mediated regenerative medicine including regeneration of NKT cells or cytotoxic T cells against tumor cells are on-going[148–151]. However, there are a lot of barriers and limitations to apply this for a clinical use, because it will take too much time and costs to be able to generate functional effector cells from patient-derived iPSCs. To isolate safe and reproducible effector cells derived from iPSCs is also a big matter. Therefore, I propose that iLS system could be replaced with the iPSC-mediated immunotherapy. The iLS cells can be quickly generated from HSPCs compared to iPSCs. Moreover, T, B, NK and myeloid cells can be easily generated from iLS cells (**Fig 2-1**). Thus, the generation of human iLS cells will be a fascinating application method for future immunotherapy.

MATERIAL AND METHODS

CHAPTER 1

Mice. *Slc39a10/ZIP10*-floxed mice is generated in our laboratory. Detailed methods including genotyping are shown in elsewhere[29]. *Cag-Cre* transgenic mice were gifted from Dr Masaru Okabe at Research Institute for Microbial Diseases, Osaka University. *mb1-Cre* transgenic mice were gifted from Dr Michael Reth at Max Planck Institute of Immunobiology and Epigenetics. *Rosa26-ER^{T2}-Cre* transgenic mice were purchased from Artemis Pharmaceuticals (Cologne, Germany). C57BL/6J mice were purchased from CLEA Japan, Inc (Tokyo. Japan). B cell specific ZIP10 conditional knockout (*Zip10*^{mb1}) mice were obtained by crossing *Zip10*-floxed mouse with *mb1-Cre* transgenic mice. Tamoxifen inducible ZIP10 conditional knockout (*Zip10*$^{Rosa\text{-}ERT2}$) mice were obtained by crossing *Zip10*-floxed mouse with *Rosa26-ER^{T2}-Cre* transgenic mice. We maintained all of the mice under nutritionally normal condition. All experiments were conducted according to guidelines approved by the RIKEN Institutional Animal Care and Use Committee.

Generation of ZIP10-specific antibody. Rabbit anti-mouse ZIP10 antibody used for FACS analysis was generated in our laboratory[29]. Epitope peptide is as follows:

^{296}ELDPDNEGELRHTRKRE^{312}

Antibodies. The following antibodies were purchased from Biolegend: CD19 (6D5), CD24 (M1/69), CD45R/B220 (RA3-6B2), CD93 (AA4.1), CD23 (B3B4) and Sca-1 (D7). Antibody against CD43 (S7) was purchased from BD Bioscience, and anti-IgM (II/41), BP-1 (6C3), c-Kit (2B8) were purchased from eBioscience. Alexa Fluor 488 F(ab')2 fragment of goat anti-rabbit IgG (H+L) was used as secondary antibody for purified ZIP10 antibody described above, and was purchased from Molecular Probes.

Flow cytometry. Single cell suspensions of BM or spleen were incubated with ice-cold red blood cell (RBC) lysing buffer containing NH_4Cl for 1 min before staining. For surface markers staining, cells were incubated with antibodies in FACS buffer (PBS with 1% FCS) for 15 min on ice. For detection of apoptotic cells, cells were stained FITC-conjugated annexin V (BD Bioscience) and 7-AAD (BD Bioscience) in annexin-V binding buffer (BD Bioscience) following manufacturer's instructions. For measurement of intracellular Zn level, cells were incubated with indicated concentration of Newport Green DCF (Invitrogen) or FluoZin-2 (Invitrogen) for 30 min at 37°C, washed PBS once and stood in PBS for 30 min at 37°C followed by FACS analysis. Data were collected by FACSCalibur or FACSCanto II (Beckton Dickinson) and analyzed by FlowJo (TreeStar).

Cell culture. For co-culture experiments, thymic storomal derived TSt-4 cell line (gifted from Dr Tomokatsu Ikawa in RIKEN Research Center for Allergy and Immunology) were used for feeder. For inducible deletion of *Zip10* gene in vitro, pro-

or pre-B cells were collected from BM of *Zip10*$^{\text{Rosa-ERT2}}$ or littermate control (*Zip10*$^{\text{wt/wt}}$ *Rosa26-ERT2-Cre*) mice, then cultured on monolayer of TSt-4 feeder cells and treated with 50 nM 4-OHT (Sigma Aldrich) for 2 d. Mouse BM-derived cell lines BAF-B03 G133 and its mutant BAF-B03 G133$^{\text{STAT3F}}$ (expresses dominant negative of STAT3 protein[57]) were maintained under IL-3 additional condition.

Treatment of zinc chelator. BAF-B03 G133 cells were incubated with 10 μM of Zn chelator TPEN (Dojindo Molecular Technologies) for 3 hrs. For rescue experiment, 10 μM $ZnSO_4$ was simultaneously added.

Gene silencing. BAF-B03 G133 cells were transfected with siRNA (siGENOME SMARTpool for mouse *Zip10*, *Stat5b* or non-targeting scramble, Thermo Fisher Scientific) using two-step electroporator CUY21Pro-Vitro (NEPA GENE). 1×10^6 cells were resuspended in 100 μL Opti-MEM (Gibco), and 400 pmol siRNA were added. Electroporation was carried out with 1 pulse for pore-formation (150 V for 10 msec) and 10 driving pulses (20 V for 50 msec) then cells were immediately resuspended in culture medium and incubated in 5% CO2 at 37°C for indicated time.

Cytokine stimulation *in vitro*. Pro-B cells were sorted from BM suspension of C57BL6/J mice using FACSAria III. Pro-B or BAF-B03 G133 cell lines were once starved in cytokine-free medium for 1 hr, then stimulated for 3 hrs by 10 ng/ml IL-7 (R&D) + SCF (R&D) or IL-3 (self-made) and/or G-CSF (R&D), respectively.

Western blotting. Tested cells were lysed with lysis buffer (20 mM Tris•HCl pH 7.4, 150 mM NaCl, 1% NP40) for 30 min at 4°C, then centrifuged at 12 k × g at 4°C for 30 min. Lysates were subjected to SDS-PAGE using 5-20% (w/v) gradient or 15% (w/v, for Caspase-3 detection) polyacrylamide gel (Wako) and transferred to PVDF membrane (Immobilon-P, Millipore). Membrane were blocked by PVDF Blocking Reagent for Can Get Signal (TOYOBO) for 1 hr under room temperature then incubated with following primary antibody diluted in Can Get Signal Solution 1 (TOYOBO) for 1 hr at room temperature: anti-Caspase 3, 8, 9, 12 (Cell Signaling, #9662, 4927, 9504 and 2202, respectively) and anti-α-tubulin (B-5-1-2: Santa Cruz Biotechnology, #sc-23948). Membrane was washed 3 times by TBS-T then incubated with secondary antibody (HRP-conjugated anti-mouse, rabbit or goat IgG: Zymed, diluted in Can Get Signal Solution 2: TOYOBO) for 1 hr at room temperature. After extensive washing (4 times) of membrane by TBS-T, immunoreactive proteins were detected by Western Lightning-ECL reagent (Perkin Elmer).

qRT-PCR. Total RNA was extracted by Sepasol Super G (Nakarai Tesque) or TRIzol reagent (Invitrogen) then reverse-transcribed with oligo-dT primer (Invitrogen) and ReverTra Ace (TOYOBO). Gene expression level was assessed by PCR using SYBR Premix ExTaq (TaKaRa). Data was collected by StepOne Plus (Applied Biosystems). Primer sequences used for qPCR is shown in **Table 1**.

Analysis of human samples. For studies involving lymphoma samples **(Fig. 1-5)**, informed consent was obtained from the human subjects, and approval was obtained from the ethics committee of the School of Dentistry, Showa University. Paraffin sections (4 μm) were cut and stained with H&E and used for immunohistochemistry with the anti-ZIP10, phospho-STAT3 (Tyr705) (Cell Signaling #9145) and phospho-STAT5 (Tyr694) (Cell Signaling #9351) antibodies. For fluorescence immunohistochemistry, the primary antibodies were detected using highly cross-adsorbed Alexa Fluor 488 goat anti-rabbit IgG (H+L) (Life Technologies) and Alexa Fluor 594 goat anti-rabbit IgG (H+L) (Life technologies), together with 4,6-diamidino-2-phenylindole (DAPI; Dojindo). All fluorescence microscopy images were captured under a fluorescence microscope (Keyence).

Statistics. All experiments were performed at least 2 times. The two-tailed Student's t-test was used to analyze differences between two groups,

CHAPTER 2

Mice. C57BL/6J (B6), B6.Rag1-KO and B6.Ly5.1 congenic mice were purchased from CLEA Japan Inc (Tokyo, Japan). NOD/Shi-scid, IL2Rg^{null} (NOG) mice were purchased from the Central Institute for Experimental Animals (Kanagawa, Japan). Nfil3 KO and B cell-specific Tg mice were kindly gifted from Dr Masato Kubo (RIKEN IMS and Tokyo University of Science). 6 to 8 week old female mice were used for transfer experiments. Embryos at 14 dpc were obtained from timed pregnancies. The day observing verginal plug was designated as 0 dpc. All experiments were conducted according to guidelines approved by the RIKEN Institutional Animal Care and Use Committee.

Antibodies and growth factors. The following antibodies were purchased from BD Pharmingen or BD Horizon: c-kit (2B8), Sca-1 (D7), Flk2 (A2F10.1), CD34 (RAM34), IL-7Ra (SB/199), CD24 (M1/69), BP-1 (6C3), CD43 (S7), erythroid lineage cells (TER119), Mac-1 (M1/70), Gr-1 (RB6-8C5), CD11c (HL3), B220 (RA3-6B2), CD8 (53-6.7), CD4 (H129.19), NK1.1 (PK136), CD3ε (145-2C11), and CD19 (1D3). IgM (II/41), IgD (11-26C) and human CD25 (M-A251). TER119, Mac-1, Gr-1, B220, CD19, NK1.1, CD3ε, CD4, and CD8 were used as Lin markers. Recombinant murine IL-3, IL-7, stem cell factor (SCF), Flt-3 ligand (Flt-3L), thrombopoietin (Tpo) were purchased from R&D.

Isolation of hematopoietic progenitors. Single cell suspensions of FL cells from 14 dpc or BM cells of B6.Ly5.1 mice were prepared as described previously[116]. Cells were then incubated with purified monoclonal antibodies specific for lineage markers (Lin: TER119, Mac-1, Gr-1, B220 and Thy1.2) for 20 min on ice. Lin^+ cells were depleted with Dynabeads Sheep anti-Rat IgG (Invitrogen) according to the manufacturer's protocol. LSK-HSCs from FL and adult BM were isolated by FACS Aria II.

Preparation and transduction of retrovirus. Retroviral vector pMCs-IRES-GFP which cloned human Id3 and modified estrogen receptor ER^{T2} fusion construct (pMCs-hId3-ER^{T2}-IG) were gifted by Dr Yasutoshi Agata (Shiga University of Medical Science). shRNA vector for KD experiments were prepared by Open Biosystems LMP system (MSCV-LTRmiR30-PIG, Thermo Scientific) which modified the expression marker to hCD25. The vector was gifted from Dr. Cornelis Murre (University of California, San Diego). Vector construction of specific target were performed according to the manufacturer's introduction, and target sequences are shown in **Table 2**. Retrovirus was generated by transfection of pMCs-hId3-ER^{T2}-IG or shRNA constract plasmid together with pantropic envelope protein VSV-G plasmid into 293T cell line using FuGENE 6 Transfection Reagent (Roche). Viral supernatant was collected at day 2 and 3 after transfection.

Establishment and B cell induction of iLS cells. LSK cells from FL or BM were transduced with hId3-ER^{T2}-IG virus supernatants by spin infection as described

previously[116]. Transduction was conducted second consecutive days, then maintained under cytokine-rich condition (IL-7, SCF, Flt-3L and Tpo; 30 ng/ml each) co-cultured with TSt-4 stromal cells for 2-3 d. After that, the transduced cells were harvested and stained with anti-mouse CD19/Mac-1/NK1.1 antibodies and $GFP^+CD19^-Mac\text{-}1^-NK1.1^-$ cells were sorted. Purified cells were maintained on TSt-4 stromal cells in the presence of 20 ng/ml IL-7, 10 ng/ml SCF, 10 ng/ml Flt-3L and 40 nM 4-OHT (SIGMA). $GFP^+CD19^-Mac\text{-}1^-NK1.1^-$ cells (correspond to iLS cells) were sorted *ad libitum*. For B cell induction from iLS cells, sorted cells were transferred to 4-OHT-free culture medium containing 5 ng/ml IL-7 on TSt-4 pre-seeded plate.

Co-culture with stromal cells. To assess myeloid potential of iLS cells, 1×10^5 cells per well were cultured with TSt-4 stromal cells in the presence of 10 ng/ml IL-3 for 10 d. For detection of T cell potential, cells were cultured with TSt-4 cells that ectopically expressed Notch ligand delta-like 1 (TSt-4/DLL1 cells[33]) in culture medium containing 5 ng/ml IL-7. All co-cultures were maintained in IMDM medium (Gibco) supplemented with 10% FCS, 50 nM 2-ME (Nakarai Tesque) and penicillin/streptomycin (1×, Gibco).

shRNA-mediated KD experiments. For iLS cells, cells were transduced with respective shRNA virus by spin infection, then cells were cultured under maintenance condition (with 4-OHT). At 2 days after infection, hCD25 (infection marker)-positive cells were collected by magnetic activatied cell sorting (MACS, Myltenyi biotec) and 1×10^5 cells of separated cells were transferred to B cell induction culture condition

(described above). For LSK cells (Nfil3 KD), virus transduction was operated similarly and co-cultured with TSt-4 and 10% FCS-containing IMDM medium for 6 days.

Adaptive transfer of iLS cells. iLS cells (5×10^6, $GFP^+Ly5.1^+$) and whole BM of B6 mice (2×10^5, $Ly5.2^+$) were intravenously injected into the tail vein of irradiated (2.4 Gy by γ-ray) NOG mice ($Ly5.2^+$). Mice were analyzed 4-6 weeks after reconstitution for donor chimerism in BM, spleen and thymus.

Flow cytometry. 6-10 wk old mice were used for all experiments. Mice were sacrificed and single cell suspensions of BM, spleen and thymus were prepared. Cell number was counted, then ~1×10^7 cells were stained with combination of antibodies in FACS buffer (1× PBS with 2% FCS and 0.05% NaN_3). Data were collected by FACSAria II or FACSCanto II (Beckton Dickinson) and analyzed by FlowJo (TreeStar).

Organelle fractionation and western blotting. Tested iLS cells (2×10^6) were fractionated using NE-PER Nuclear and Cytoplasmic Extraction Reagents (Pierce). Each lysates were subjected to SDS-PAGE using Mini-Protean TGX precast gel (Bio-Rad) then transferred to PVDF membrane by Transblot Turbo Transfer System (Bio-Rad). Membrane were blocked by PVDF Blocking Reagent for Can Get Signal (TOYOBO) for 1 hr under room temperature then incubated with following primary antibody diluted in Can Get Signal Solution 1 (TOYOBO) for 1 hr at room temperature: anti-human ID3 (Cell Signaling, #9837), anti-a-tubulin (Santa Cruz Biotechnology,

#sc-8035) and anti-Lamin A/C (Santa Cruz Biotechnology, #sc-7292). Membrane was washed 3 times by TBS-T then incubated with secondary antibody (HRP-conjugated anti-mouse or rabbit IgG: Life Technologies, diluted in Can Get Signal Solution 2: TOYOBO) for 1 hr at room temperature. After extensive washing (4 times) of membrane by TBS-T, immunoreactive proteins were detected by Western Lightning Plus-ECL reagent (Perkin Elmer).

RNA extraction. Total RNA is extracted by Maxwell 16 LEV simplyRNA Purification Kit (Promega) followed by the manufacturer's protocol.

qRT-PCR. cDNA is synthesized with VILO cDNA Synthesis Kit (Invitrogen). Quantitative PCR is performed with SYBR Premix Ex Taq (TaKaRa). Primer sequences are shown in **Table 3**.

PCR analysis for genomic rearrangement of IgH locus. Genomic DNA is extracted by DNeasy Blood and Tissue Kit (Qiagen). PCR is performed with KAPATaq Extra HotStart ReadyMix with dye (KAPA Biosystems). Primer sequences are shown in **Table 3**.

RNA sequence (RNA-seq). Poly(A)$^+$ mRNA was isolated from total RNA by NEBNext Poly(A) mRNA Magnetic Isolation Module (New England Biolabs) then library was prepared by NEBNext Ultra RNA Library Prep Kit for Illumina (New

England Biolabs). Average size and quantity of each library were measured by Agilent 2100 Bioanalyzer (Agilent Technologies) and KAPA Library Quantification Kit (KAPA Biosystems), respectively. Sequences were read by HiSeq 1500 system (Illumina).

ChIP and ChIP-seq. Detailed ChIP protocol was described at elsewhere[152]. Cells were fixed with 1% formaldehyde solution for 10 (for methylated histone) or 20 (for TFs) at 25°C. Soluble chromatin was immunoprecipitated with normal rabbit IgG (as negative control, Santa Cruz Biotechnology, #sc-2027), anti-H3K4me3 (Millipore, #07-473), anti-H3K27me3 (Millipore, #07-449), anti-H3K9me3 (Medical & Biological Laboratories, #MABI0308), anti-E2A (Santa Cruz Biotechnology, #sc-349X). For quantification, precipitated and input DNA were purified with MinElute PCR Purification Kit (Qiagen) and performed quantitative PCR with SYBR Premix Ex Taq (TaKaRa). For sequencing, purified DNA were fragmented with DNA shearing system M220 (Covaris) then libraries were prepared with NEBNext Ultra DNA Library Prep Kit for Illumina (New England Biolabs). Procedures for quality check of libraries and sequencing were corresponded to RNA-seq.

Data analysis. Sequences obtained in RNA-seq experiments were aligned on mouse genome (NCBI build 37, mm9) using tophat2 (version 2.1.0)[153] and assigned to mouse genes using cufflinks (version 2.1.1)[154] with gene annotation provided by iGenomes. Fold changes and p-values of gene expression between Eμ-Nfil3 and WT expression

was performed using cuffdiff (version 2.1.1)[155]. Expression similarity among experimental replicates was estimated using Pearson correlation of RPKM values of all genes. In the PCA plot, we used 1,182 representative genes that had different expression among time points with less than 0.01 p-value corrected Bonfferoni adjustment using ANOVA. ChIP-Seq reads were aligned on mouse genome (mm9) using bowtie 2.1.0 and compared with gene locations Mapping to reference genome is performed with Integrative Genomics Viewer (https://www.broadinstitute.org/igv). To see epigenetic changes of differently expressed genes before and after differentiation, we evaluated expression changes between 0 hr and 144 hr samples using DESeq2 package[156] and collected significant genes (q-value < 0.01) expressed more than 2 times (410 genes) or less than 0.5 times (304 genes). RPKM around TSS (-5kb to +2kb, 100bp window size) was subtracted between two time points and represented.

PCA, heat maps, correlation plots, k-means clustering, GO analysis, ChIP-seq subtraction diagrams were analyzed using in-house computer programs developed by Dr Takaho A Endo, RIKEN IMS.

Network construction based on time-course transcriptome. DNA binding factors were picked-up by their gene ontology term. Read counts for the genes annotated in UCSC mm9 were assembled using featureCounts[157], and differential gene expression was determined using DESeq2 version 1.8.1[156]. We integrated additional data obtained from the gene expression omnibus database (GEO, www.ncbi.nlm.nih.gov/geo/) with the ChEA2 database (http://amp.pharm.mssm.edu/ChEA2/)[158] to construct a ChIP

database containing a total of 25,468,840 binding interactions for 486 transcription regulators (constructed by Dr Eiryo Kawakami, RIKEN IMS). The network is shown in an organic layout using Cytoscape (http://www.cytoscape.org)[159]. The node colors indicate the Enrichment Scores of TFs calculated with weighted parametric enrichment analysis indicating the weighted average expression changes of their target genes in each stage (early, mid and late) of B cell commitment. The width of the line represents the experimental score of the interaction obtained from STRING database v10 (http://string-db.org)[160].

Statistics. All experiments were performed at least 2 times. The two-tailed Student's t-test was used to analyze differences between two groups,

TABLES FOR MATERIAL AND METHODS

Table 1. Primer sequences for qRT-PCR used in CHAPTER 1.

mouse *Zip6*	Forward	GCAAGAAGCAGCTGTCCAAA
	Reverse	TGCATGGGCTATCATGACCT
mouse *Zip8*	Forward	AGCTTGAACACACCCTGCAGAA
	Reverse	AATCCCAGAGCATGGCAAGAC
mouse *Zip10*	Forward	GCATCAGCACATCCATAGCC
	Reverse	TTGGCATACTGACCGACTGC
mouse *Zip13*	Forward	ACCGATGGACGGCAGCTAAG
	Reverse	AACACATTCACCAGGGCGATATAGA
mouse *Zip14*	Forward	TGGTGCCTCCTTCACTGTGT
	Reverse	AGGCCAGACCCAAATAGCAG
mouse *c-myc*	Forward	CCTAGTGCTGCATGAGGAGACAC
	Reverse	GGATGGAGATGAGCCCGACT
mouse *Socs3*	Forward	CCCAAGGCCGGAGATTTC
	Reverse	GGAGCCAGCGTGGATCTG
mouse *Stat5b*	Forward	CCATTTGCACCCTAATTTGACATC
	Reverse	TGCAGGTCCCATTCCTACCA

Table 2. Sequence of shRNA constructs used in CHAPTER 2.

Target	Sequence
Cbx2	TGCTGTTGACAGTGAGCGAAGACACTCTATGCTTTGCAAGTAGTGAAGCCACAGATGTACTTGCAAAGCATAGAGTGTCTCTGCCTACTGCCTCGGA
Uhrf1	TGCTGTTGACAGTGAGCGCGGCCACACACTCTTCGATTATTAGTGAAGCCACAGATGTAATAATCGAAGAGTGTGTGGCCATGCCTACTGCCTCGGA
Mysm1	TGCTGTTGACAGTGAGCGAATAGATAATGTGAGAAGGAAGTAGTGAAGCCACAGATGTACTTCCTTCTCACATTATCTATGTGCCTACTGCCTCGGA
Pax5	TGCTGTTGACAGTGAGCGAGCAGAGCGAGTCTGTGACAATTAGTGAAGCCACAGATGTAATTGTCACAGACTCGCTCTGCCTGCCTACTGCCTCGGA
Nr4a2	TGCTGTTGACAGTGAGCGACCTGTCACTCTTCTCCTTTAATAGTGAAGCCACAGATGTATTAAAGGAGAAGAGTGACAGGCTGCCTACTGCCTCGGA
Klf4	TGCTGTTGACAGTGAGCGCTCTGCCTTGCTGATTGTCTATTAGTGAAGCCACAGATGTAATAGACAATCAGCAAGGCAGATTGCCTACTGCCTCGGA
Egr1	TGCTGTTGACAGTGAGCGCATTCTTGATGTGAAGATAATTTAGTGAAGCCACAGATGTAAATTATCTTCACATCAAGAATATGCCTACTGCCTCGGA
Nfil3	TGCTGTTGACAGTGAGCGACTGCTCTCCCTGAAATTAAAGTAGTGAAGCCACAGATGTACTTTAATTTCAGGGAGAGCAGCTGCCTACTGCCTCGGA

Nucleotides shown in magenta are gene-specific sequences.

Table 3. Primer sequences used in CHAPTER 2.

Primer for qRT-PCR

	Forward	Reverse
qE2A	CAGAACTGGAAACAAAGCAG	TGGTGGCTCTGAAGTAGAAG
qE47	TTGACCCTAGCCGGACATACA	GCATAGGCATTCCGCTCACT
qCD79a	TATGTCTGACTCCAGCATCC	GGGAAGGACAAGATTAGGTG
qlambda5	GTTCTAATGGGATGCTAGGC	AGCGTCCTTCTCTTATCAGG
qEBF1	TGGGTTACAGGTCATATTCG	GAACTGCTTGGACTTGTACG
qPax5	CATTCGGACAAAAGTACAGC	GATGCCACTGATGGAGTATG
qFlt3	AGTTCACCAAAATGTTCACG	ACTTCTTCCAGGTCCAAGAG
qCd34_1	ATGCTGGTGCTAGTGTCTGC	TGGATCCCCAGCTTTCTCAAG

Primer for ChIP-qPCR

	Forward	Reverse
Cd79a	CCACGCACTAGAGAGAGACTCAA	CCGCCTCACTTCCTGTTCAGCCG
EBF1	CCACGCTCCTTCCAGTTTAG	ATCCTTCCGCCTTATCACAG
Igll1	GGGTTAAGACAGGCAGCTGTGAG	CAAACCCCAGGCTGTCTCTAGTT
Igk_3' enhancer	ATAGCAACTGTCATAGCTACCGT	GCAGGTGTATGAGGCTTTGGAAA

Primer for rearrangement PCR

DHL	MTTTTTGTSAAGGGATCTACTACTGTG
VH7183	GAASAMCCTGTWCCTGCAAATGASC
VHQ52	ACTGARCATCASCAAGGACAAYTCC
VHJ558	CARCACAGCCTWCATGCARCTCARC
JH3	CTCACAAGAGTCCGATAGACCCTGG
mVkdeg-F1	GSTTCAGTGGCAGTGGRTCWGGRAC
mJk2-R1	TTTCCAGCTTGGTCCCCCCTCCGAA
Acta1-F	GGCATCGTGTTGGATTCTG
Acta1-R	CACGAAGGAATAGCCACGC

REFERENCE

1. Osawa, M., Hanada, K., Hamada, H. & Nakauchi, H. Long-term lymphohematopoietic reconstitution by a single CD34-low/negative hematopoietic stem cell. *Science* **273,** 242–245 (1996).
2. Adolfsson, J. *et al*. Identification of Flt3+ lympho-myeloid stem cells lacking erythro-megakaryocytic potential: A revised road map for adult blood lineage commitment. *Cell* **121,** 295–306 (2005).
3. Kondo, M., Weissman, I. L. & Akashi, K. Identification of clonogenic common lymphoid progenitors in mouse bone marrow. *Cell* **91,** 661–672 (1997).
4. Hardy, R. R., Kincade, P. W. & Dorshkind, K. The Protean Nature of Cells in the B Lymphocyte Lineage. *Immunity* **26,** 703–714 (2007).
5. Hardy, R. R., Carmack, C. E., Shinton, S. a, Kemp, J. D. & Hayakawa, K. Resolution and characterization of pro-B and pre-pro-B cell stages in normal mouse bone marrow. *J. Exp. Med.* **173,** 1213–1225 (1991).
6. Rumfelt, L. L., Zhou, Y., Rowley, B. M., Shinton, S. a & Hardy, R. R. Lineage specification and plasticity in CD19- early B cell precursors. *J. Exp. Med.* **203,** 675–687 (2006).
7. Rothenberg, E. V. Transcriptional control of early T and B cell developmental choices. *Annu. Rev. Immunol.* **32,** 283–321 (2014).
8. Nagasawa, T. Microenvironmental niches in the bone marrow required for B-cell development. *Nat. Rev. Immunol.* **6,** 107–116 (2006).

9. Morrison, S. J. & Scadden, D. T. The bone marrow niche for haematopoietic stem cells. *Nature* **505,** 327–34 (2014).

10. Mendelson, A. & Frenette, P. S. Hematopoietic stem cell niche maintenance during homeostasis and regeneration. *Nat. Med.* **20,** 833–846 (2014).

11. Ding, L. & Morrison, S. J. Haematopoietic stem cells and early lymphoid progenitors occupy distinct bone marrow niches. *Nature* **495,** 231–235 (2013).

12. Visnjic, D. *et al*. Conditional ablation of the osteoblast lineage in Col2.3deltatk transgenic mice. *J. Bone Miner. Res.* **16,** 2222–2231 (2001).

13. Zhu, J. *et al*. Osteoblasts support B-lymphocyte commitment and differentiation from hematopoietic stem cells. *Blood* **109,** 3706–12 (2007).

14. Clark, M. R., Mandal, M., Ochiai, K. & Singh, H. Orchestrating B cell lymphopoiesis through interplay of IL-7 receptor and pre-B cell receptor signalling. *Nat. Rev. Immunol.* **14,** 69–80 (2013).

15. Corfe, S. A. & Paige, C. J. The many roles of IL-7 in B cell development; mediator of survival, proliferation and differentiation. *Semin Immunol* **24,** 198–208 (2012).

16. Dolence, J. J., Gwin, K., Frank, E. & Medina, K. L. Threshold levels of Flt3-ligand are required for the generation and survival of lymphoid progenitors and B-cell precursors. *Eur. J. Immunol.* **41,** 324–334 (2011).

17. Waskow, C., Paul, S., Haller, C., Gassmann, M. & Rodewald, H.-R. Viable c-Kit(W/W) mutants reveal pivotal role for c-kit in the maintenance of lymphopoiesis. *Immunity* **17,** 277–88 (2002).

18. Kong, Y. Y. *et al*. OPGL is a key regulator of osteoclastogenesis, lymphocyte development and lymph-node organogenesis. *Nature* **397,** 315–323 (1999).

19. Dougall, W. C. *et al*. RANK is essential for osteoclast and lymph node development. *Genes Dev*. **13,** 2412–2424 (1999).

20. Tokoyoda, K., Egawa, T., Sugiyama, T., Choi, B. Il & Nagasawa, T. Cellular niches controlling B lymphocyte behavior within bone marrow during development. *Immunity* **20,** 707–718 (2004).

21. Bain, G. *et al*. E2A proteins are required for proper B cell development and initiation of immunoglobulin gene rearrangements. *Cell* **79,** 885–892 (1994).

22. Lin, Y. C. *et al*. A global network of transcription factors, involving E2A, EBF1 and Foxo1, that orchestrates B cell fate. *Nat. Immunol*. **11,** 635–643 (2010).

23. Seo, W., Ikawa, T., Kawamoto, H. & Taniuchi, I. Runx1-Cbfβ facilitates early B lymphocyte development by regulating expression of Ebf1. *J. Exp. Med*. **209,** 1255–62 (2012).

24. Nechanitzky, R. *et al*. Transcription factor EBF1 is essential for the maintenance of B cell identity and prevention of alternative fates in committed cells. *Nat. Immunol*. **14,** 867–75 (2013).

25. Boller, S. & Grosschedl, R. The regulatory network of B-cell differentiation: A focused view of early B-cell factor 1 function. *Immunol. Rev*. **261,** 102–115 (2014).

26. Nutt, S. L., Heavey, B., Rolink, a G. & Busslinger, M. Commitment to the B-lymphoid lineage depends on the transcription factor Pax5. *Nature* **401,** 556–

562 (1999).

27. King, J. C., Shames, D. M. & Woodhouse, L. R. Zinc and Health: Current Status and Future Directions Zinc Homeostasis in Humans 1. *J. Nutr.* **130,** 1360–1366 (2000).

28. Eide, D. J. Zinc transporters and the cellular trafficking of zinc. *Biochim. Biophys. Acta - Mol. Cell Res.* **1763,** 711–722 (2006).

29. Miyai, T. *et al.* Zinc transporter SLC39A10/ZIP10 facilitates antiapoptotic signaling during early B-cell development. *Proc. Natl. Acad. Sci. U. S. A.* **111,** 11780–11785 (2014).

30. Choukrallah, M. A. & Matthias, P. The Interplay between Chromatin and Transcription Factor Networks during B Cell Development: Who Pulls the Trigger First? *Front. Immunol.* **5,** 1–11 (2014).

31. Yamamoto, R. *et al.* Clonal analysis unveils self-renewing lineage-restricted progenitors generated directly from hematopoietic stem cells. *Cell* **154,** 1112–1126 (2013).

32. Morita, Y., Ema, H. & Nakauchi, H. Heterogeneity and hierarchy within the most primitive hematopoietic stem cell compartment. *J. Exp. Med.* **207,** 1173–1182 (2010).

33. Ikawa, T. *et al.* Induced Developmental Arrest of Early Hematopoietic Progenitors Leads to the Generation of Leukocyte Stem Cells. *Stem Cell Reports* **5,** 716–727 (2015).

34. Fukada, T., Yamasaki, S., Nishida, K., Murakami, M. & Hirano, T. Zinc

homeostasis and signaling in health and diseases. *JBIC J. Biol. Inorg. Chem.* **16,** 1123–1134 (2011).

35. Fukada, T. & Kambe, T. Molecular and genetic features of zinc transporters in physiology and pathogenesis. *Metallomics* **3,** 662–674 (2011).

36. Kabu, K. *et al.* Zinc Is Required for Fc{epsilon}RI-Mediated Mast Cell Activation. *J. Immunol.* **177,** 1296–1305 (2006).

37. Yu, M. *et al.* Regulation of T cell receptor signaling by activation-induced zinc influx. *J. Exp. Med.* **208,** 775–785 (2011).

38. Kitamura, H. *et al.* Toll-like receptor-mediated regulation of zinc homeostasis influences dendritic cell function. *Nat. Immunol.* **7,** 971–7 (2006).

39. Shankar, A. H. & Prasad, A. S. Zinc and immune function: the biological basis of altered resistance to infection. *Am. J. Clin. Nutr.* **68,** 447S–463S (1998).

40. Fraker, P. J. & King, L. E. Reprogramming of the Immune System During Zinc Deficiency. *Annu. Rev. Nutr.* **24,** 277–298 (2004).

41. Vallee, B. L. & Falchuk, K. H. *The biochemical basis of zinc physiology. Physiological reviews* **73,** (1993).

42. Prasad, A. S. Zinc: an overview. *Nutrition* **11,** 93–9 (1995).

43. Andreini, C., Banci, L., Bertini, I. & Rosato, A. Counting the zinc-proteins encoded in the human genome. *J. Proteome Res.* **5,** 196–201 (2006).

44. Blindauer, C. a & Leszczyszyn, O. I. Metallothioneins: unparalleled diversity in structures and functions for metal ion homeostasis and more. *Nat. Prod. Rep.* **27,** 720–741 (2010).

45. Kambe, T., Hashimoto, A. & Fujimoto, S. Current understanding of ZIP and ZnT zinc transporters in human health and diseases. *Cell. Mol. Life Sci.* 3281–3295 (2014). doi:10.1007/s00018-014-1617-0

46. Küry, S. *et al.* Identification of SLC39A4, a gene involved in acrodermatitis enteropathica. *Nat. Genet.* **31,** 239–240 (2002).

47. Fukada, T. *et al. The zinc transporter SLC39A13/ZIP13 is required for connective tissue development; its involvement in BMP/TGF-beta signaling pathways. PloS one* **3,** e3642 (2008).

48. Bin, B. H. *et al.* Biochemical characterization of human ZIP13 protein: A homo-dimerized zinc transporter involved in the spondylocheiro dysplastic Ehlers-Danlos syndrome. *J. Biol. Chem.* **286,** 40255–40265 (2011).

49. Bin, B.-H. *et al.* Molecular pathogenesis of spondylocheirodysplastic Ehlers-Danlos syndrome caused by mutant ZIP13 proteins. *EMBO Mol. Med.* **6,** 1028–42 (2014).

50. Hojyo, S. *et al.* The zinc transporter SLC39A14/ZIP14 controls G-protein coupled receptor-mediated signaling required for systemic growth. *PLoS One* **6,** e18059 (2011).

51. Kim, J. H. *et al.* Regulation of the catabolic cascade in osteoarthritis by the zinc-ZIP8-MTF1 axis. *Cell* **156,** 730–743 (2014).

52. Liu, M. J. *et al.* ZIP8 Regulates Host Defense through Zinc-Mediated Inhibition of NF-κB. *Cell Rep.* **3,** 386–400 (2013).

53. Fukada, T., Hojyo, S. & Furuichi, T. Zinc signal: a new player in osteobiology. *J.*

Bone Miner. Metab. **31,** 129–35 (2013).

54. Yamashita, S. *et al.* Zinc transporter LIVI controls epithelial-mesenchymal transition in zebrafish gastrula organizer. *Nature* **429,** 298–302 (2004).

55. Rönnstrand, L. Signal transduction via the stem cell factor receptor/c-Kit. *Cell. Mol. Life Sci.* **61,** 2535–48 (2004).

56. Broudy, V. C. Stem Cell Factor and Hematopoiesis. *Blood* **90,** 1345–1364 (1997).

57. Fukada, T. *et al.* Two Signals Are Necessary for Cell Proliferation Induced by a Cytokine Receptor gp130: Involvement of STAT3 in Anti-Apoptosis. *Immunity* **5,** 449–460 (1996).

58. Bowman, T., Garcia, R., Turkson, J. & Jove, R. STATs in oncogenesis. *Oncogene* **19,** 2474–2488 (2000).

59. Bromberg, J. & Darnell, J. E. The role of STATs in transcriptional control and their impact on cellular function. *Oncogene* **19,** 2468–2473 (2000).

60. Rink, L. & Haase, H. Zinc homeostasis and immunity. *Trends Immunol.* **28,** 1–4 (2007).

61. Hirano, T. *et al.* Roles of zinc and zinc signaling in immunity: zinc as an intracellular signaling molecule. *Adv. Immunol.* **97,** 149–76 (2008).

62. Osati-Ashtiani, F., King, L. E. & Fraker, P. J. Variance in the resistance of murine early bone marrow B cells to a deficiency in zinc. *Immunology* **94,** 94–100 (1998).

63. Ibs, K.-H. & Rink, L. Zinc-altered immune function. *J. Nutr.* **133,** 1452S–6S

(2003).

64. Hojyo, S. *et al*. Zinc transporter SLC39A10/ZIP10 controls humoral immunity by modulating B-cell receptor signal strength. *Proc. Natl. Acad. Sci. U. S. A.* **111,** 11786–11791 (2014).

65. Nagata, S. Apoptosis by death factor. *Cell* **88,** 355–365 (1997).

66. Perry, D. K. *et al*. Zinc is a potent inhibitor of the apoptotic protease, caspase-3. A novel target for zinc in the inhibition of apoptosis. *J. Biol. Chem.* **272,** 18530–3 (1997).

67. Peterson, Q. P. *et al*. PAC-1 Activates Procaspase-3 in Vitro through Relief of Zinc-Mediated Inhibition. *J. Mol. Biol.* **388,** 144–158 (2009).

68. Schrantz, N. *et al*. Zinc-mediated regulation of caspases activity: dose-dependent inhibition or activation of caspase-3 in the human Burkitt lymphoma B cells (Ramos). *Cell Death Differ.* **8,** 152–61 (2001).

69. Stennicke, H. R. & Salvesen, G. S. Biochemical characteristics of caspases-3, -6, -7, and -8. *J. Biol. Chem.* **272,** 25719–23 (1997).

70. Huber, K. L. & Hardy, J. A. Mechanism of zinc-mediated inhibition of caspase-9. *Protein Sci.* **21,** 1056–65 (2012).

71. Velázquez-Delgado, E. M. & Hardy, J. a. Zinc-mediated allosteric inhibition of caspase-6. *J. Biol. Chem.* **287,** 36000–36011 (2012).

72. Haase, H. & Rink, L. Functional significance of zinc-related signaling pathways in immune cells. *Annu. Rev. Nutr.* **29,** 133–152 (2009).

73. Meng, T. C., Fukada, T. & Tonks, N. K. Reversible oxidation and inactivation of

protein tyrosine phosphatases in vivo. *Mol. Cell* **9,** 387–399 (2002).

74. Wilson, M., Hogstrand, C. & Maret, W. Picomolar concentrations of free zinc(II) ions regulate receptor protein-tyrosine phosphatase β activity. *J. Biol. Chem.* **287,** 9322–9326 (2012).

75. Maret, W. Molecular aspects of human cellular zinc homeostasis: Redox control of zinc potentials and zinc signals. *BioMetals* **22,** 149–157 (2009).

76. Van Wart, H. E. & Birkedal-Hansen, H. The cysteine switch: a principle of regulation of metalloproteinase activity with potential applicability to the entire matrix metalloproteinase gene family. *Proc. Natl. Acad. Sci. U. S. A.* **87,** 5578–82 (1990).

77. Pabo, C. O. & Sauer, R. T. Transcription factors: structural families and principles of DNA recognition. *Annu. Rev. Biochem.* **61,** 1053–1095 (1992).

78. Rebollo, A. & Schmitt, C. Ikaros, Aiolos and Helios: transcription regulators and lymphoid malignancies. *Immunol. Cell Biol.* **81,** 171–5 (2003).

79. Joshi, I. *et al.* Loss of Ikaros DNA-binding function confers integrin-dependent survival on pre-B cells and progression to acute lymphoblastic leukemia. *Nat. Immunol.* **15,** 294–304 (2014).

80. Fukada, T. *et al.* Signaling through Gp130: toward a general scenario of cytokine action. *Growth Factors* **17,** 81–91 (1999).

81. Hirano, T., Ishihara, K. & Hibi, M. Roles of STAT3 in mediating the cell growth, differentiation and survival signals relayed through the IL-6 family of cytokine receptors. *Oncogene* **19,** 2548–2556 (2000).

82. Dumon, S. *et al*. IL-3 dependent regulation of Bcl-xL gene expression by STAT5 in a bone marrow derived cell line. *Oncogene* **18,** 4191–4199 (1999).

83. Shirogane, T. *et al*. Synergistic roles for Pim-1 and c-Myc in STAT3-mediated cell cycle progression and antiapoptosis. *Immunity* **11,** 709–719 (1999).

84. Silva, M. *et al*. Erythropoietin can induce the expression of Bcl-x(L) through Stat5 in erythropoietin-dependent progenitor cell lines. *J. Biol. Chem.* **274,** 22165–22169 (1999).

85. Meffre, E., Casellas, R. & Nussenzweig, M. C. Antibody regulation of B cell development. *Nat. Immunol.* **1,** 379–385 (2000).

86. Melchers, F. Checkpoints that control B cell development. **125,** 1–8 (2015).

87. Melchers, F. The pre-B-cell receptor: selector of fitting immunoglobulin heavy chains for the B-cell repertoire. *Nat. Rev. Immunol.* **5,** 578–584 (2005).

88. Keenan, R. a *et al*. Censoring of autoreactive B cell development by the pre-B cell receptor. *Science (80-.).* **321,** 696–699 (2008).

89. Rolink, A. G., Andersson, J. & Melchers, F. Characterization of immature B cells by a novel monoclonal antibody, by turnover and by mitogen reactivity. *Eur. J. Immunol.* **28,** 3738–3748 (1998).

90. Cohen, J. J., Duke, R. C., Fadok, V. a & Sellins, K. S. Apoptosis and programmed cell death in immunity. *Annu. Rev. Immunol.* **10,** 267–93 (1992).

91. Kagara, N., Tanaka, N., Noguchi, S. & Hirano, T. Zinc and its transporter ZIP10 are involved in invasive behavior of breast cancer cells. *Cancer Sci.* **98,** 692–7 (2007).

92. Kohlmann, A. *et al*. An international standardization programme towards the application of gene expression profiling in routine leukaemia diagnostics: The Microarray Innovations in LEukemia study prephase. *Br. J. Haematol*. **142,** 802–807 (2008).

93. Kridel, R., Sehn, L. H. & Gascoyne, R. D. Pathogenesis of follicular lymphoma. *J. Clin. Invest*. **122,** 3424–31 (2012).

94. Nutt, S. L. & Kee, B. L. The transcriptional regulation of B cell lineage commitment. *Immunity* **26,** 715–25 (2007).

95. Vilagos, B. *et al*. Essential role of EBF1 in the generation and function of distinct mature B cell types. *J. Exp. Med*. **209,** 775–792 (2012).

96. Revilla-i-Domingo, R. *et al*. The B-cell identity factor Pax5 regulates distinct transcriptional programmes in early and late B lymphopoiesis. *EMBO J*. **31,** 3130–3146 (2012).

97. Schwickert, T. a *et al*. Stage-specific control of early B cell development by the transcription factor Ikaros. *Nat. Immunol*. **15,** 283–93 (2014).

98. Massari, M. E. & Murre, C. Helix-loop-helix proteins: regulators of transcription in eucaryotic organisms. *Mol. Cell. Biol*. **20,** 429–440 (2000).

99. Engel, I. & Murre, C. The function of E- and Id proteins in lymphocyte development. *Nat. Rev. Immunol*. **1,** 193–199 (2001).

100. Mansson, R. *et al*. Positive intergenic feedback circuitry, involving EBF1 and FOXO1, orchestrates B-cell fate. *Proc. Natl. Acad. Sci. U. S. A*. **109,** 21028–33 (2012).

101. Welinder, E. *et al*. The transcription factors E2A and HEB act in concert to induce the expression of FOXO1 in the common lymphoid progenitor. *Proc. Natl. Acad. Sci.* **108,** 17402–17407 (2011).

102. Lukin, K. *et al*. Compound haploinsufficiencies of Ebf1 and Runx1 genes impede B cell lineage progression. *Proc. Natl. Acad. Sci. U. S. A.* **107,** 7869–74 (2010).

103. O'Riordan, M. & Grosschedl, R. Coordinate regulation of B cell differentiation by the transcription factors EBF and E2A. *Immunity* **11,** 21–31 (1999).

104. Sigvardsson, M., O'Riordan, M. & Grosschedl, R. EBF and E47 collaborate to induce expression of the endogenous immunoglobulin surrogate light chain genes. *Immunity* **7,** 25–36 (1997).

105. Decker, T. *et al*. Stepwise activation of enhancer and promoter regions of the B cell commitment gene Pax5 in early lymphopoiesis. *Immunity* **30,** 508–20 (2009).

106. Ng, S. Y. M., Yoshida, T., Zhang, J. & Georgopoulos, K. Genome-wide Lineage-Specific Transcriptional Networks Underscore Ikaros-Dependent Lymphoid Priming in Hematopoietic Stem Cells. *Immunity* **30,** 493–507 (2009).

107. Liu, P. *et al*. Bcl11a is essential for normal lymphoid development. *Nat. Immunol.* **4,** 525–532 (2003).

108. Yu, Y. *et al*. Bcl11a is essential for lymphoid development and negatively regulates p53. *J. Exp. Med.* **209,** 2467–83 (2012).

109. Fahl, S. P., Crittenden, R. B., Allman, D. & Bender, T. P. c-Myb is required for pro-B cell differentiation. *J. Immunol.* **183,** 5582–92 (2009).

110. Greig, K. T., Carotta, S. & Nutt, S. L. Critical roles for c-Myb in hematopoietic

progenitor cells. *Semin. Immunol.* **20,** 247–256 (2008).

111. Spooner, C. J., Cheng, J. X., Pujadas, E., Laslo, P. & Singh, H. A Recurrent Network Involving the Transcription Factors PU.1 and Gfi1 Orchestrates Innate and Adaptive Immune Cell Fates. *Immunity* **31,** 576–586 (2009).

112. Li, H., Ji, M., Klarmann, K. D. & Keller, J. R. Repression of Id2 expression by Gfi-1 is required for B-cell and myeloid development. *Blood* **116,** 1060–1069 (2010).

113. Motomura, Y. *et al.* The transcription factor E4BP4 regulates the production of IL-10 and IL-13 in CD4+ T cells. *Nat. Immunol.* **12,** 450–459 (2011).

114. Geiger, T. L. *et al.* Nfil3 is crucial for development of innate lymphoid cells and host protection against intestinal pathogens. *J. Exp. Med.* **211,** 1723–1731 (2014).

115. Seillet, C. *et al.* Nfil3 is required for the development of all innate lymphoid cell subsets. *J. Exp. Med.* **211,** jem.20140145– (2014).

116. Ikawa, T., Kawamoto, H., Wright, L. Y. T. & Murre, C. Long-Term Cultured E2A-Deficient Hematopoietic Progenitor Cells Are Pluripotent. *Immunity* **20,** 349–360 (2004).

117. Kashiwada, M., Pham, N. L., Pewe, L. L., Harty, J. T. & Rothman, P. B. NFIL3/E4BP4 is a key transcription factor for CD8alpha(+) dendritic cell development. *Blood* **117,** 6193–6197 (2011).

118. Sanulli, S. *et al.* Jarid2 Methylation via the PRC2 Complex Regulates H3K27me3 Deposition during Cell Differentiation. *Mol. Cell* **57,** 769–783 (2015).

119. Su, I.-H. *et al*. Ezh2 controls B cell development through histone H3 methylation and Igh rearrangement. *Nat. Immunol*. **4,** 124–131 (2003).

120. Jiang, X.-X. *et al*. Control of B cell development by the histone H2A deubiquitinase MYSM1. *Immunity* **35,** 883–96 (2011).

121. Bossen, C. *et al*. The chromatin remodeler Brg1 activates enhancer repertoires to establish B cell identity and modulate cell growth. *Nat. Immunol*. **16,** 775–784 (2015).

122. Guo, C. *et al*. CTCF-binding elements mediate control of V(D)J recombination. *Nature* **477,** 424–430 (2011).

123. Okuno, H. Regulation and function of immediate-early genes in the brain: Beyond neuronal activity markers. *Neurosci. Res*. **69,** 175–186 (2011).

124. Watson, R. J. & Clements, J. B. A herpes simplex virus type 1 function continuously required for early and late virus RNA synthesis. *Nature* **285,** 329–330 (1980).

125. Kelly, K., Cochran, B. H., Stiles, C. D. & Leder, P. Cell-specific regulation of the c-myc gene by lymphocyte mitogens and platelet-derived growth factor. *Cell* **35,** 603–10 (1983).

126. Greenberg, M. E. & Ziff, E. B. Stimulation of 3T3 cells induces transcription of the c-fos proto-oncogene. *Nature* **311,** 433–438 (1984).

127. Almendral, J. M. *et al*. Complexity of the early genetic response to growth factors in mouse fibroblasts. *Mol. Cell. Biol*. **8,** 2140–2148 (1988).

128. Muse, G. W. *et al*. RNA polymerase is poised for activation across the genome.

Nat. Genet. **39,** 1507–11 (2007).

129. Zeitlinger, J. *et al.* RNA polymerase stalling at developmental control genes in the Drosophila melanogaster embryo. *Nat. Genet.* **39,** 1512–6 (2007).

130. Margaritis, T. & Holstege, F. C. P. Poised RNA Polymerase II Gives Pause for Thought. *Cell* **133,** 581–584 (2008).

131. Gaertner, B. *et al.* Poised RNA Polymerase II Changes over Developmental Time and Prepares Genes for Future Expression. *Cell Rep.* **2,** 1670–1683 (2012).

132. Tullai, J. W. *et al.* Immediate-early and delayed primary response genes are distinct in function and genomic architecture. *J. Biol. Chem.* **282,** 23981–95 (2007).

133. Wang, Z. Q. *et al.* Bone and haematopoietic defects in mice lacking c-fos. *Nature* **360,** 741–745 (1992).

134. Fujita, K. *et al.* B cell development is perturbed in bone marrow from c-fos/v-jun doubly transgenic mice. *Int. Immunol.* **5,** 227–30 (1993).

135. Hu, L., Hatano, M., Rüther, U. & Tokuhisa, T. Overexpression of c-Fos induces apoptosis of CD43+ pro-B cells. *J. Immunol.* **157,** 3804–11 (1996).

136. Gururajan, M. *et al.* Early growth response genes regulate B cell development, proliferation, and immune response. *J. Immunol.* **181,** 4590–602 (2008).

137. Li, S. *et al.* Early growth response gene-2 (egr-2) regulates the development of b and t cells. *PLoS One* **6,** 1–9 (2011).

138. Yosef, N. *et al.* Dynamic regulatory network controlling TH17 cell differentiation. *Nature* **496,** 461–8 (2013).

139. Okuyama, K. *et al*. MicroRNA-126-mediated control of cell fate in B-cell myeloid progenitors as a potential alternative to transcriptional factors. *Proc. Natl. Acad. Sci. U. S. A.* **110,** 13410–5 (2013).

140. Mehta, A. *et al*. The microRNA-212 / 132 cluster regulates B cell development by targeting Sox4. **212,** 1679–1692 (2015).

141. Li, J., Wan, Y., Ji, Q., Fang, Y. & Wu, Y. The role of microRNAs in B-cell development and function. *Cell. Mol. Immunol.* **10,** 107–112 (2013).

142. Petri, A. *et al*. Long Noncoding RNA Expression during Human B-Cell Development. *PLoS One* **10,** e0138236 (2015).

143. Casero, D. *et al*. Long non-coding RNA profiling of human lymphoid progenitor cells reveals transcriptional divergence of B cell and T cell lineages. *Nat. Immunol.* **16,** (2015).

144. Fatica, A. & Bozzoni, I. Long non-coding RNAs: new players in cell differentiation and development. *Nat. Rev. Genet.* **15,** 7–21 (2014).

145. Pott, S. & Lieb, J. D. What are super-enhancers? *Nat. Publ. Gr.* **47,** 8–12 (2015).

146. Whyte, W. A. *et al*. Master transcription factors and mediator establish super-enhancers at key cell identity genes. *Cell* **153,** 307–319 (2013).

147. Adam, R. C. *et al*. Pioneer factors govern super-enhancer dynamics in stem cell plasticity and lineage choice. *Nature* **521,** 366–70 (2015).

148. Vizcardo, R. *et al*. Regeneration of human tumor antigen-specific T cells from iPSCs derived from mature CD8+ T cells. *Cell Stem Cell* **12,** 31–36 (2013).

149. Watarai, H. *et al*. Murine induced pluripotent stem cells can be derived from and

differentiate into natural killer T cells. *J. Clin. Invest.* **120,** 2610–8 (2010).

150. Nishimura, T. *et al*. Generation of rejuvenated antigen-specific T cells by reprogramming to pluripotency and redifferentiation. *Cell Stem Cell* **12,** 114–126 (2013).

151. Tabar, V. & Studer, L. Pluripotent stem cells in regenerative medicine: challenges and recent progress. *Nat. Rev. Genet.* **15,** 82–92 (2014).

152. Agata, Y. *et al*. Histone acetylation determines the developmentally regulated accessibility for T cell receptor gamma gene recombination. *J. Exp. Med.* **193,** 873–880 (2001).

153. Kim, D. *et al*. TopHat2: accurate alignment of transcriptomes in the presence of insertions, deletions and gene fusions. *Genome Biol.* **14,** R36 (2013).

154. Trapnell, C. *et al*. Transcript assembly and quantification by RNA-Seq reveals unannotated transcripts and isoform switching during cell differentiation. *Nat. Biotechnol.* **28,** 511–515 (2010).

155. Trapnell, C. *et al*. Differential analysis of gene regulation at transcript resolution with RNA-seq. *Nat. Biotechnol.* **31,** 46–53 (2013).

156. Love, M. I., Huber, W. & Anders, S. Moderated estimation of fold change and dispersion for RNA-seq data with DESeq2. *Genome Biol.* **15,** 550 (2014).

157. Liao, Y., Smyth, G. K. & Shi, W. FeatureCounts: An efficient general purpose program for assigning sequence reads to genomic features. *Bioinformatics* **30,** 923–930 (2014).

158. Kou, Y. *et al*. ChEA2: Gene-set libraries from ChIP-X experiments to decode the

transcription regulome. *Lect. Notes Comput. Sci. (including Subser. Lect. Notes Artif. Intell. Lect. Notes Bioinformatics)* **8127 LNCS,** 416–430 (2013).

159. Shannon, P. *et al*. Cytoscape: a software environment for integrated models of biomolecular interaction networks. *Genome Res*. **13,** 2498–504 (2003).

160. Snel, B., Lehmann, G., Bork, P. & Huynen, M. a. STRING: a web-server to retrieve and display the repeatedly occurring neighbourhood of a gene. *Nucleic Acids Res*. **28,** 3442–3444 (2000).

FIGURES

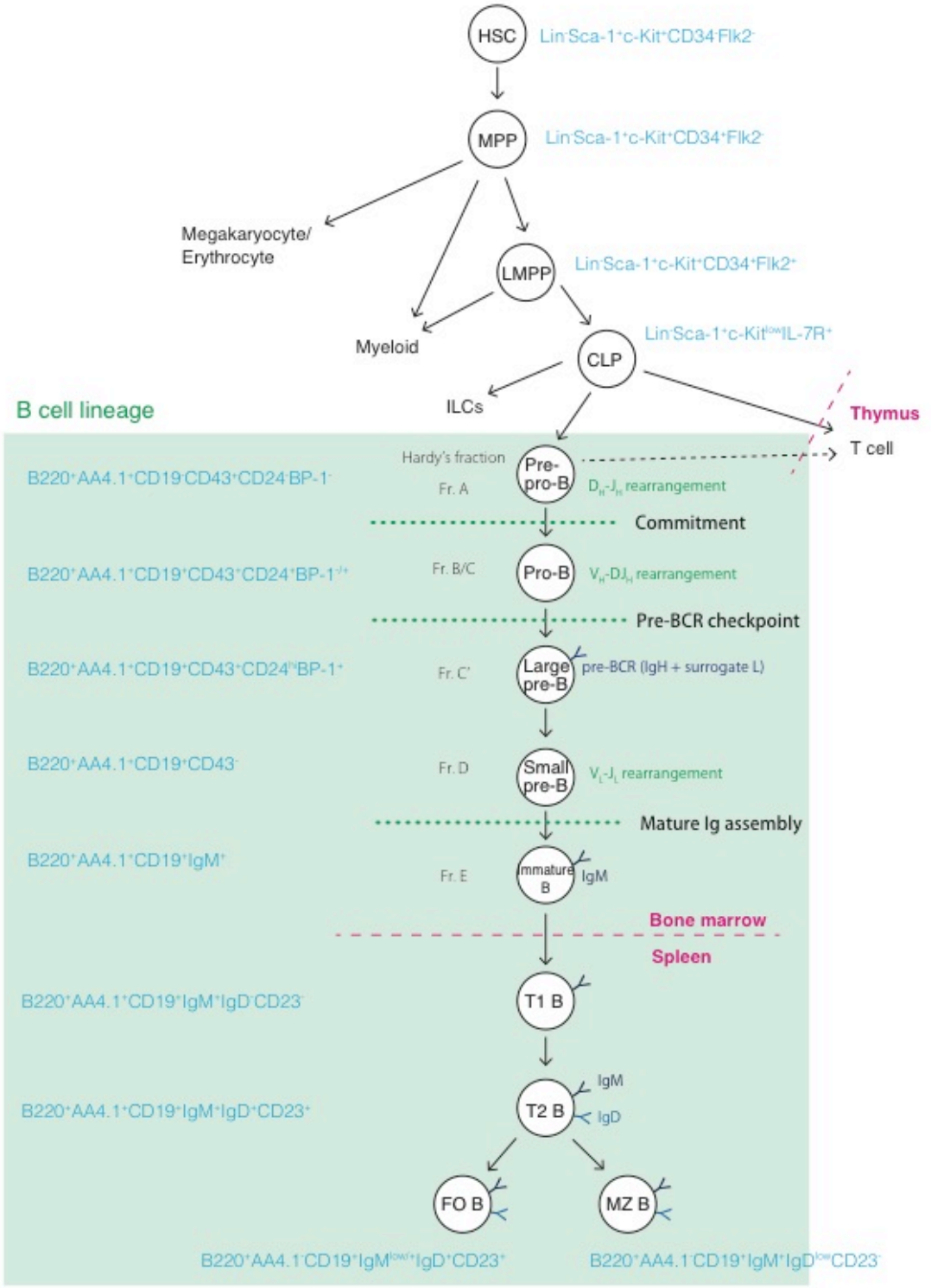

Figure G-1. Development of B lineage cells from HSC.

A model of B cell developmental process is shown. Cell surface markers of individual subpopulations are shown in blue and the place of differentiation is shown in magenta, respectively.

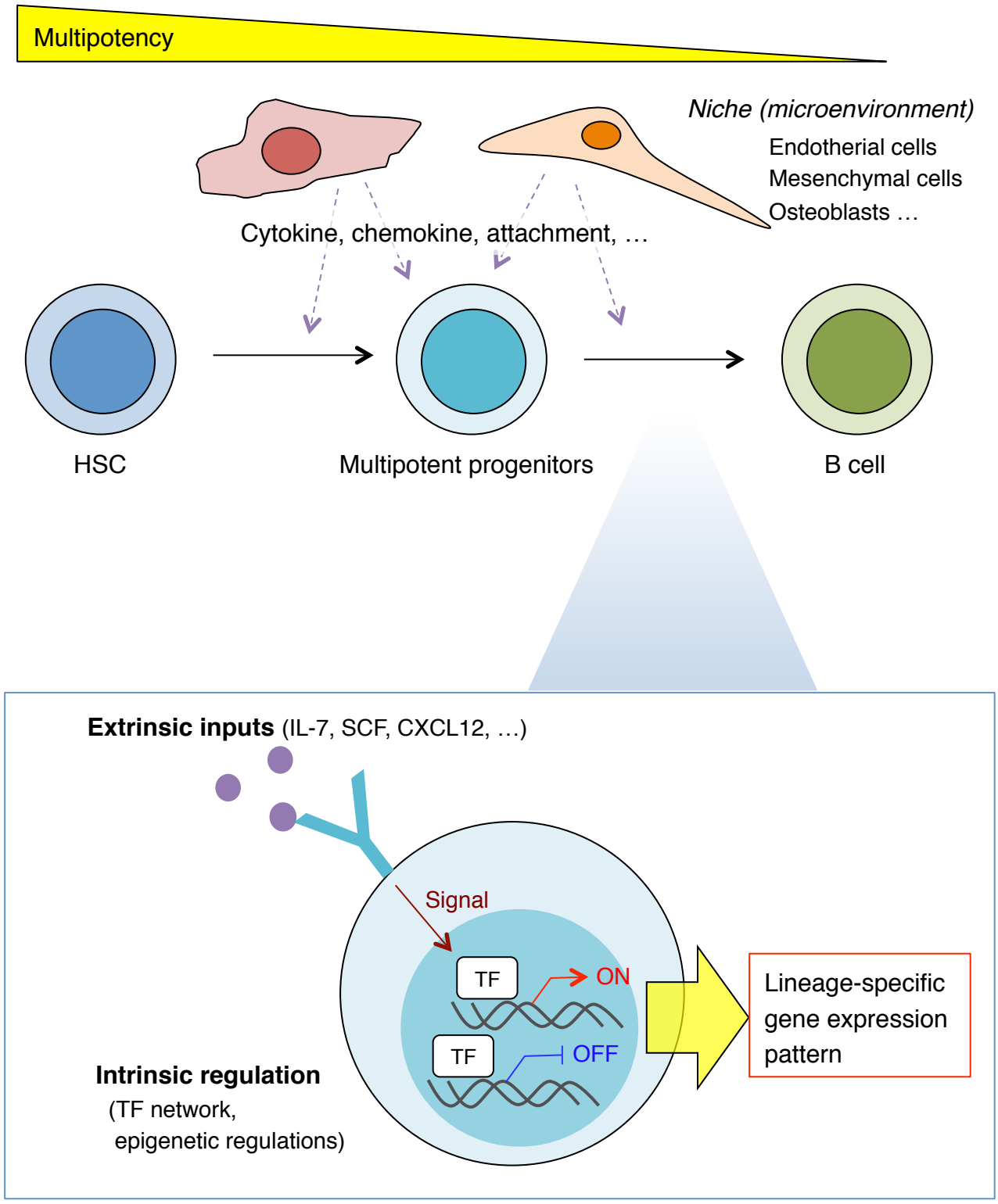

Figure G-2. Outline of the intrinsic and extrinsic regulations during B cell fate decision process.

During B lineage differentiation process, progenitors receive a multiple signals from environment called niche , and lineage specific gene programs are gradually induced by TF networks and epigenetic regulations. Finally, uncommitted progenitors determine their fates into B cell lineage.

A

Tissue	Zinc concentrate (μg/g wet weight)	% of total body zinc (%)
Skeletal muscle	51	57
Bone	100	29
Skin	32	6
Liver	58	5
Brain	11	1.5
Kidney	55	0.7
Heart	23	0.4
Hair	150	~ 0.1
Blood plasma	1	~ 0.1

C

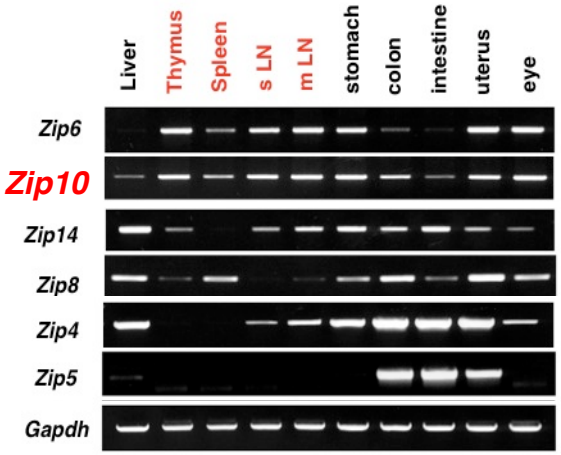

B

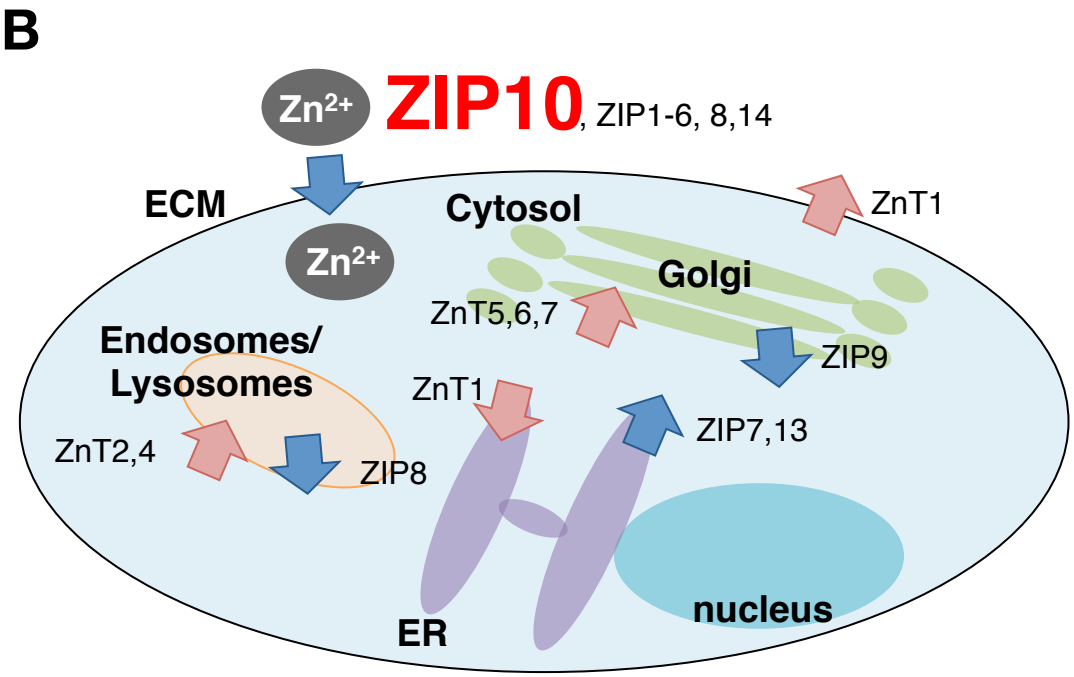

Figure G-3. Zinc and its transporters – What is the function of ZIP10 in B cell development?

A. Distribution of zinc within the body (in 70 kg adult man, adapted from King et al., 2000.).

B. Cellular localization of zinc transporters. Blue and red arrows represent ZIP and ZnT transporters, respectively. ECM, extracellular matrix; Golgi, Golgi apparatus; ER, endoplasmic reticulum.

C. mRNA expression of surface-localized ZIP transporters in the cells among various tissues.

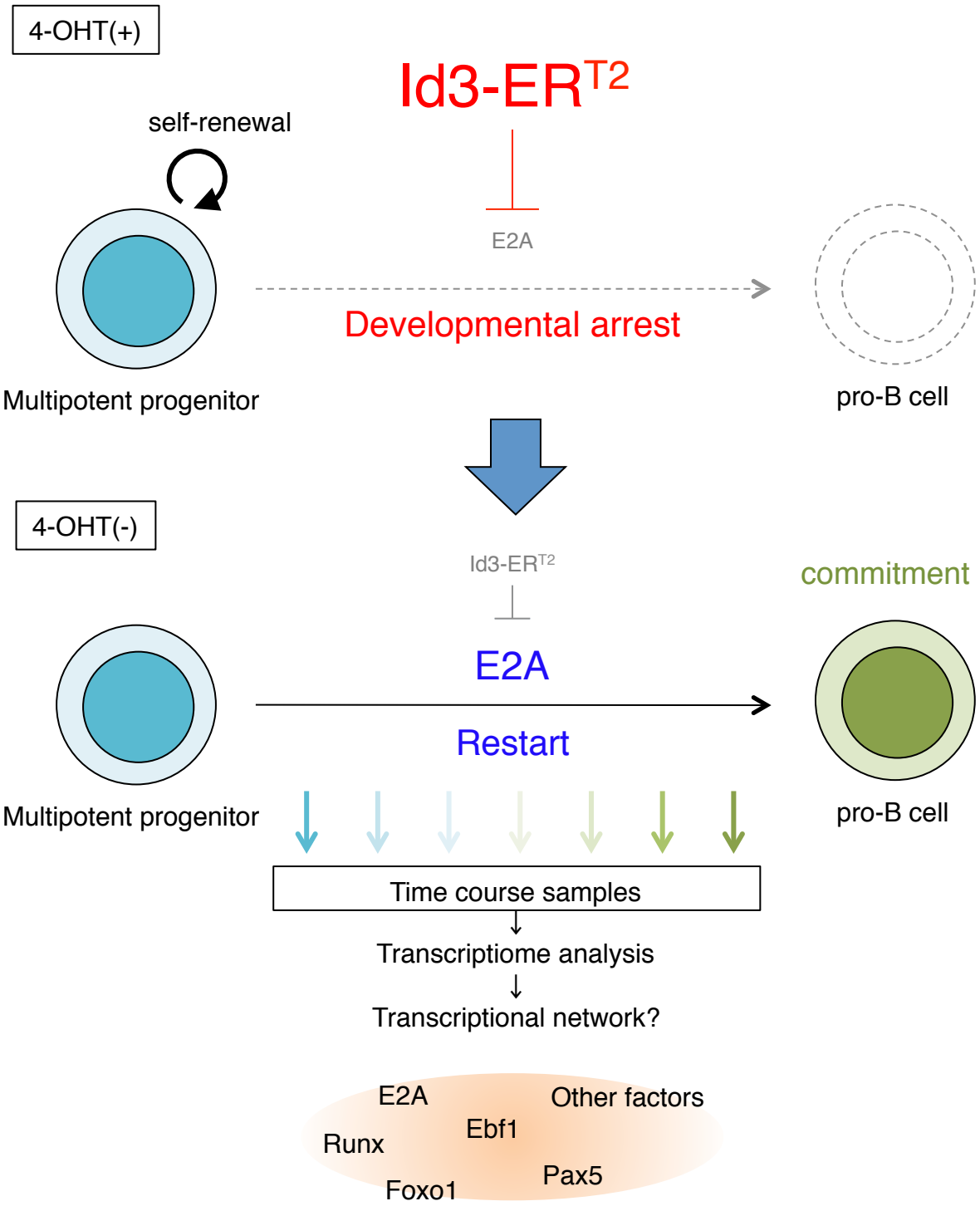

Figure G-4. Strategy of arrest/restart control of B cell differentiation by inducible overexpression of Id3.

We have recently reported the self-renewing multipotent progenitors by ectopic expression of Id3 in HSPCs (Ikawa et al. 2015). In this study, I established the inducible multipotent progenitors by introducing Id3-ERT2 into HSPCs to control the progression of B cell differentiation in a 4-OHT-dependent manner . Using this system, I collected a series of time course samples and performed transcriptome analysis to reveal the TF networks during B cell fate determination.

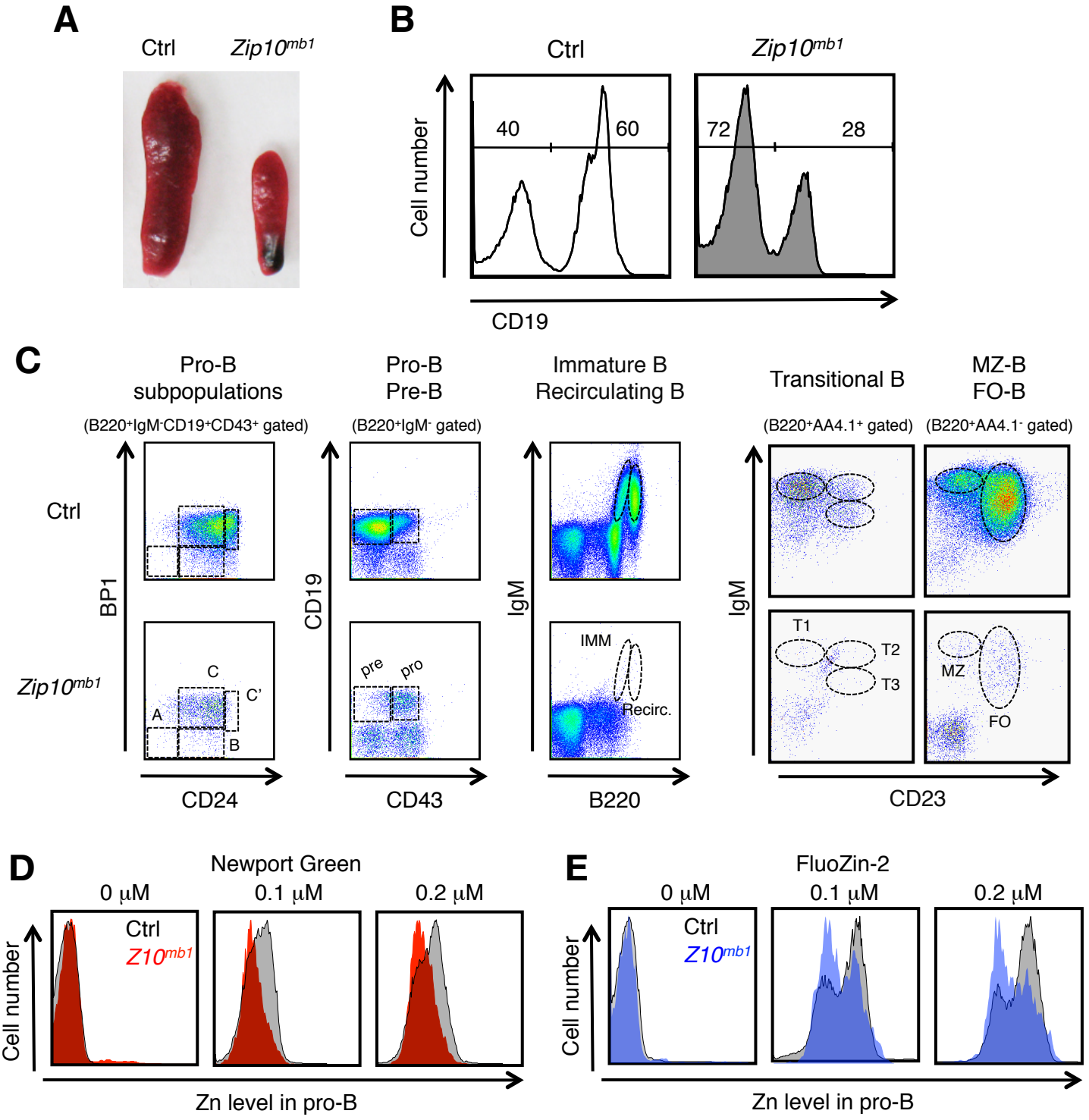

Figure 1-1. *Zip10*^{mb1} mice showed a dramatic loss of B lymphocytes.

A. Representative image of spleen in control (Ctrl) and *Zip10*^{mb1} mice.

B. Flow cytometric analysis of splenocytes in Ctrl and *Zip10*^{mb1} mice.

C. Flow cytometric profiles of B-cell subsets in BM (pro-, pre-, immature and recirculating B) and spleen (transitional, MZ and FO B) of Ctrl and *Zip10*^{mb1} mice are shown. MZ: marginal zone; FO: follicular.

D and E. Flow cytometric profiles of intracellular Zn^{2+} level in pro B cells assessed by Newport Green (**D**) or FluoZin-2 (**E**) zinc indicators are shown. Grey and red or blue histograms are represents the Zn level in Ctrl and *Zip10*^{mb1}, respectively.

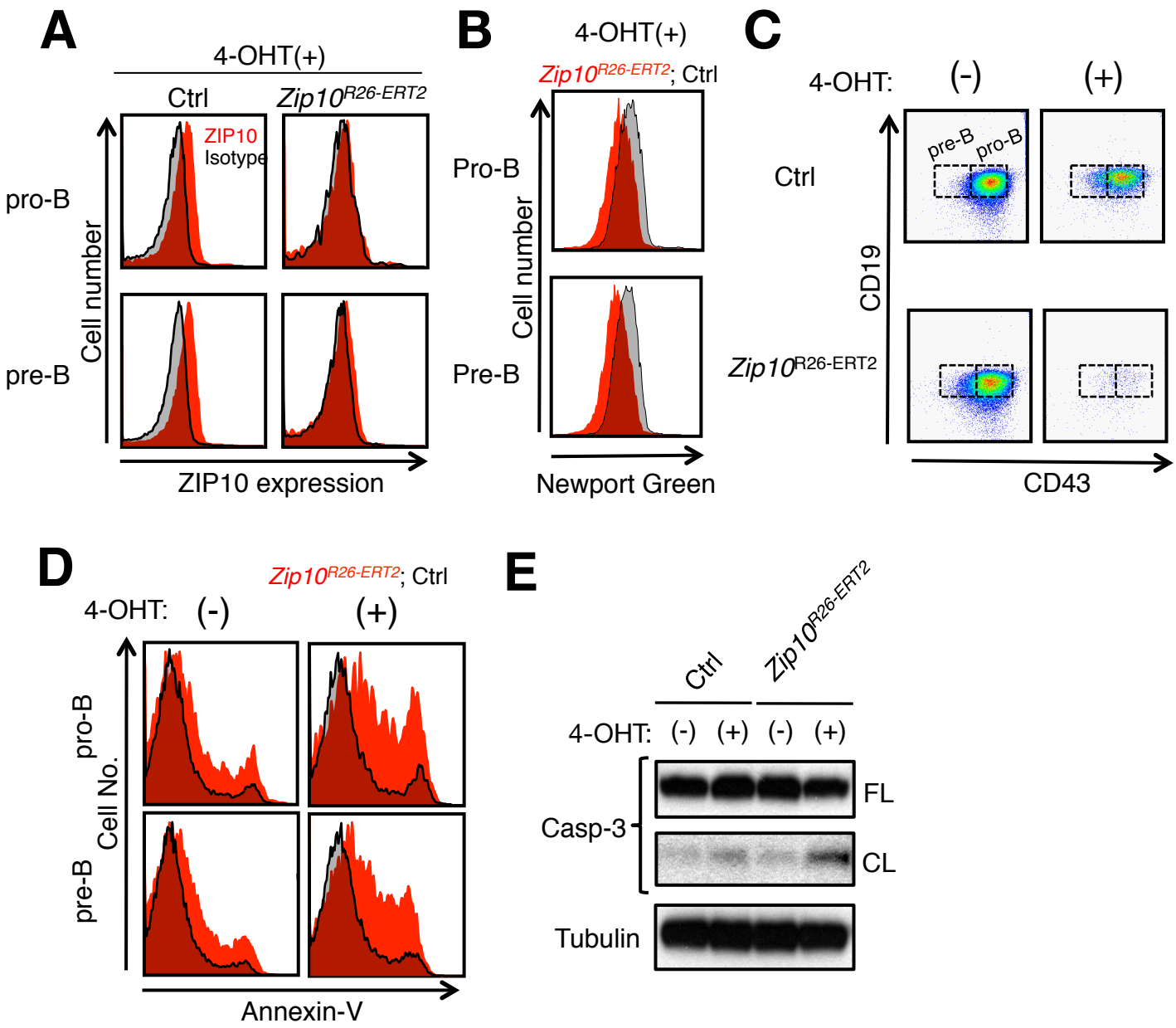

Figure 1-2. Inducible deletion of ZIP10 triggers caspase-dependent apoptosis in B cell progenitors.

A-D. Flow cytometric profiles of surface ZIP10 protein expression (**A**), intracellular Zn^{2+} level (stained by 0.1 μM Newport Green) (**B**), B cell progenitor populations (**C**), and annexin-V staining (**D**) in pro-B and pre-B cells in BM from Ctrl or *Zip10*$^{R26\text{-}ERT2}$ mice after 4-OHT treatment.

E. Western blot of caspase-3 in cultured B cell progenitors after 4-OHT treatment. Tubulin is shown as a loading control.

Ctrl: control; *Zip10*$^{R26\text{-}ERT2}$: *Zip10*$^{flox/flox}$::*Rosa26-Cre-ER*^{T2}; Casp-3: caspase-3; FL: full-length; CL: cleaved.

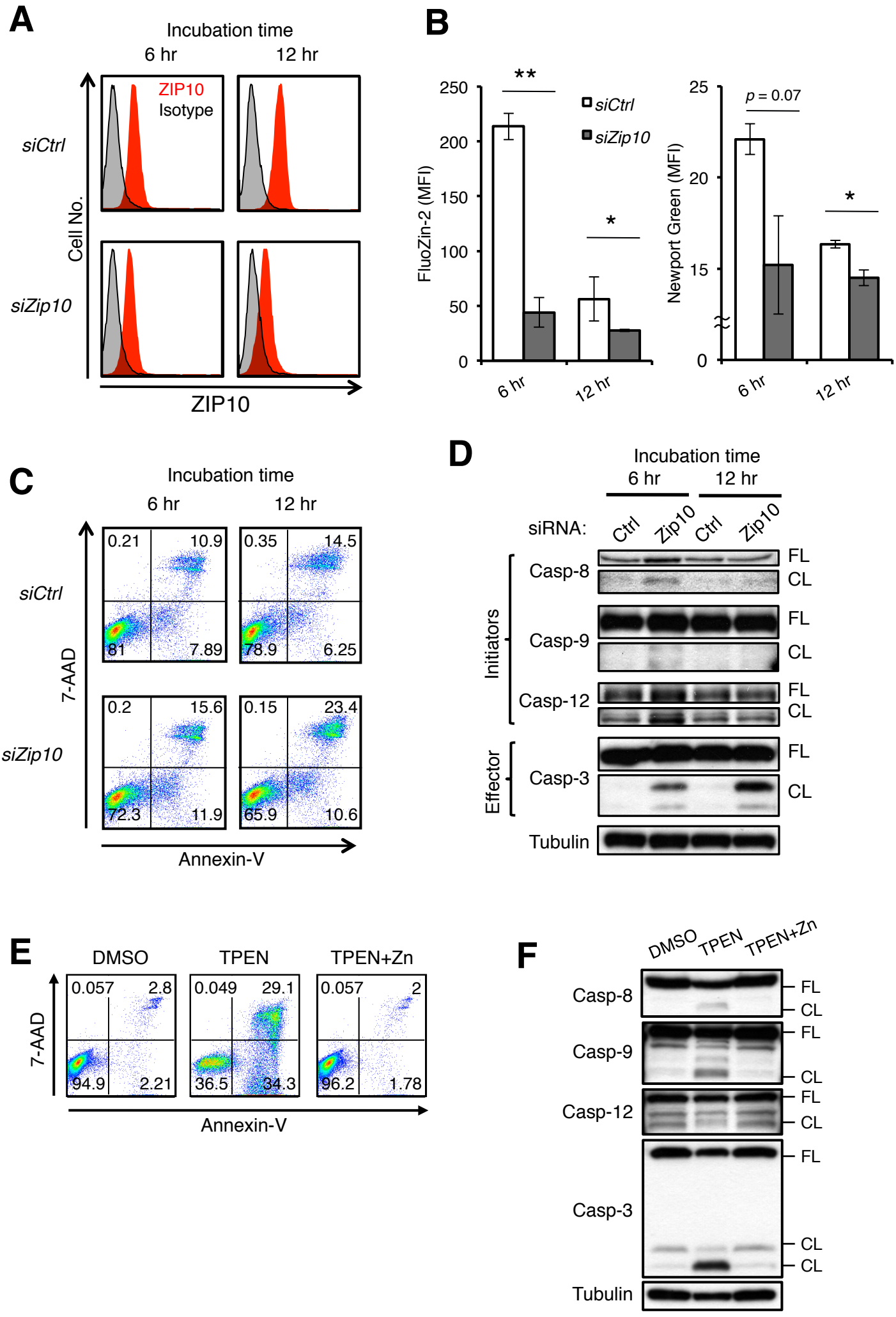
A
Incubation time
6 hr
12 hr
ZIP10
Isotype
siCtrl
siZip10
Cell No.
ZIP10
B
**
*
siCtrl
siZip10
FluoZin-2 (MFI)
250
200
150
100
50
0
6 hr
12 hr
p = 0.07
*
Newport Green (MFI)
25
20
15
0
6 hr
12 hr
C
Incubation time
6 hr
12 hr
siCtrl
siZip10
7-AAD
0.21
10.9
81
7.89
0.35
14.5
78.9
6.25
0.2
15.6
72.3
11.9
0.15
23.4
65.9
10.6
Annexin-V
D
Incubation time
6 hr
12 hr
siRNA:
Ctrl
Zip10
Ctrl
Zip10
Initiators
Effector
Casp-8
Casp-9
Casp-12
Casp-3
Tubulin
FL
CL
E
DMSO
TPEN
TPEN+Zn
7-AAD
0.057
2.8
94.9
2.21
0.049
29.1
36.5
34.3
0.057
2
96.2
1.78
Annexin-V
F
DMSO
TPEN
TPEN+Zn
Casp-8
Casp-9
Casp-12
Casp-3
Tubulin
FL
CL

Figure 1-3. ZIP10 specifically modulates enzymatic activity of caspases in a zinc-dependent manner.

A. Surface ZIP10 protein level in *Zip10*-KD BAF-B03 cells.

B. Intracellular Zn^{2+} level in *Zip10*-KD BAF-B03 cells stained by 0.1 μM FluoZin-2 (*left*) or 0.1 μM Newport Green (*right*) Zn indicators.

C. Annexin-V/7-AAD staining in *Zip10*-KD BAF-B03 cells.

D. Activation of various caspases in *Zip10*-KD BAF-B03 cells. Tubulin is shown as a loading control.

E. Annexin-V/7-AAD staining in Baf-B03 cells with treatment of DMSO (as control), TPEN and combination of TPEN and $ZnSO_4$.

F. Activation of various caspases in BAF-B03 cells by treatment of DMSO (as control), TPEN and combination of TPEN and $ZnSO_4$. Tubulin is shown as loading control.

siCtrl: scrambled non-targeting siRNA; *siZip10*: Zip10-targeting siRNA; MFI: mean fluorescence intensity; Casp: caspase; FL: full length; CL: cleaved. Values represent means ± S.D of three independent experiments. * $P < 0.05$; ** $P < 0.01$.

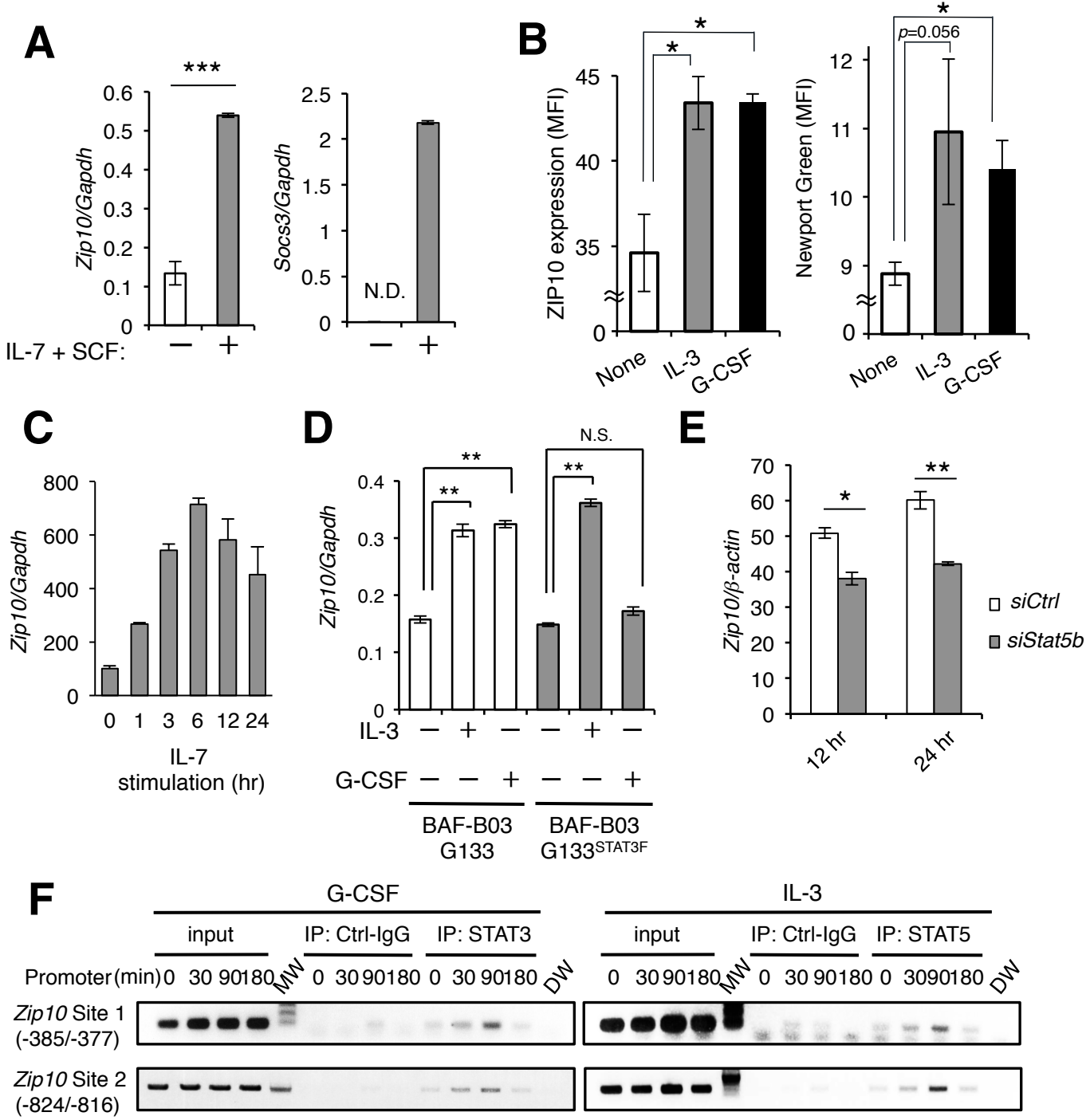

Figure 1-4. JAK-STAT-mediated cytokine signaling pathway regulates *Zip10* expression.

A. *Zip10* (*left*) and *Socs3* (*right*) expression levels in normal pro-B cells after stimulation by IL-7+SCF for 3 h.

B: Surface ZIP10 expression (*left*) and intracellular Zn^{2+} levels (*right*, stained by 0.1 μM Newport Green) in BAF- B03 G133 cells after stimulation by IL-3 or G-CSF for 12 h.

C: *Zip10* expression levels in pre-B cell line 2E8 after IL-7 stimulation.

D. *Zip10* expression levels in STAT3-mutated BAF-B03 cells.

E. *Zip10* expression levels in *Stat5*-KD BAF-B03 cells.

F. ChIP assay for STAT3 (*left*) or STAT5 (*right*) binding to putative binding sites of *Zip10* locus in BAF-B03 cells under cytokine stimulation.

N.D.: not detected; MFI: mean fluorescence intensity; N.S.: no significance; *siCtrl*: scrambled non-targeting siRNA; *siStat5b*: Stat5b-targeting siRNA. Values represent means ± S.D of three independent experiments. * $P < 0.05$; ** $P < 0.01$; *** $P < 0.001$.

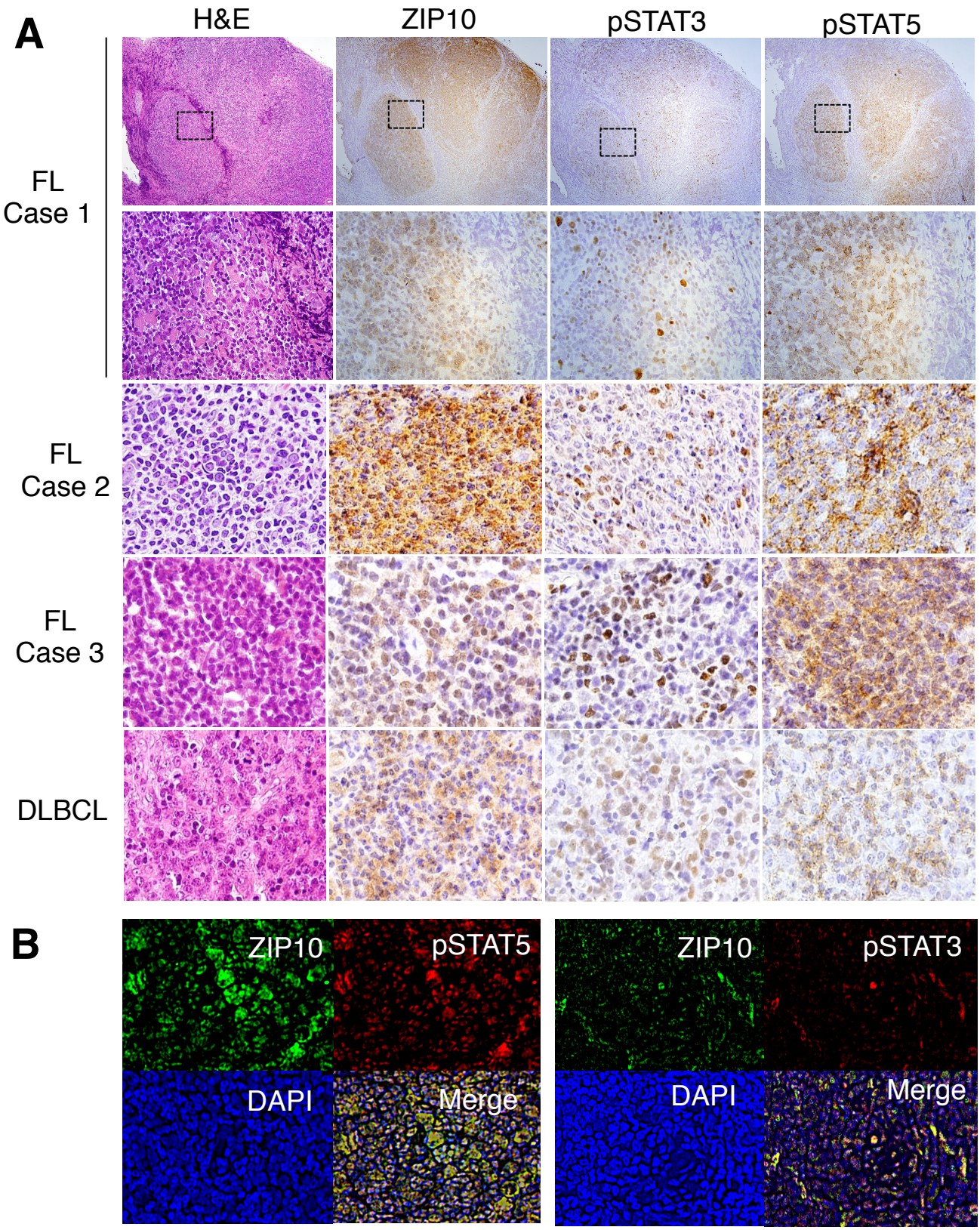

Fig 1-5. Co-localization of ZIP10 and phosphorylated STAT proteins in human B cell lymphoma.

A. Human follicular lymphoma sample (3 cases of follicular lymphoma (FL) and 1 case of diffuse large B-cell lymphoma(DLBCL)) isolated from salivary glands is staind by Hematoxylin & eosin (H&E) and immunohistochemistry for ZIP10, phospho-STAT3 (pSTAT3) and phospho-STAT5 (pSTAT5). In the FL case 1, magnifications of images are 40x (*upper*) and 400x (*lower*), respectively. In other cases, magnifications of images are 400x.

B. Immunofluorescence for ZIP10, pSTAT3 and pSTAT5 using human follicular lymphoma. Magnification of image is 600x.

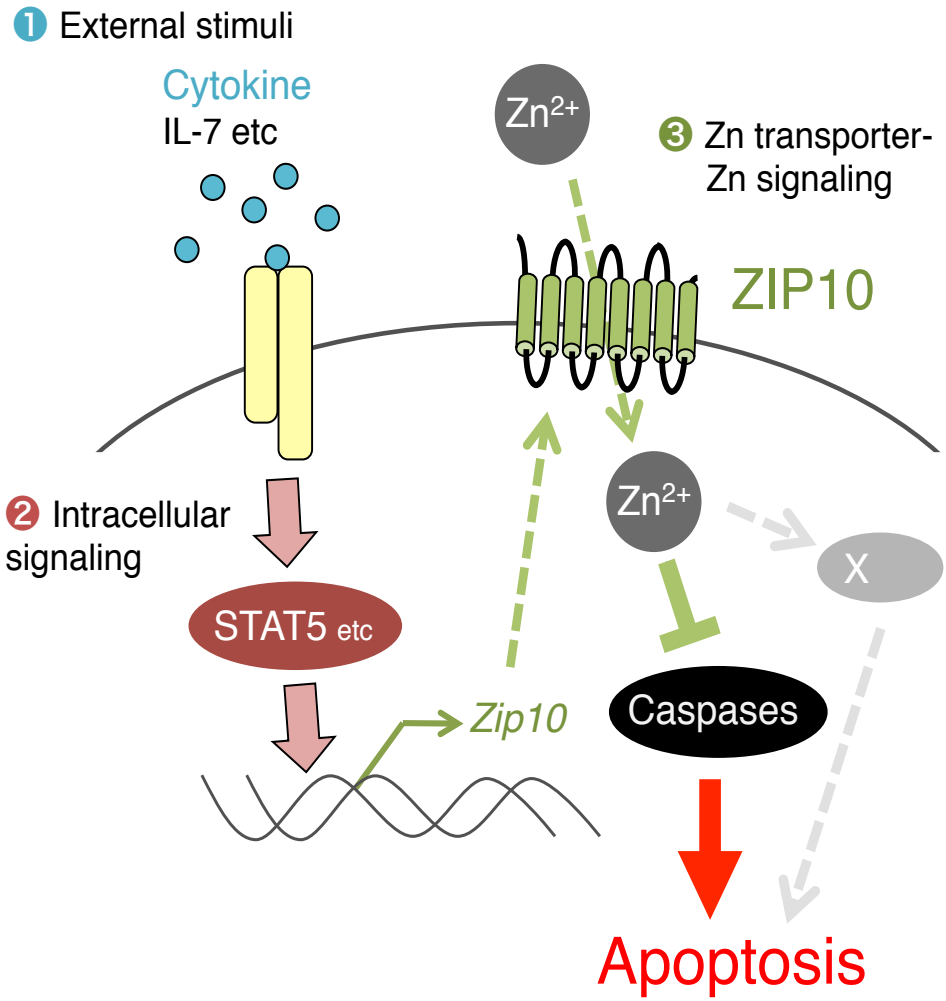

Figure 1-6. ZIP10-mediated zinc signal promotes anti-apoptotic effect by suppressing the enzymatic activity of caspases.

Cytokine signal, such as IL-7 (❶) from extracellular space induces JAK-STAT activation (❷) and *Zip10* gene expression. ZIP10, then, promotes the influx of Zn into the cells and suppresses the caspase activities. This could be regarded as a conversion of cytokine signal to Zn signal. (❸). This sequential signal conversion (with unknown mechanism mediated by factor 'X') facilitates anti-apoptosis during early B cell development. Disruption of this serial signal coversion process interrupts survival mechanism, resulting in B cell lymphopenia.

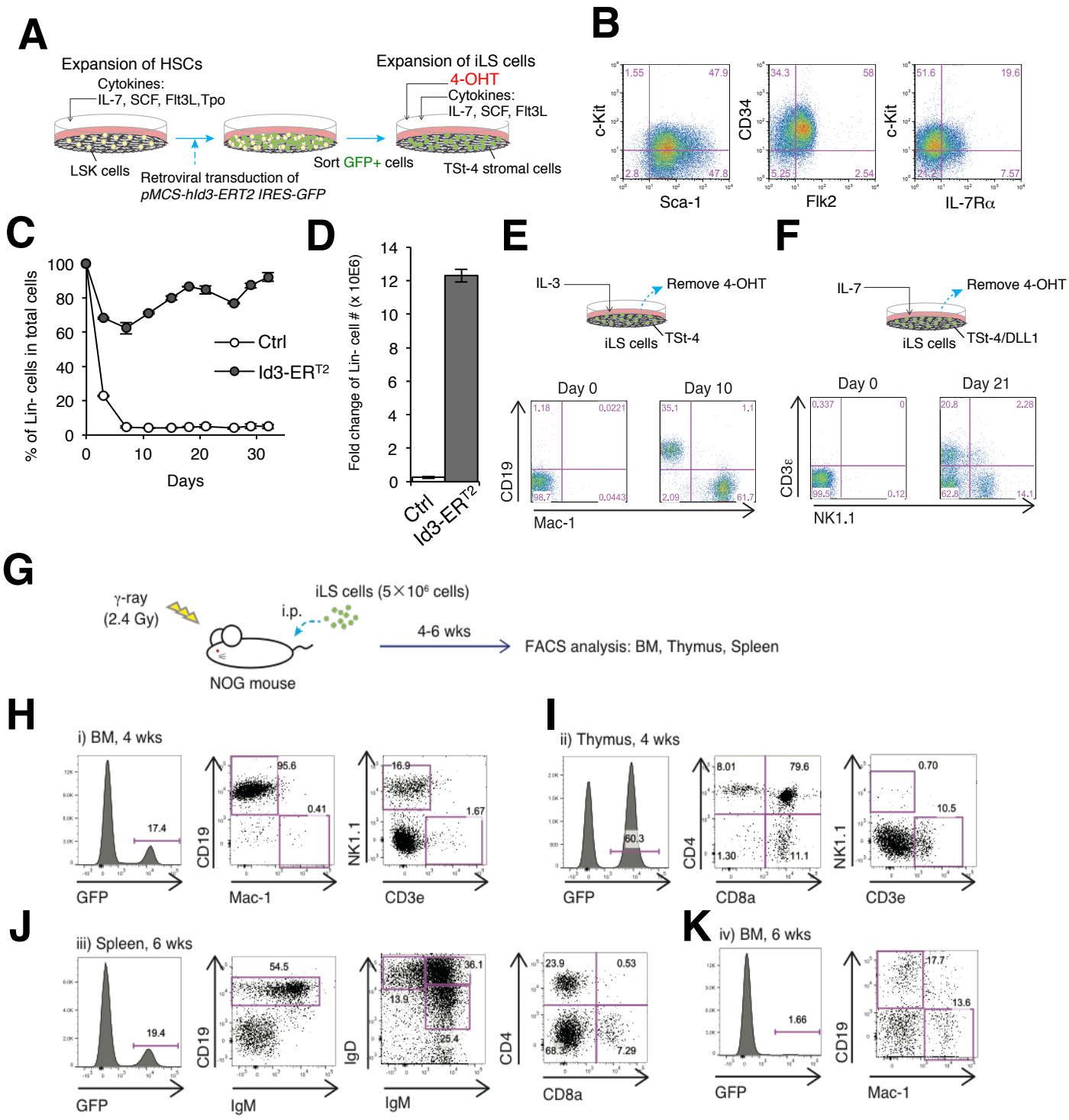

Figure 2-1. Establishment and characterization of iLS cells.

A. Scheme for establishment of iLS cell line.

B. Flow cytometric profiles of Id3-ER^{T2} transduced cells.

C. Proportion of lineage negative (Lin$^-$: CD19$^-$Mac-1$^-$NK1.1$^-$) population of LSK(control) or Id3-ER^{T2} transduced cells.

D. Number of Lin$^-$ cells after 1 month culture in LSK or Id3-ER^{T2} transduced cells.

E. Myeloid lineage potential of iLS cells *in vitro*. iLS cells were cultured in the presence of 10 ng/ml IL-3 on TSt-4 feeder cells for 10 days (*upper*). FACS profiles before (*lower, left*) and after (*lower, right*) the culture are shown.

F. T and NK lineage potential of iLS cells *in vitro*. iLS cells were cultured in the presence of 5 ng/ml IL-7 on TSt-4/DLL1 feeder cells for 3 wks (upper). FACS profiles of before (*lower, left*) and after (*lower, right*) the culture are shown.

G-K. Hematopoietic reconstitution potential of iLS cells. iLS cells were transferred into γ-ray-irradiated NOG mice, then primary and secondary lymphoid organs (BM, thymus and spleen) were analyzed at 4 to 6 wks after injection.

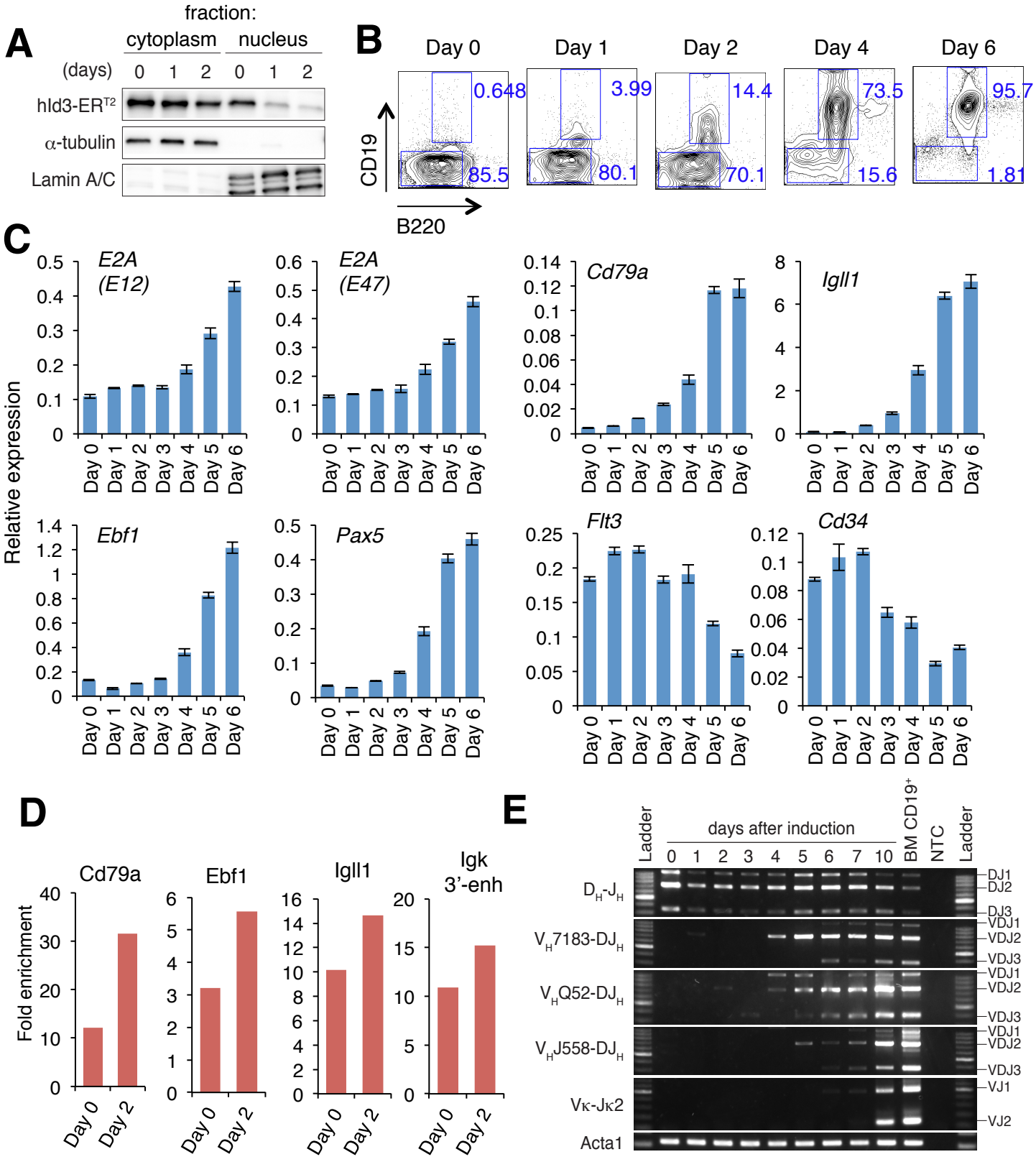

Figure 2-2. Induction into B lineage committed cells from iLS cells.

A. Western blot analysis for localization of hId3-ER^{T2} fusion protein. a-tubulin and Lamin A/C are shown as loading control for cytosolic and nuclear fraction.

B. Flow cytometric profiles of B220 and CD19 expression during B cell commitment.

C. qRT-PCR analysis of TFs (E2A, Ebf1, Pax5), Cd79a (mb-1), Igll1 (λ5) for B lineage-associated genes, and Flt3, Cd34 for stem cell-associated genes. Values represent means ± S.D of two independent experiments.

D. ChIP-qPCR analysis for E2A occupancy at the indicated loci.

E. VDJ rearrangement in Igh locus during B cell differentiation. Acta1 is shown as a loading control.

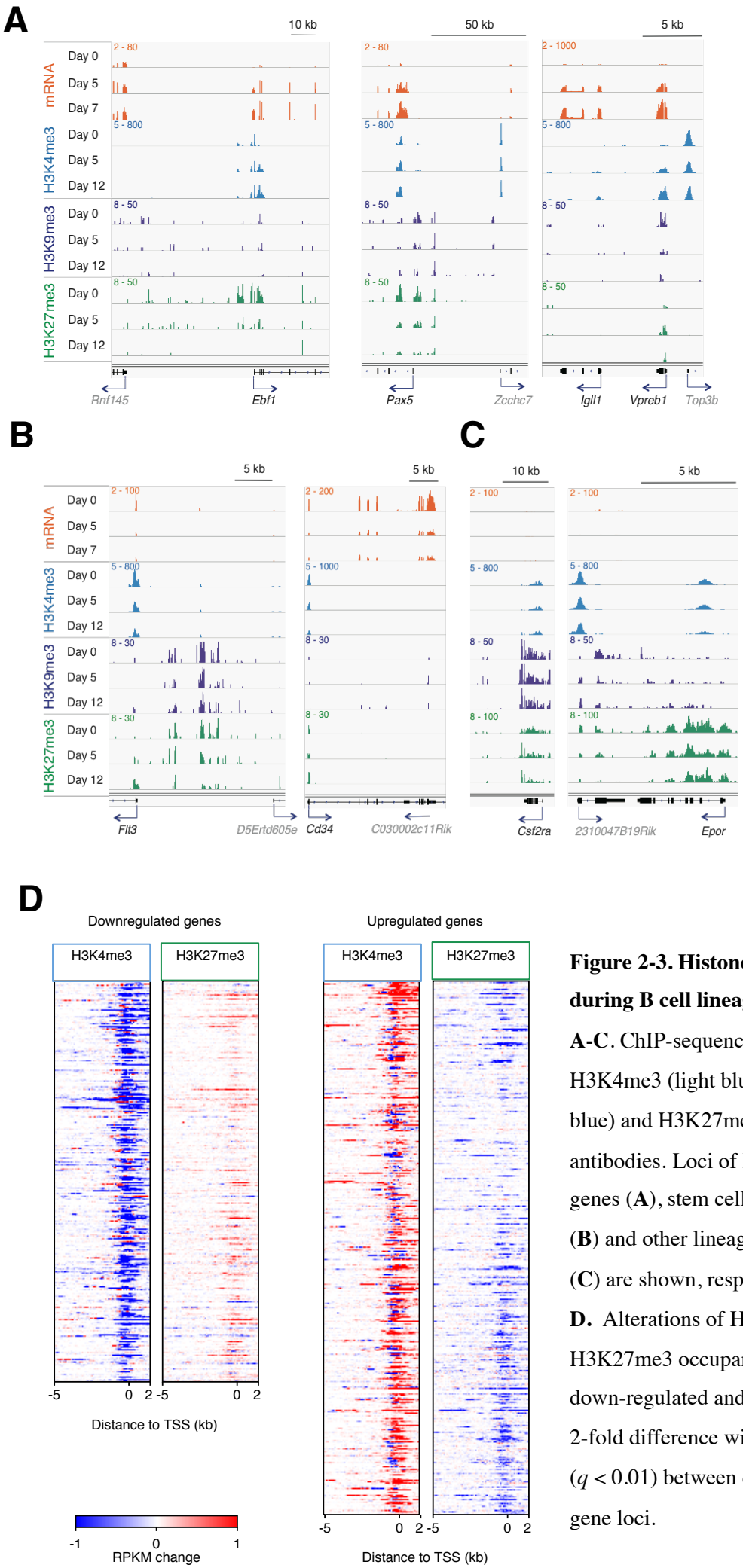

Figure 2-3. Histone modification during B cell lineage commitment.

A-C. ChIP-sequencing analysis using H3K4me3 (light blue), H3K9me3 (dark blue) and H3K27me3 (green) –specific antibodies. Loci of B cell-associated genes (**A**), stem cell-associated genes (**B**) and other lineage-associated genes (**C**) are shown, respectively.

D. Alterations of H3K4me3 and H3K27me3 occupancy around TSS of down-regulated and up-regulated (over 2-fold difference with high significance ($q < 0.01$) between day 0 and day 6) gene loci.

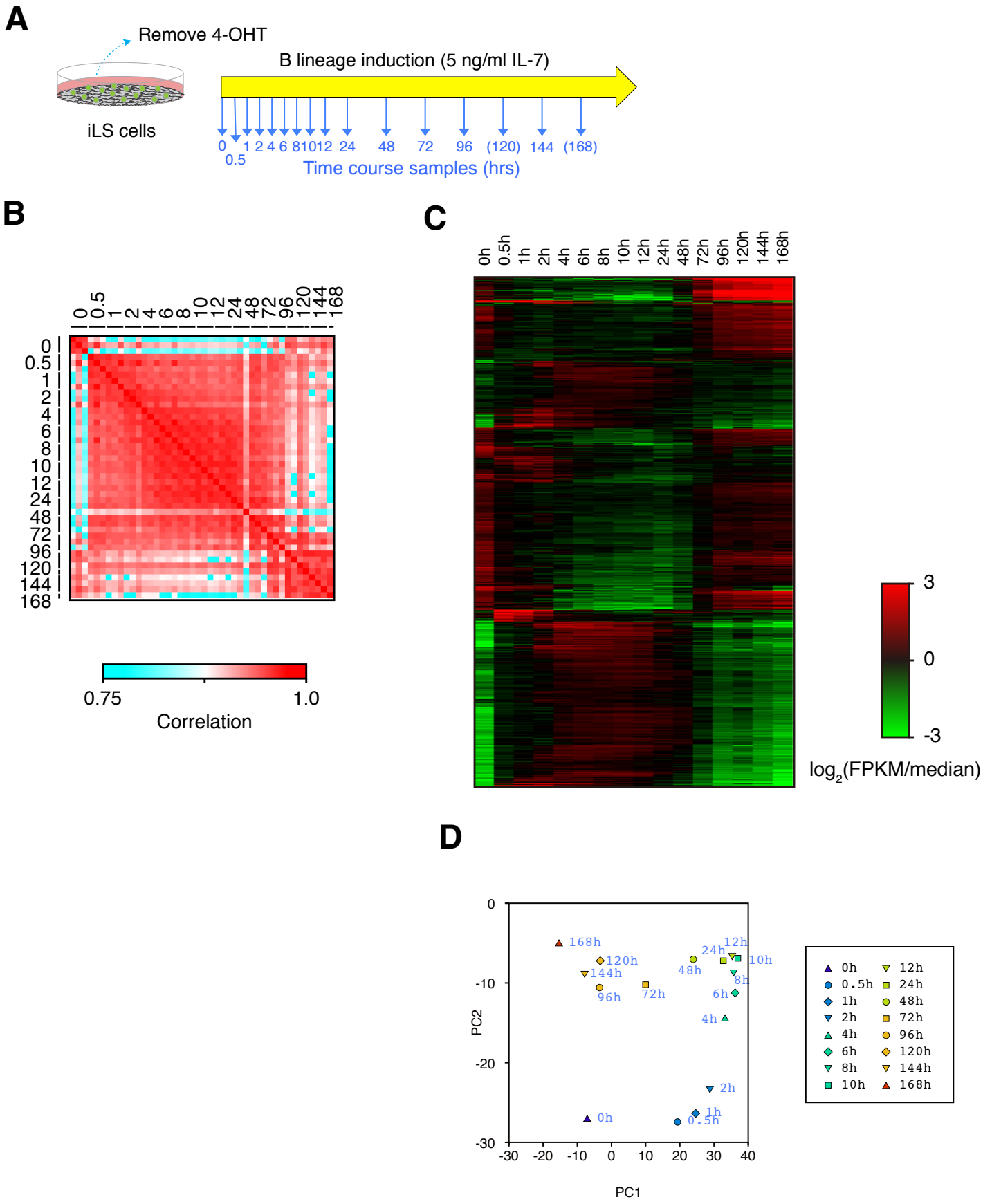

Fig 2-4. Genome-wide analysis using time course samples during B cell commitment from iLS cells.

A. Scheme for sample collection. Samples at 120 and 168 hr are collected in only single experiment.

B. Reproducibility matrix of three independent experiments.

C. Differentially expressed genes (n=1182) extracted by ANOVA with Boferroni-correction.

D. Principal component analysis of gene expression pattern in each time points.

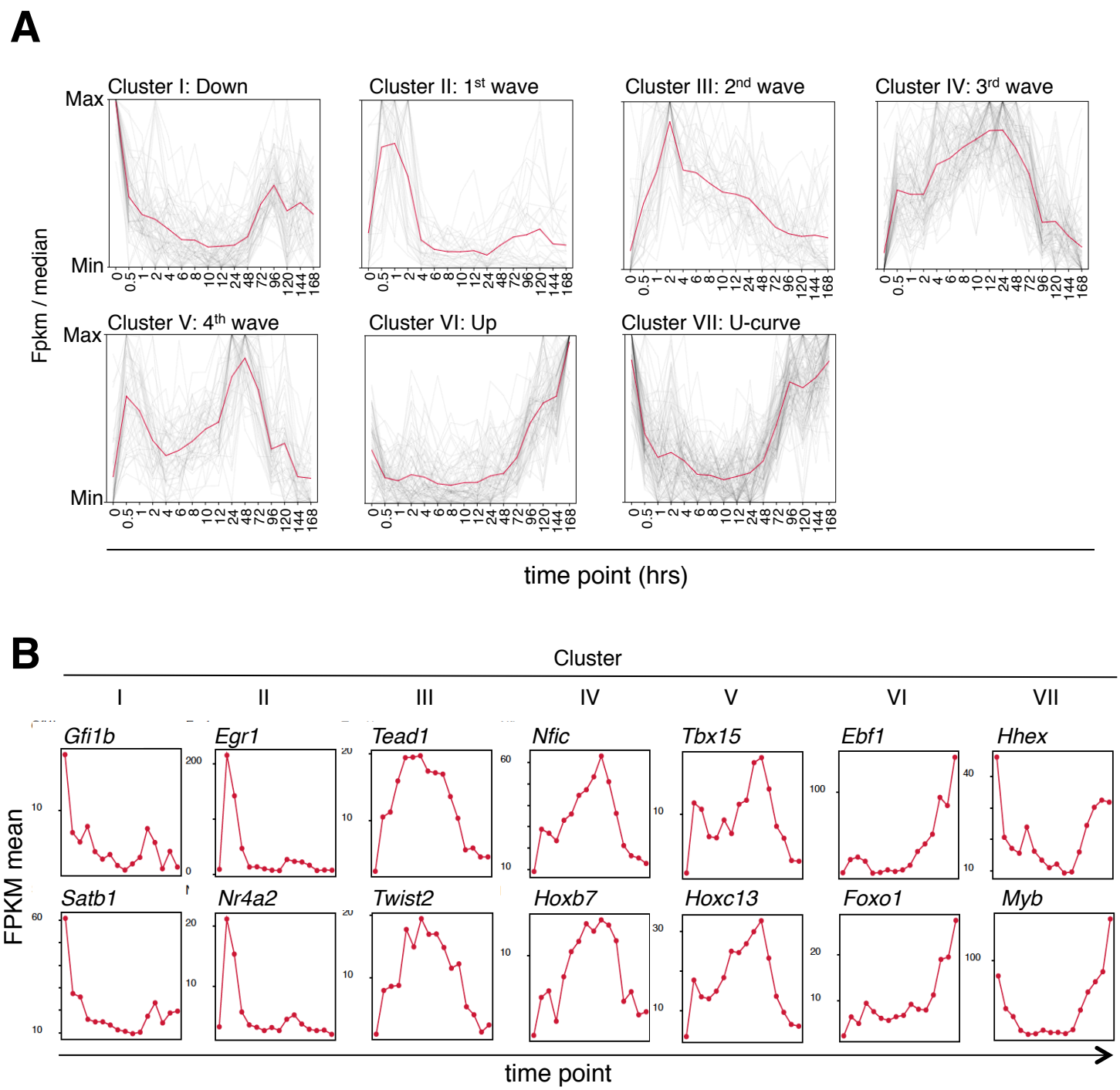

Fig 2-5. TF waves during B cell commitment in iLS cells.

A. *k*-means clustering in 1144 DNA-binding factors. Genes were filtered by expression level (FPKM > 1) and range of variance.

B. Gene expression pattern of representative genes of each cluster.

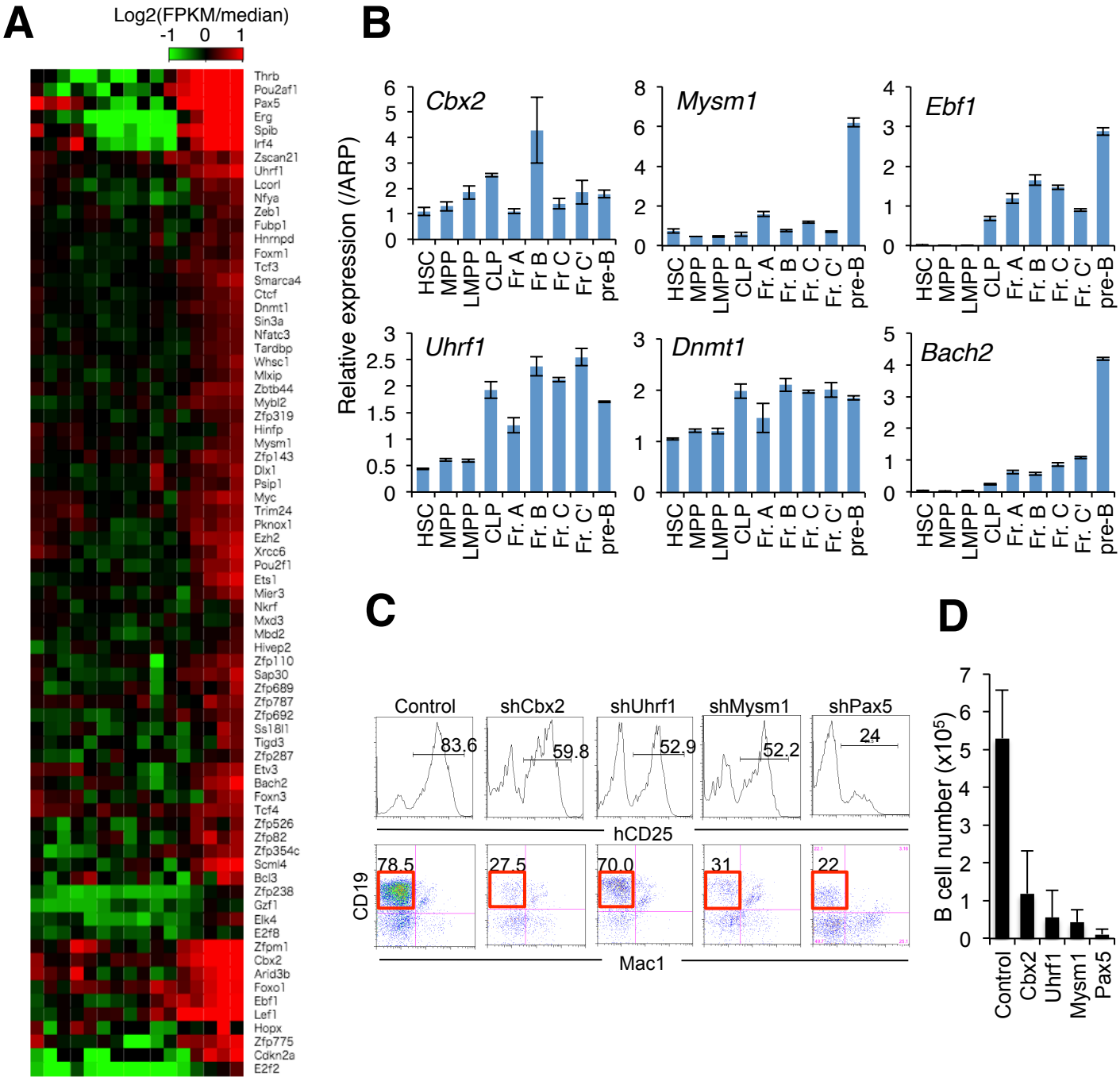

Fig 2-6. Up-regulated TFs during B cell commitment in iLS cells.

A. Heat map of cluster VI (in **Fig 2-5A**) composed genes.

B. qRT-PCR of indicated genes in HSPC and B cell progenitor fractions in BM. Values represent mean ± S.D. in two independent experiments.

C,D. shRNA-mediated KD of indicated factors. Flow cytometric profiles (**C**) and B cell numbers (**D**) are shown. shRNA-induced cells (hCD25^{+}) are gated for Mac1 vs CD19 profiles. Values represent mean in three independent experiments.

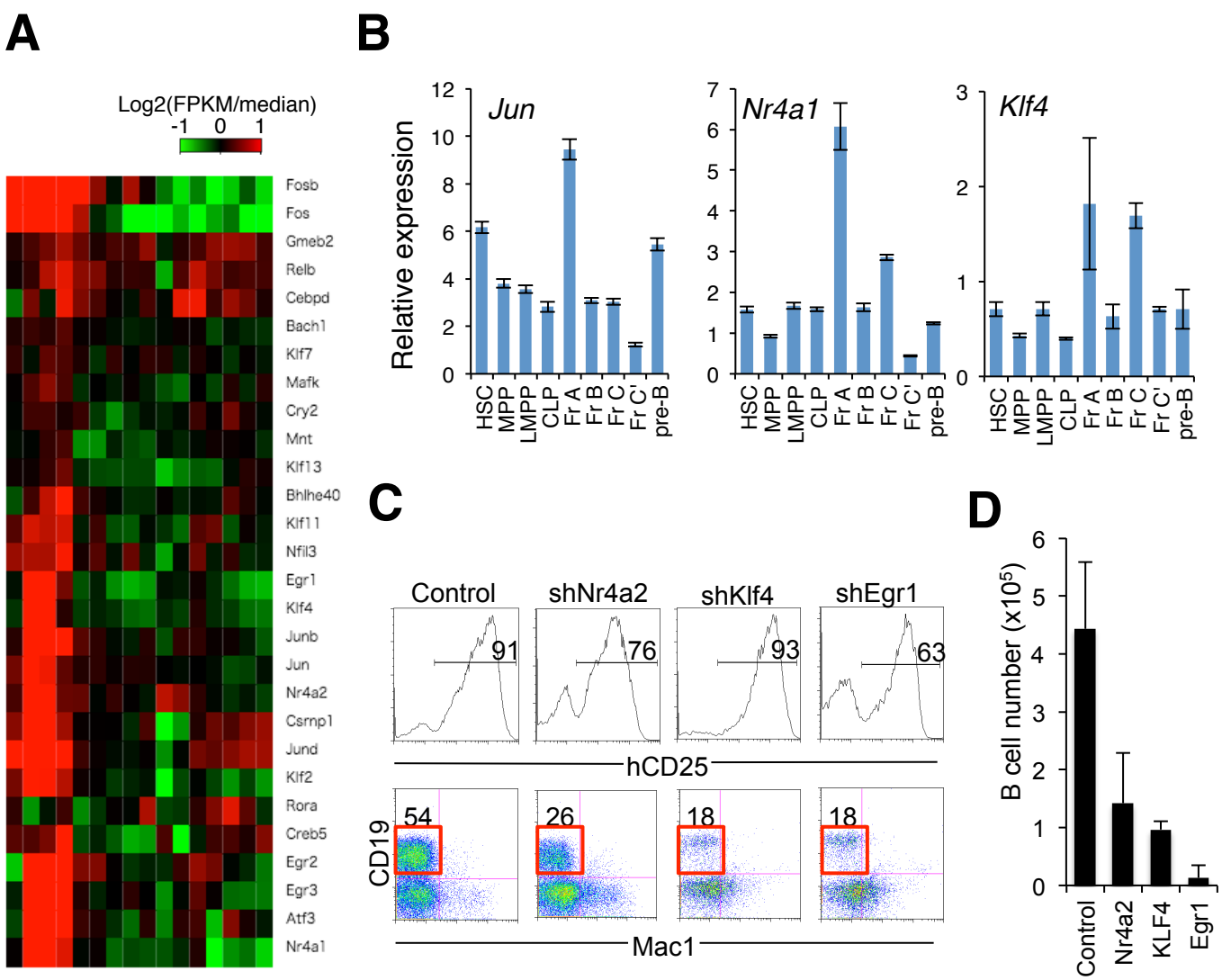

Fig 2-7. Early responding TFs during B cell commitment in iLS cells.

A. Heat map of genes in cluster II (**Fig 2-5A**).

B. qRT-PCR analysis of indicated factors in HSPC and B cell progenitor fractions in BM. Values represent mean ± S.D. in two independent experiments.

C,D. shRNA-mediated KD of indicated factors in iLS cells. Flow cytometric profiles (**C**) and cell numbers (**D**) are shown. shRNA-induced cells (hCD25$^+$) are gated for Mac1 vs CD19 profiles. Values represent mean in three independent experiments.

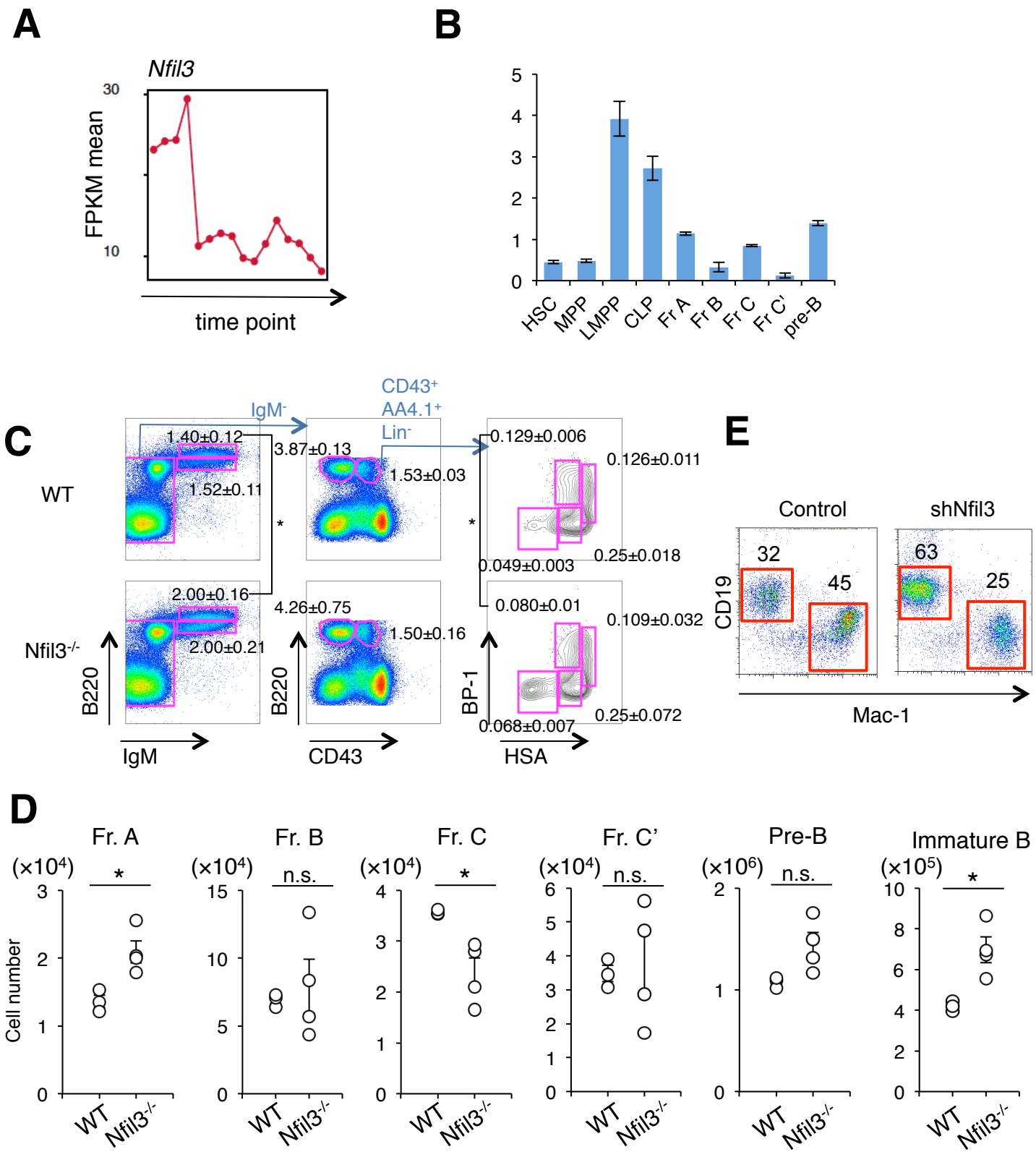

Figure 2-8: *continued to next page*

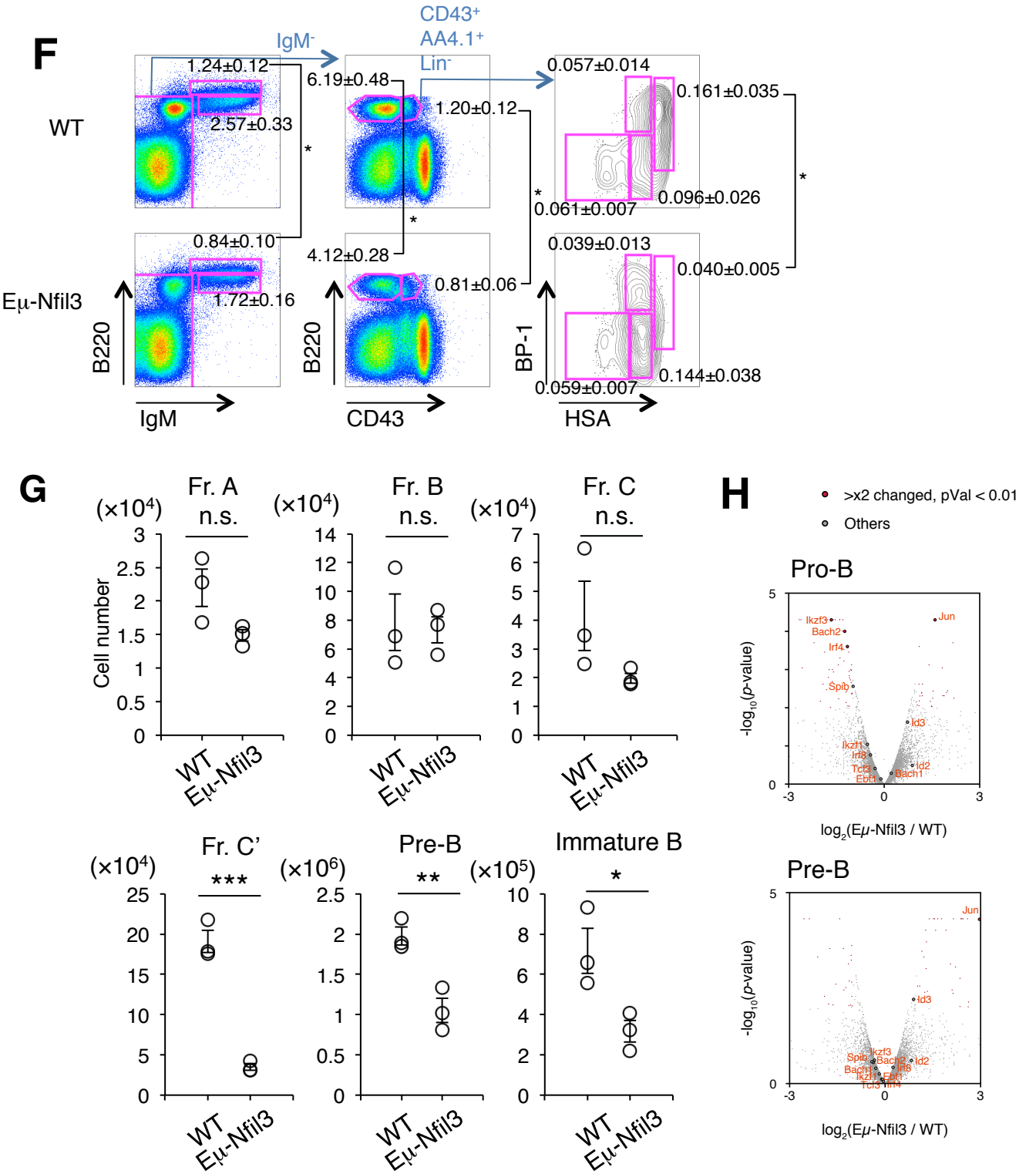

Fig 2-8. Prolonged *Nfil3* expression perturbs normal B cell commitment.

A. Expression pattern of *Nfil3* in iLS cells differentiating into B cells by RNA-seq analysis.

B. qRT-PCR analysis of *Nfil3* in HSPCs and early B cell progenitors in BM. Values represent mean ± S.D. in two independent experiments.

C,D. FACS profiles (**C**) and actual cell number (**D**) of B cell progenitor population in wild type (WT) and Nfil3$^{-/-}$ mice. Values represent mean ± S.D. in three independent experiments. * p<0.05.

E. shRNA-mediated KD of Nfil3 in BM LSK cells differentiating into B cells. Cells were cultured on TSt-4 stromal cells for _ days after shRNA induction.

F,G. FACS profiles (**F**) and cell number (**G**) of B cell progenitor population in WT and Eμ-Nfil3 mice. Values represent mean ± S.D. in three independent experiments. * p<0.05, ** p<0.01, *** p<0.001.

H. Volcano plot for comparison of gene expression status in pro- (upper) or pre- (lower) B cells between WT and Eμ-Nfil3 mice. x-axis indicates the expression ratio of Eμ-Nfil3 versus WT cells, and y-axis shows the statistical significance.

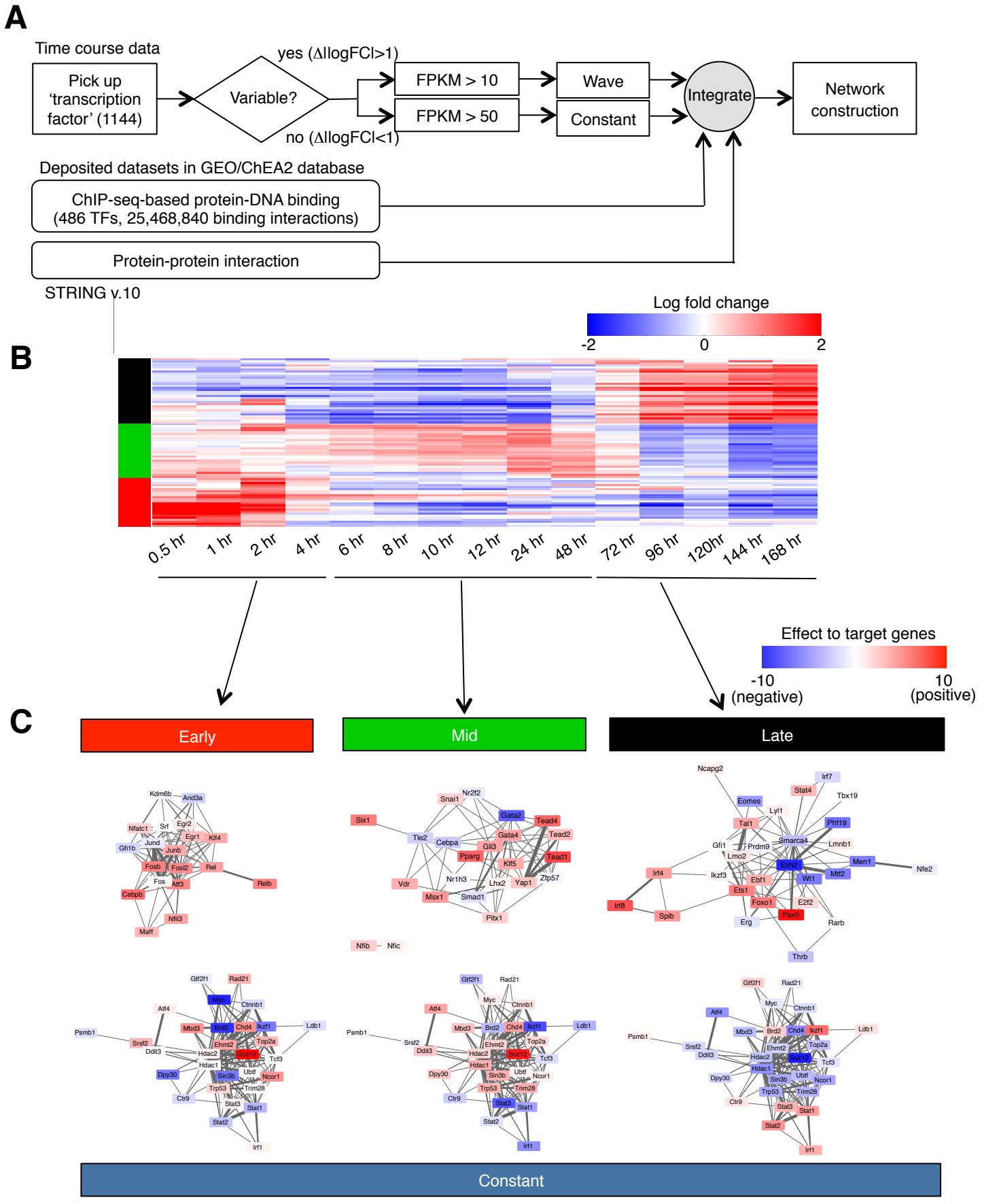

Fig 2-9. Proposed gene regulatory network using time course dataset.

A. Strategy for construction of network.

B. Heat map of highly variable TFs (Δllog fold changel > 1 between time points).

C. Transcriptional regulatory network during B cell commitment process. Color of each node represents the correlation between variations of itself and its downstream at indicated time phase. Thickness of edge means the probability of protein-protein interaction (experimental score in STRING database).

SUPPREMENTAL MATERIALS

PC1	Loading	PC2	Loading
Vpreb3	0.0825287	Fosb	0.14816
Crhbp	0.0696208	Mir5133	-0.121299
Cd19	0.0690726	Fos	0.115014
Atp1b1	0.0632793	Vsig2	0.101583
Pou2af1	0.0604032	Ptgds	0.0963023
Vpreb2	0.0590817	Rgs1	0.092486
Rsph9	0.0587511	Ccl3	0.0897232
Clgn	0.0581369	Pyhin1	-0.0823654
Mmp10	-0.0573116	Hist1h1a	0.082263
Sit1	0.0568714	Ccl4	0.0756985
Vat1l	0.0564397	Otof	0.0748536
Ak4	0.0563374	Pou2af1	-0.073318
Vpreb1	0.0553119	Arc	0.0731184
Fgf2	-0.0539506	BC094916	-0.0713442
H19	0.0534769	Nr4a1	0.0711058
Ctse	0.0521164	Fhit	0.070303
Bst1	0.0520466	Egr3	0.069886
Erg	0.0516747	Gzmc	0.067658
Igll1	0.0513681	Nlrp2	-0.0661532
Cd79a	0.0506846	Rhov	0.0660256
Tmem90a	0.0506597	Kcnq3	0.0659719
Gm266	0.0498864	Gm6460	0.0657927
Fam70a	0.0496094	Cox6a2	0.0625638
Rag1	0.0493889	Fam70a	-0.0623653
Thrb	0.0493875	Fam46c	0.0621678
Ngf	-0.0483881	Gipr	-0.0613108
Bfsp2	0.0482731	1110017F19Rik	0.0607115
Ereg	-0.0479209	Ccl20	0.0598765
Krtap1-5	-0.0476314	Ereg	0.0596722
Gimap4	0.0473689	Cd19	-0.0595481
Cdkn2a	0.0471986	Nr4a3	0.0568375
Pax5	0.0470134	Gldc	-0.0565984
Lta	0.0467812	Omp	0.0557894
Cyp4f18	0.0466245	Pmaip1	0.0547102
Tubb3	0.0465662	5430421N21Ri	-0.0541029
Cd79b	0.046501	Tesc	0.0538147
1700027J07Rik	0.0460879	Pde2a	-0.0537603
2010001M09Ri	0.0459131	Zfp36	0.0533756
Blnk	0.0452393	Rtn4rl2	-0.0519788
Kcng1	0.0450534	4933402N22Ri	0.0515298
Car2	0.0443147	Psg17	0.0513392
Gimap7	0.0442929	Pydc3	-0.0500646
Cecr2	0.043988	Gpr35	-0.0500223
7530420F21Rik	-0.0438843	Armc3	0.049902
Mir5133	-0.0436891	Beta-s	0.049672
Gimap3	0.0434153	Otor	0.0489658
Ctgf	-0.043329	Gpr160	0.0489277
Ccdc135	0.0432818	Hist1h1d	0.0479679
Gng4	0.0427166	Gm266	-0.0479467
Clic6	0.0426181	Mest	0.0474506

Supplement table 1. Loadings for PC1 and PC2, *related to Fig 2-4D*. Top 50 genes contributed to generate each dimension and their loading scores are shown.

Organism	Mus musculus
Geneset	Transcription factor (1144)
Cutoff (FPKM)	1
Cutoff (variance)	0.2

Cluster #	1	2	3	4	5	6	7
Feature	Down	1st wave	2nd wave	3rd wave	4th wave	Up-regulated	U curve
	Runx2	Egr3	E2f5	Zfp827	Tcf7l2	Tigd3	Jarid2
	Mycl1	Jun	Klf9	Jrk	Lhx9	Trim24	Srebf1
	Mef2c	Junb	Maff	Klf3	Foxc1	Mxd3	Zfp653
	Meis1	Jund	Nr1d2	Foxp4	Nr2f1	Gzf1	Pogz
	Foxf1a	Klf2	Nfkb2	Lhx2	Zfp516	Mbd2	Taf1
	Ssbp2	Klf4	Srf	Lhx6	Smarca2	Mysm1	Ttf2
	Chd4	Mafk	Lrrfip1	Taf12	Nfia	Whsc1	Runx1
	Homez	Mnt	Klf16	Atf5	Nfib	Mybl2	Mxi1
	Nfe2	Klf13	Jrkl	Meis2	Nfix	Myc	Lyl1
	Nfkb1	Nfil3	Bcl6	Meis3	Lass4	Tardbp	Hic2
	Mll3	Csrnp1	Thoc1	Zfp532	Rcor3	Zfp787	Mecp2
	Zfp422	Relb	Klf5	Zhx3	Zfp821	Nfatc3	Mef2d
	Mycn	Rora	Zfat	Sall2	Pou6f1	Uhrf1	Rad54b
	Camta1	Klf7	Nr1d1	Taf13	Pparg	Nfya	Men1
	Kdm5b	Atf3	Med6	Glis2	Ahr	Dnmt1	Zfp629
	Foxp1	Bach1	Cebpb	Nfe2l1	Zfp521	Spib	Msl3
	Zkscan3	Cebpd	Npas4	Nfic	Six5	Pax5	Hmg20a
	Hoxa7	Bhlhe40	Taf1a	Creb3l1	Olig3	Zfp143	E2f6
	Batf3	Cry2	Tead4	Otx1	Snai2	Pknox1	Patz1
	Irf5	Egr1	Hivep3	Pbx1	Cebpa	Etv3	Myb
	Rreb1	Egr2	Tgif1	Pbx3	Hoxc10	Pou2af1	Zfp329
	Rb1	Fos	Klf10	Pitx1	Zfp13	Pou2f1	Zfp191
	Rbl2	Fosb	Elk1	Prrx1	Tbx15	Fubp1	Hmgn5
	Tet1	Klf11	Epas1	Znx2	Tcf7l1	Zfp82	Zbtb48
	Gpbp1l1	Nr4a2	Erf	Tbx18	Maf	Sap30	Nrf1
	Rorc	Nr4a1	Etv5	Zfp697	Dlx5	Mlxip	Dedd2
	Sub1	Creb5	Foxc2	Zfp513	Tef	Psip1	Arid5a
	Trerf1	Gmeb2	Foxf2	Csrnp2	Ebf3	Hopx	Akna
	Satb1		Foxs1	Rarg	Tcea3	Nkrf	Zfp260
	Mbd1		Fosl1	Aebp1	Trp63	Bach2	Pbx2
	Runx3		Fosl2	E2f7	Mecom	Bcl3	Zfp639
	Zfp219		Zfa	Nr2f2	Nr1h3	Sin3a	Gon4l
	Rcor1		Gata2	Rxra	Vdr	Hinfp	Pnn
	Crem		Zfp28	Prrx2	Gata3	Smarca4	Pou2f2
	Tcea2		Sp7	Lass6	Pcgf2	Cbx2	Rere
	Tcf7		Hes1	Scx	Zkscan5	Xrcc6	Phtf2
	Arid3a		Klf8	Shox2	Sox9	Cdkn2a	Rfc1
	Terf2		Irx3	Six1	Hlx	Lef1	Rfx1
	Elf1			Ncor2	Hmg20b	Ctcf	Rfx2
	Txk			Cenpb	Hoxa10	Lcorl	Rfx3
	Zbtb16			Zfp768	Hoxb8	Tcf4	Zfp628
	Fli1			Clock	Hoxc6	Zeb1	Zfp580
	Rcor2			Mier2	Hoxc8	Tcf3	Arid1a
	Zfp1			Glis3	Mypop	Dlx1	Elf2
	Zfp35			Bnc2	Nfatc4	Zfp526	Ing2
	Gfi1b			Ddit3	Satb2	Ebf1	Rxrb
	Ikzf1			Twist2	Jdp2	Thrb	Phf21a
	Gtf2i			Irx5	Irx1	Zfp319	Sfpi1
	Hes6			Prdm5	Thra	Elk4	Zfp592
	Dnmt3a			Tead1	Irf1	Zfp692	Batf
	Zfp131			Tead2		Zfp689	Zfp280c
	Ssbp3			Tead3		Mier3	Banp
	Zfp369			Taf9b		Erg	Sox4
	Hoxa5			Atoh8		Zbtb44	Sp4
	Hoxa6			Twist1		Zfp775	Zfp182
	Hoxa9			Arid5b		Foxn3	Cebpg
	Foxo3			Mkx		Ezh2	Zfp710
	Yy2			Zfp30		Foxm1	Zfp800
	Gtf2ird2			Zfp57		Scml4	Nono
				Zscan12		E2f2	Zbtb5
				Zfpm2		Zscan21	Zfp553
				Gli3		Zfp238	Zfp687
				Creb3l2		Zfp354c	Creb1
				Hoxb2		Zfpm1	Zfp784
				Foxg1		Hnrnpd	Cux1
				Foxd1		E2f8	Taf1c
				Hmga2		Zfp287	Dbp
				Hoxb3		Hivep2	Irf3
				Hoxb4		Arid3b	Taf5
				Hoxb5		Ss18l1	Hnf1b
				Hoxb6		Foxo1	E2f3
				Hoxb7		Ets1	Tfdp1
				Hoxc13		Zfp110	Foxo4
				Hoxc4		Irf4	Trim28
				Hoxc5			Zfp292
				Hoxc9			Gfi1
				Kcnip3			Mier1
				Ets2			Zfp184
				Vax2			Nr2c2
				Gtf2ird1			Ercc2
				Six4			Spata24
				Zfp672			Nfrkb
				Irx2			Esr1
							Etv6
							Nr1h2
							Usf2
							Cic
							Zfp239
							Zscan2
							Zfp652
							Zbtb1
							Zfp654
							Taf8
							Tfdp2
							Pbx4
							Hhex
							Zfp668
							Tbl1xr1
							Elf4
							Tgif2
							Gtf2e2
							Zbtb33
							Irf8
							Gpbp1
							Chd7
							Zbtb22
							Zfp667
							Irf2

Supplement table 2.

The gene list of TF waves, *related to Fig 2-5A***.**

	0.5hr	1hr	2hr	4hr	6hr	8hr	10hr	12hr	24hr	48hr	72hr	96hr	120hr	144hr	168hr
RARB	0.53777464	0.35995014	-0.78367558	-1.07354911	-0.17920647	-0.15940396	0.11867908	0.56042622	0.23533385	0.31602885	0.35739494	0.13067725	0.08629846	-0.18905708	0.12368878
EOMES	-0.65683839	-0.65091438	-0.02220823	-0.33335918	-0.47860647	-0.69174245	-0.48696144	-0.43464346	-0.06017503	0.30484922	0.79355774	1.08544577	-0.01015637	1.29438354	0.18839426
IRF7	-0.36025165	-0.37650916	-0.393736	-0.06620776	0.0642542	0.05894337	-0.0212374	0.14505345	-0.37231107	0.3610899	1.00379146	0.5957355	0.45717022	0.08768823	-0.08782718
BACH2	-0.38330405	-0.36464747	-0.83921973	0.57028595	0.14836545	-0.02984486	-0.46971205	-0.56862984	-0.88532878	-0.84994109	-0.31259215	0.53823893	0.75353163	0.99678402	1.50613225
FOXO1	-0.32159318	-0.6852053	0.24608518	-0.07471087	-0.26441816	-0.24598314	-0.17310373	-0.22303496	0.4242099	-0.00548095	0.00731553	0.34352915	0.72184843	0.68400329	1.18193816
TAL1	-0.11380471	-0.79779378	-0.74525952	0.38524592	-0.23072226	-1.16143976	-1.52957663	-1.02596531	-0.52848766	-0.59358781	0.41814205	1.19529041	0.88416851	1.52919409	1.59837047
WT1	-0.88787014	-0.7743502	-0.48315865	-0.78611518	-0.87596971	-0.80451699	-1.23075787	-0.94704941	0.47661129	0.14419106	0.78547714	1.71231835	1.68454501	1.62157844	1.57587447
CNDG2	-0.29637485	-0.26837161	-0.1101518	-0.10668088	-0.3240852	-0.50441463	-0.52434837	-0.61779373	-0.13329778	-0.19738251	-0.08748431	0.5773386	0.51649229	0.77053403	1.02466252
LMNB1	-0.17306449	-0.34926524	-0.44016244	-0.38709343	-0.60550615	-0.66525703	-0.77681493	-0.69859401	-0.14820544	-0.18476595	0.25895407	0.7291987	0.69529012	1.07874451	1.15577096
EZH2	-0.18220787	-0.44019035	-0.72616329	-0.46963389	-0.46912461	-0.57888514	-0.58179573	-0.64824009	-0.16901893	-0.3348718	0.10060354	0.76205129	0.7788558	1.13309692	1.32956487
ERG	-0.20143339	-0.27671487	-0.31044255	-0.47065316	-0.52541661	-0.5169766	-0.54365538	-0.54991805	-0.55179677	-0.35300404	0.15196904	0.78042179	0.76651897	1.33064044	1.18991859
MTF2	-0.3180572	-0.38460173	-0.28645771	-0.30267544	-0.30907096	-0.30511002	-0.39208888	-0.57607601	-0.55346286	-0.36390211	0.05607255	0.6289563	0.75856232	0.78542366	1.10352013
TBX19	-0.56485257	-0.83009429	-0.27344496	-0.84122148	-0.76487497	-1.17425892	-1.17247082	-1.01987707	-0.83321291	-0.38757535	1.09198202	1.77187453	1.3018501	2.2745836	1.55082879
MEN1	-0.27704251	-0.55167142	-0.52365412	-0.31060326	-0.45923084	-0.46521908	-0.42025365	-0.27417241	-0.30752907	-0.16095487	0.25618197	0.59813976	0.75589016	0.80877262	1.03476747
THB	-0.92769864	-1.07328287	-1.36035768	-1.67312	-1.4544295	-1.50994145	-1.61779736	-1.62088295	-1.33515684	-0.14168761	1.13784012	2.48244956	2.5696735	3.42492991	3.75830788
IKZF3	-0.70047439	-1.29836425	-0.92842367	-0.73540828	-1.25685238	-1.33487173	-1.50299136	-1.34874462	-1.13224106	0.0610555	0.90241241	2.38685519	2.59715446	2.72828076	2.42633658
ETS1	-0.26903138	-0.28133117	-0.11506163	-0.28161827	-0.19287899	-0.24208893	-0.30644024	-0.45128661	-0.45391002	-0.36173942	-0.11951921	0.44616281	0.78337356	0.94038353	1.56578422
SMCA4	-0.1890754	-0.2199194	-0.3320919	-0.41491545	-0.42385557	-0.34491491	-0.34056697	-0.2569331	-0.14861361	-0.23892264	0.00288092	0.33809058	0.51451416	0.66657823	1.21131043
RAG2	-0.05249285	-0.92722556	-1.56959182	-1.32480024	-0.74804236	-0.38742721	-0.60258141	-0.59947328	-0.9640766	-0.55948894	0.51884262	1.41449486	1.2268489	1.4773119	1.82237589
PRDM9	0.19646093	-0.1022697	-0.6223736	-0.37017228	-0.28678271	-0.29662177	-0.69468391	-0.68018341	-0.67683976	-0.53713119	-0.05439374	0.56987329	0.85249649	0.90136838	1.14640223
PHF19	-0.31230875	-0.16835827	1.19642404	-0.00465457	-0.2284936	-0.44096215	-0.75503434	-1.09444817	-0.69017596	-0.83036881	-0.01564466	0.57850044	0.77182066	0.88394617	0.89318318
E2F2	-0.44196543	-0.5705218	0.93797319	-0.12724839	-0.90019772	-1.00591925	-1.3376761	-1.33399819	-1.21631553	-0.66766105	0.29822709	1.16008095	1.1567653	1.60483489	1.94124575
IRF4	-0.04482653	0.75375532	1.30790848	-0.09882332	-1.23256218	-1.54528862	-1.82628779	-1.88240274	-1.8587584	-1.30060851	0.12840943	1.28122069	1.70148684	2.08255492	2.42248587
NFE2	0.56254622	-0.07242705	-0.09377609	-0.4752578	-1.01405913	-0.8863192	-0.85244932	-0.85000912	-1.51744377	-0.39031422	0.64380981	0.99120487	0.56346433	0.63575436	0.88685588
RBTN2	0.31364548	0.10474426	-0.09252815	-0.36568706	-0.36167352	-0.41048418	-0.44955233	-0.39561709	-1.02595132	-0.39349742	0.15100158	0.52735282	0.25245334	0.51560076	0.53903477
COE1	0.25342594	0.38113371	0.24158591	-1.14816999	-0.92923324	-0.8380967	-0.78354281	-0.8281649	-0.19917448	0.26748891	0.35404302	0.601865	1.01041925	1.09854024	1.59998914
STAT4	0.01484422	-0.14840971	-0.36401113	-0.64129853	-1.06448479	-0.44908595	-0.6395614	-0.4945736	-0.6741556	-0.33492339	0.13973259	0.79627709	0.81976164	1.02532741	1.31540778
PAX5	0.063401	-0.12011457	-0.91327614	-1.27999373	-1.68539045	-1.53260816	-1.41957305	-1.49182609	-1.48038157	-0.31374959	1.07519376	1.85463395	1.83350198	2.3160917	2.20845209
IRF8	0.15575846	-0.12740395	0.22851082	-0.70922747	-0.9625926	-0.68172504	-0.83864825	-0.80456272	-1.29453768	-1.02149653	0.23577151	1.05373144	0.86967069	1.35497687	1.36148914
SPIB	0.00714552	0.07658508	0.25207583	-1.03555733	-1.33263425	-1.37672362	-1.35837742	-1.27602618	-1.19129499	-0.55488874	0.54165771	1.82759925	1.07960385	2.11445012	1.32687383
GFI1	0.20353862	-0.34767985	0.03145231	-0.62111879	-1.0348589	-1.02170069	-0.98587677	-0.84118804	-1.20597375	-0.13224033	0.47088836	0.89834055	1.03246841	1.0992963	1.13957967
LYL1	0.34844067	0.25365909	0.14368772	-0.67263302	-1.29734901	-1.00404766	-1.3338246	-1.19188416	-1.20978104	-0.44488102	0.54595034	1.07699526	1.01539956	1.25368525	1.23440013
SNAI1	-0.63008261	-0.20576551	1.01584933	0.88099558	0.55879217	0.51468938	0.52359003	0.63561682	0.9587703	0.44024682	0.03178126	-0.61096318	-0.30706724	-1.00993294	-1.01409049
TEAD1	0.00391964	0.16859739	0.76812415	1.01311653	0.98655684	0.94164654	0.74553452	0.56937767	0.78304949	0.24930659	-0.35581329	-0.99470333	-0.60618831	-1.26990706	-1.21273474
TEAD4	-0.08212338	-0.01083278	1.36917318	0.98243634	0.88385453	1.10104031	1.10282866	1.08419579	0.68458354	-0.10858764	-0.4101015	-1.22615639	-1.09951252	-1.53824835	-1.12040482
KLF5	-0.14753395	0.6761104	1.39464055	0.16520453	0.3756155	0.704623	0.75498981	1.01126739	1.11583791	-0.02622105	-0.4920455	-0.96297477	-0.66217914	-1.16829801	-1.00207804
SMAD1	0.14024045	0.32208493	0.59612616	0.32441744	0.42265807	0.47187445	0.47810078	0.3963413	0.66501849	0.27448155	-0.16064467	-0.56366197	-0.55095803	-0.85335312	-1.04247265
TAF9B	0.44427551	0.27747496	0.44964982	0.26948801	0.46422224	0.52441089	0.7667586	0.34730098	1.18972974	0.66880236	-0.14938358	-0.75140304	-0.93791347	-1.32152215	-1.09607498
LHX2	0.09671382	0.11575275	-0.02827432	-0.04813782	0.12981342	0.35973911	0.83069368	1.02461022	0.86329124	0.72491791	0.09131146	-0.69620663	-0.42710105	-0.74359802	-0.74754457
TEAD2	0.21779445	0.21926587	0.16596812	0.08830525	0.42348862	0.55644478	0.63399452	0.97802128	1.07046379	0.54559529	0.11634808	-0.93219154	-0.60803914	-0.9633631	-1.0256107
COT2	-0.15226611	-0.12794177	0.03373595	0.44801021	0.60210928	0.69820106	0.9657278	0.84729598	1.14981216	0.35346271	-0.16542463	-0.81994927	-0.32400433	-0.80974317	-0.82012292
NFIC	-0.01849131	-0.07954858	-0.20878415	0.09563785	0.22439151	0.49000696	0.64862307	0.835614	1.19097904	0.56927478	0.01254233	-0.53572265	-0.2213793	-0.73094134	-0.8326337
GATA4	0.06276216	-0.07173933	0.03872961	0.16470331	0.68410357	0.71436865	0.55028308	0.64205775	0.943364	0.48528966	0.45750456	-0.57645247	-0.38248327	-1.55805731	-0.91990369
PITX1	0.05623132	-0.25515777	0.04747755	0.42894885	0.36225119	0.56352626	0.7047847	0.93838095	0.89369813	0.70825494	0.3870808	-0.62354934	-0.4702465	-1.09814387	-1.17721492
MSX1	-0.15062721	0.16678234	0.47756055	0.45213886	0.34775024	0.3037077	0.71969949	0.81911884	0.56887008	0.63891168	0.26216587	-0.87281666	-0.46242052	-1.06274443	-0.87480234
ZFP57	0.21098784	0.15205248	0.04374781	0.38482292	0.76580832	0.76820459	0.76099434	0.74865138	0.53263894	0.37373894	0.02982184	-0.66753168	-0.30971445	-0.98320712	-1.05892988
GATA2	0.30227931	0.16428696	0.35473526	0.40913512	0.53686867	0.7996827	0.96940448	0.85123793	0.72808412	0.68251041	0.11156913	-1.08570662	-0.75096824	-1.19732509	-1.33098369
YAP1	0.09153753	0.19473302	0.31370939	0.39008231	0.55153011	0.62612591	0.70796918	0.68286372	0.58608086	0.55474643	0.11113142	-0.67704217	-0.30412029	-0.98072174	-1.03987863
SIX1	0.59292031	0.06886481	-0.01152323	0.04128323	0.16241961	0.35348697	0.443851	0.49021319	0.7911515	0.77552637	0.53798927	-0.61189406	-0.31237016	-0.92577908	-1.03164998
HXC9	0.11495859	0.10692412	0.11333947	-0.00290907	0.04315769	0.22683223	0.48291925	0.5103009	1.10340954	0.86760648	0.49388054	-0.26675565	-0.30267211	-1.08201604	-0.8442898
VDR	0.7271984	0.52290933	0.08074954	0.18269282	0.29216636	0.31065422	0.26419749	0.16115023	0.64432475	0.91686575	0.15985507	-0.85900001	-0.45499636	-1.22217129	-1.0294409
GLI3	0.3779395	0.48829362	0.10523212	0.47480873	0.40303708	0.41565148	0.57332433	0.49593992	0.99744228	0.62797808	0.16249993	-0.52565799	-0.3921383	-1.0167046	-1.36354693
PPARG	0.30570151	0.37223001	0.27576451	0.19937993	0.26384703	0.2406102	0.66641273	0.54690216	0.96366158	0.64700055	0.24029607	-0.597215	-0.26133692	-0.98400303	-1.05986703
NR1H3	0.24763409	0.30899945	-0.03812505	-0.33557815	-0.16523926	0.08673962	0.06488426	-0.14660459	0.66483108	1.05249613	0.69985273	-0.03843698	-0.50070257	-0.89686347	-0.4489581
SCML2	0.27690484	0.51655271	0.04071418	-0.17772865	0.0972594	0.04862231	0.25000104	0.28061742	1.24168749	0.82451358	0.07309523	-0.30519216	-0.16667492	-0.79973869	-0.99421669
NFIB	0.49304349	0.60821416	0.02196622	-0.23271372	-0.12092999	-0.03551166	0.28144805	0.18417211	1.02906456	0.77812422	0.29159354	-0.24412312	-0.13265358	-0.61459454	-0.70742716
PER2	0.37625971	1.3929503	0.83631988	-0.05527716	-0.46034208	-0.74809305	-0.71901281	-0.66648175	0.61303015	0.50285251	0.27152264	-0.12893843	0.15672082	-0.28909757	-0.38449701
TLE2	0.76906164	0.66139473	0.34777862	-0.20897684	-0.50119896	-0.46186788	-0.45474396	-0.360307	0.30085117	1.18621962	1.08789034	-0.01100349	0.25804538	-0.78507307	-0.68924969
CEBPA	1.06744522	0.68433255	0.60776771	0.38003129	-0.02957246	-0.20801069	-0.19922955	-0.11714431	0.00369803	0.86324738	0.6469677	-0.41852638	-0.63965844	-1.27989733	-1.43520796
RELB	-0.1814158	0.76319478	1.48208318	0.74650628	0.30769573	0.05484394	-0.25233103	-0.10727865	-0.56255537	-0.05717417	-0.03528446	-0.29636043	-0.34872271	-0.30358183	-0.57781841
NFAC1	0.08686852	0.36531645	1.09332841	0.48887001	-0.1958365	-0.22790181	-0.30759098	-0.35048495	-0.43760476	-0.64168759	-0.41526204	-0.07455053	-0.14044605	0.00245875	0.14448823
OVOL2	-0.27489833	0.12869371	3.27112644	0.29617096	-0.49086422	-0.52731046	-0.0876729	-0.09506049	-0.27779689	-0.53598771	-0.11103697	-0.30872322	-0.21354928	-0.28447401	-0.2069299
CEBPD	0.55647404	0.0206292	1.40181923	0.28646803	-0.35193423	-0.40202896	-0.65139788	-0.32023231	-0.26476247	0.71839502	0.81993069	-0.01668993	0.18766609	-0.0915327	-0.47990778
ARI3A	0.08486659	0.00868805	1.03838283	0.07472807	-0.46174008	-0.3924641	-0.54231277	-0.54197499	-0.69167232	-0.55689263	0.04156568	0.53321536	0.04382229	0.17166733	0.01406041
GFI1B	0.68024128	0.29957632	0.86700655	0.05909019	-0.82544337	-0.69099281	-0.91240126	-1.24394126	-0.51387853	-0.02833736	0.6475709	0.80630013	-0.42888947	-0.2078283	-0.43373685
FOSL2	0.5249542	1.14974896	1.05671998	0.27735683	0.17381263	0.09225749	0.08979047	0.08495374	0.1249256	0.29707624	-0.04381104	-0.66012694	-0.11766494	-0.75962167	-0.78852141
CEBPB	0.28824474	0.6987223	1.23547818	0.33981876	0.08062245	0.11283422	0.07803265	0.28033197	-0.03307146	0.12300714	0.1350007	-0.52603067	-0.25035632	-0.77112559	-0.91593851
NPAS4	0.33593779	1.46960145	1.78499978	1.06389124	1.12710863	0.89917361	0.72310783	0.62815263	0.48466042	-0.30727908	-0.74284586	-1.23950268	-0.53858088	-1.43477803	-1.54862166
MAFF	1.00558613	1.60962912	1.70841614	0.85027027	0.67860278	0.61445869	0.16656693	0.16658982	-0.3335927	-0.71880177	-0.74257198	-1.12033095	-0.6748637	-0.91610366	-0.73284773
SRF	0.6110747	1.03140602	1.14922647	0.68104519	0.54231333	0.44648395	0.15054953	0.17783133	-0.14991132	-0.29651455	-0.53863888	-0.71930542	-0.82381558	-0.72447651	-0.84302493
NFIL3	0.71768083	0.87944067	1.02269501	-0.14286613	-0.03224648	-0.1789143	-0.35098765	-0.42224828	-0.36222257	-0.13169759	0.08480097	-0.16368222	-0.28544118	-0.49846807	-0.69622048
FOS	4.52085512	2.35795401	1.41696442	0.17626143	-0.62661254	-1.26778031	-1.49771894	-1.51612958	-0.60230836	-0.821345	-0.07485354	-1.57000565	-0.81188472	-1.20593546	-0.86093615
FOSB	5.14462825	4.54278303	2.3550527	0.408282	-0.44518673	-0.87423152	-1.29844869	-1.5772891	-1.5118671	-1.4767598	-1.19220841	-2.37842404	-0.95751526	-2.27664462	-1.12378072
ATF3	2.85488729	2.91333131	1.58737882	0.17331434	-0.04159714	-0.4073734	-0.71129207	-0.80201464	-1.08308697	-0.5871075	-0.40640127	-0.79664472	-0.04904013	-0.7510188	-0.435776
EGR2	3.63709778	3.23008837	1.93004135	0.51521919	0.12174684	-0.25960492	-1.07359506	-1.20302745	-0.13696923	0.09937932	-0.23038883	-0.89682649	-0.70485938	-1.30491898	-1.43445213
JUNB	2.2634396	2.00662723	1.54499216	0.30567259	-0.2261224	-0.3407095	-0.53801161	-0.34903717	-0.33697231	-0.252983	-0.35098171	-0.82221598	-0.49681643	-0.72958772	-1.05287072
EGR1	3.28067274	2.67830722	0.90541799	-0.40306401	-0.26481088	-0.67929586	-1.06330674	-0.9896757	0.62472141	0.38838021	0.20279418	-0.83632421	-0.53302655	-1.08738638	-1.21658824
KLF4	1.64600564	1.62163984	0.46061638	-0.08836882	0.08791203	0.10078462	-0.10268285	-0.0654277	-0.12079435	-0.15629021	-0.08317255	-0.61316696	-0.33752353	-0.75965981	-0.81297145
JUN	2.41813337	1.29974622	0.42357391	0.00693563	0.00990599	-0.08457451	-0.15891177	0.02370941	-0.04266375	-0.39706137	-0.47237737	-0.97943417	-0.65246613	-0.76800879	-0.70469208
REL	0.78091111	1.2616986	0.44972546	0.08945928	-0.07761132	0.0009872	-0.31222841	-0.54399584	-0.62460401	-0.67156263	-0.64667637	-0.03766266	-0.15114714	-0.06036255	0.08975287
JUND	1.31506877	1.40692327	0.78746771	-0.5885613	-0.87584931	-0.75302855	-0.8962873	-0.66334926	-0.84655641	-0.58680032	-0.00264215	0.14751228	0.01426147	0.26088971	0.23829608
PER1	1.88014375	1.88138827	0.45002384	-0.62551446	-0.57575368	-0.64009971	-0.73251843	-0.58053583	-0.04427613	-0.04598422	-0.02524448	-0.35860184	-0.0313891	-0.48096864	-0.27376635
KDM6B	1.01946983	1.35545554	0.7046736	-0.39350552	-0.53779223	-0.39802856	-0.55158915	-0.52223966	-0.25587502	-0.34310169	-0.09875646	-0.15668198	0.17371414	-0.20604591	-0.02883808

Supplement table 3. The list of detailed genes and expression changes (Log fold change) in "wave" of TF network, *related to Fig 2-9***.**

	0hr	0.5hr	1hr	2hr	4hr	6hr	8hr	10hr	12hr	24hr	48hr	72hr	96hr	120hr	144hr	168hr
STAT3	-0.16397157	0.05204201	0.37574583	0.61924554	0.37867968	0.08452366	-0.04811651	-0.04482876	-0.09964097	-0.0988314	0.19550194	0.05002201	-0.21588927	-0.1685551	-0.46566529	-0.45026181
MYC	-0.17289402	-0.16973336	0.25523084	0.07792109	-0.19069387	-0.27813287	-0.34285149	-0.51792794	-0.36463974	-0.43846028	-0.6821902	-0.01118654	0.49767889	0.59322335	0.83634461	0.90831152
DDIT3	-1.52085927	0.2349328	0.30900342	0.20594111	-0.00921582	0.53277259	0.49288355	0.32045232	0.40091277	-0.21209429	0.11209402	0.31542361	-0.34727642	0.14350897	-0.46385714	-0.51462221
CHD4	0.66276749	0.11808506	0.09320084	-0.20754152	-0.42058695	-0.34496569	-0.22799259	-0.2112274	-0.26147422	-0.15696184	-0.1395654	0.08279488	0.24329076	0.16945983	0.2384497	0.36226706
TFE2	0.02646359	-0.1734174	-0.25650392	-0.35092392	-0.37012082	-0.47804162	-0.352204	-0.34760269	-0.17884757	-0.23578744	-0.10644784	0.21375766	0.42228624	0.53069454	0.74058858	0.91610661
IRF1	-0.66686534	0.0140489	-0.05808356	0.21645994	0.09766211	0.02574748	-0.13338553	-0.11874573	-0.09494695	-0.33578836	0.20782459	0.57442273	0.15425601	0.23400576	0.01123101	-0.12784305
HDAC1	0.51671612	0.2161909	0.22012832	0.04973913	-0.21901849	-0.19369965	-0.24003745	-0.24269567	-0.30528342	-0.15809377	-0.02148796	0.07256808	0.18606749	-0.08559802	0.13153062	0.07297379
IKZF1	1.18292761	0.35887992	0.03884205	0.22473978	0.21157328	-0.27154601	-0.35862275	-0.58793659	-0.70888232	-0.88180428	-0.51113181	0.14530995	0.56612443	0.12927964	0.28585918	0.17638792
TIF1B	0.50158968	0.0331406	-0.06710186	-0.18882048	-0.22439289	-0.28612918	-0.3363604	-0.28727029	-0.21671316	-0.4884558	-0.12758344	0.20596341	0.33616109	0.2869756	0.48988864	0.36910846
DNJC2	0.25973703	-0.23231035	-0.25896206	-0.18799055	-0.00707325	-0.02473125	-0.15337023	-0.06533205	-0.18818963	0.09467737	-0.20852836	-0.04403169	0.30411802	0.08896053	0.41547666	0.20754982
T2FA	-0.02667313	-0.08578206	-0.02217173	0.07610888	0.11450849	0.19571334	0.18380542	0.12330828	0.16382546	0.20235345	-0.05303531	-0.06389522	-0.09544684	-0.30933545	-0.1040382	-0.2992454
CTNB1	-0.26351737	-0.04192588	0.11263741	0.31953281	0.1676018	0.15568489	0.0826186	0.10544261	0.07863601	0.04652384	0.17111382	-0.02233192	-0.21808485	-0.1710848	-0.29936881	-0.22347814
P53	0.10522828	-0.06828048	-0.11359824	-0.13242102	-0.09761342	0.00825588	0.01621711	0.07528977	0.11922059	0.2360924	-0.07015311	-0.02899253	0.00040883	-0.06094815	0.05830176	-0.04700768
MBD3	-0.11927686	-0.09350972	-0.11265726	-0.18482079	-0.12553798	-0.0642997	0.05165474	0.09681709	0.2559631	0.10063283	0.17533231	0.13845419	0.01213572	-0.06969959	0.05612425	-0.11731234
ATF4	-0.39099944	0.32091282	0.45807054	0.32488737	0.22334854	0.34369072	0.2078476	0.08325937	0.01707058	-0.06681546	-0.15165511	-0.19029503	-0.30466375	-0.31338965	-0.22383666	-0.33743246
SRSF2	0.14129289	-0.11259069	-0.06957731	0.18234432	0.17856844	-0.08343779	-0.20618986	-0.35051872	-0.38746313	-0.10287292	-0.19244082	-0.09982729	0.19653676	0.153804	0.40043975	0.35193235
PSB1	0.08082106	0.06840643	0.09393332	0.08277469	-0.06604077	0.02334962	-0.07575808	0.04358203	-0.02344823	0.05733375	0.0686729	0.01605372	-0.04543296	-0.22418735	-0.04276125	-0.05729888
TOP2A	0.31626693	-0.19890455	-0.38068177	-0.66016603	-0.35947663	-0.29210614	-0.42676751	-0.458298	-0.53524192	0.16342133	-0.04956242	0.01938162	0.55911026	0.57342339	0.74859807	0.98100337
CBX3	0.28098397	-0.03573672	-0.04775397	-0.3069002	-0.41151387	-0.34894981	-0.35413388	-0.29074293	-0.42021907	-0.00326585	0.02060608	0.03995909	0.41478512	0.33131282	0.54820611	0.58336309
BRD2	-0.02763167	0.30354579	0.3259021	0.30709981	0.20969243	0.1007573	0.07659214	0.0165776	0.01427724	0.03993635	-0.15310433	-0.12148815	-0.25808362	-0.27262485	-0.25257217	-0.30887597
CTR9	1.68238364	0.69964977	0.24832237	-0.27487447	-0.09036145	-0.09839593	-0.12195041	-0.33015186	-0.35895073	-0.10459838	-0.16032286	0.07893227	0.15592741	-0.45683139	-0.21729467	-0.65148332
RAD21	0.02947512	-0.14526429	-0.15688117	-0.1942564	-0.17183935	-0.12761937	-0.14740704	-0.09879261	-0.20182723	0.4303857	0.05733513	-0.09541624	0.15274325	0.08493639	0.21510332	0.36932478
HDAC2	0.03272172	-0.01597339	-0.08534479	-0.1947511	-0.10469152	-0.00207331	-0.02111549	0.06634112	-0.06286798	0.36299924	0.03736984	-0.10783435	0.01526415	-0.06857571	0.04764937	0.10088221
CSN1	-0.32195703	-0.10627887	-0.0481312	0.08114509	0.18719275	0.21888168	0.33775752	0.33968642	0.46563007	0.21761668	0.08653244	-0.12762487	-0.28109561	-0.50285644	-0.17887745	-0.36762116
STAT1	-0.99054088	-0.17132205	-0.24199645	-0.42774016	-0.01299665	0.09972509	-0.07460389	-0.08040009	-0.05451533	-0.06121973	0.56946464	0.7745109	0.36049581	0.29620333	0.08377027	-0.0688348
LDB1	0.73006431	0.26913449	0.05596397	-0.26473155	-0.44805246	-0.44366736	-0.24932596	-0.24177407	-0.11695403	-0.21180923	-0.14349458	0.15352552	0.26543055	0.2063977	0.22253111	0.2167616
UBF1	-0.02294871	-0.15756424	-0.12416366	-0.00077472	0.18053397	-0.00495299	-0.04167904	0.0144833	0.04611625	0.14679656	-0.00507971	0.07347437	0.0388344	-0.0768264	0.14167455	-0.20792393
DPY30	0.22339473	-0.10214269	-0.13956203	-0.31933864	-0.23780879	-0.08977598	-0.17381988	-0.0450222	-0.1629039	0.32794636	-0.032128	-0.10082295	0.28755204	0.1301941	0.30174893	0.13248889
SIN3B	-0.03114582	-0.01403102	-0.03052232	0.03169477	0.2212155	0.12141819	0.12693251	0.10097611	0.13548716	-0.20554314	-0.06033208	-0.01129835	-0.1227881	-0.07120659	-0.11657532	-0.07428152
STAT2	-0.98170373	-0.07317112	-0.36506629	-0.55645759	0.16641275	0.25756189	0.03321499	0.05352567	0.04692805	0.07275117	0.60841862	0.8024166	0.17714524	0.24797308	-0.20881013	-0.28113919
EHMT2	0.45688406	0.14651756	-0.1205831	-0.36773198	-0.41225485	-0.36652324	-0.18784607	-0.11444469	0.03583583	-0.07481731	0.08859161	0.25335069	0.15234444	0.24247855	0.15182904	0.11636947
SUZ12	0.46272732	-0.01641958	-0.15294441	-0.26424888	-0.1989708	-0.30385994	-0.37777298	-0.3250284	-0.48134965	-0.23041924	-0.26776387	-0.01224637	0.51186541	0.43672504	0.55342663	0.66627973
NCOR1	0.356871	0.09528797	0.03899885	-0.06579252	-0.2047063	-0.23274298	-0.26914662	-0.23246509	-0.28796665	0.06892563	-0.07829979	0.01406053	0.14611366	0.17488582	0.18195057	0.2940259

Supplement table 4. The list of detailed genes and expression changes (Log fold change) in "constant" of TF network, *related to Fig 2-9***.**

ACKNOWLEDGEMENTS

I would like to express the deepest appreciation to Dr. Toshiyuki Fukada and Dr. Tomokatsu Ikawa for generous supervision. They gave me a lot of valuable advises for daily experiments, and opportunity to make presentations in various meetings.

I'm also grateful to Drs. Toshio Hirano, Ichiro Taniuchi, Shigeo Koyasu, Haruhiko Koseki, Kazuyo Moro and all members in Hirano laboratory, Koyasu laboratory, Moro laboratory and Koseki laboratory for fruitful discussions and heartfelt supports.

I'd like to thanks to Drs. Kenji Mishima and Taro Irie in Showa University for histological analysis of human leukemia samples, Dr. Hideki Ogura for ChIP analysis in ZIP10 study, Dr. Yasutoshi Agata for the kind gift of Id3-ER^{T2} vector, and Drs. Masato Kubo and Yasutaka Motomura for kind gifts of Nfil3 knockout and Eμ-transgenic mice.

I am particularly grateful for the assistance given by Dr. Sharif Jafar for library preparation of RNA-seq and ChIP-seq, Drs. Takaho A Endo and Eiryo Kawakami for bioinformatics analysis, Mss. Mika Ikegaya-Nakano, Asako Shibano-Sato, Mrs. Masami Kawamura and Masanao Ohno for their technical assistance and Mss. Reiko Kimura, Noriko Shibasaki and Norie Takeuchi for their secretarial assistance.

Finally, I owe my deepest gratitude to my family.

This study was supported by RIKEN Junior Research Associate Program.

ACHIEVEMENTS

ORIGINAL PAPERS

1. Bin BH, Fukada T, Hosaka T, Yamasaki S, Ohashi W, Hojyo S, Miyai T, Nishida K, Yokoyama S, Hirano T. (2011) Biochemical characterization of human ZIP13 protein: a homo-dimerized zinc transporter involved in the spondylocheiro dysplastic Ehlers-Danlos syndrome.

J Biol Chem. 286(46):40255-65. doi: 10.1074/jbc.M111.256784.

Contribution: Discussion and revision of manuscript.

2. Fukushima Y, Miyai T, Kumagae M, Horiuchi H, Furusawa S. (2012) Molecular cloning of chicken interleukin-5 receptor α-chain and analysis of its binding specificity.

Dev Comp Immunol. 37(3-4):354-62. doi: 10.1016/j.dci.2012.02.013.

Contribution: Cloning of chicken IL-5Ra gene and gene expression analysis.

3. Bin BH*, Hojyo S*, Hosaka T, Bhin J, Kano H, Miyai T, Ikeda M, Kimura-Someya T, Shirouzu M, Cho EG, Fukue K, Kambe T, Ohashi W, Kim KH, Seo J, Choi DH, Nam YJ, Hwang D, Fukunaka A, Fujitani Y, Yokoyama S, Superti-Furga A, Ikegawa S, Lee TR, Fukada T. (*equal contribution) (2014) Molecular pathogenesis of Spondylocheirodysplastic Ehlers-Danlos syndrome caused by mutant ZIP13 proteins.

EMBO Mol Med. 6(8):1028-42. doi: 10.15252/emmm.201303809.

Contribution: Establishment of stable cell lines expressing mutated ZIP13 protein and biochemical analysis.

4. Miyai T*, Hojyo S*, Ikawa T, Kawamura M, Irié T, Ogura H, Hijikata A, Bin BH, Yasuda T, Kitamura H, Nakayama M, Ohara O, Yoshida H, Koseki H, Mishima K, Fukada T. (*equal contribution) (2014) Zinc transporter SLC39A10/ZIP10 facilitates antiapoptotic signaling during early B-cell development.
Proc Natl Acad Sci U.S.A. 111:11780-11785. doi: 10.1073/pnas.1323549111.

5. Hojyo S*, Miyai T*, Fujishiro H, Kawamura M, Yasuda T, Hijikata A, Bin BH, Irié T, Takana J, Atsumi T, Murakami M, Nakayama M, Ohara O, Himeno S, Yoshida H, Koseki H, Ikawa T, Mishima K, Fukada T. (*equal contribution) (2014) Zinc transporter SLC39A10/ZIP10 controls humoral immunity by modulating B-cell receptor signal strength.
Proc Natl Acad Sci U.S.A. 111:11786-11791. doi: 10.1073/pnas.1323557111.

6. Ikawa T, Masuda K, Huijskens MJAJ, Satoh R, Kakugawa K, Agata Y, Miyai T, Germeraad WTV, Katsura Y, Kawamoto H. (2015) Induced developmental arrest of early hematopoietic progenitors leads to the generation of leukocyte stem cells.
Stem Cell Reports. pii: S2213-6711(15)00274-X. doi: 10.1016/j.stemcr.2015.09.012.
Contribution: Determination of suitable concentration of 4-OHT for iLS cell culture, cell cycle assay and revision of manuscript.

7. Miyai T, Takano J, Endo T, Kawakami E, Agata Y, Motomura Y, Kubo M, Kawamoto H and Ikawa T. Dynamic transcriptional cascades and regulatory networks that orchestrate B cell fate determination.
In preparation.

REVIEW ARTICLES

1. 伊川 友活，宮井 智浩 (2014) B 細胞系列への運命決定を制御する転写因子

臨床免疫・アレルギー科. 61(6): 704-10.

Contribution: Revision of manuscript.

2. 深田 俊幸，宮井 智浩，北條 慎太郎 (2015) なぜ亜鉛は生体防御に必要なのか？ B 細胞における亜鉛シグナルの役割

実験医学. 33(3): 462-5.

Contribution: Figure preparation and revision of manuscript.

3. Hojyo S, Miyai T, Fukada T. (2015) B-cell receptor signal strength and zinc signaling: unraveling the role of zinc transporter ZIP10 in humoral immunity

Receptor Clin Invest. 2: e387. doi: 10.14800/rci.387. Research highlight.

Contribution: Figure preparation and revision of manuscript.

PRESENTATIONS (*: Selected for fellowship or award)

[ORAL PRESENTATIONS]

*1. 宮井 智浩 (2013) 亜鉛トランスポーターZIP10 は B 細胞発生における生存に必須である

メタルバイオサイエンス研究会, 静岡.

2. Miyai T, Kawamoto H, Ikawa T. (2013) A novel system to clarify the gene regulatory networks in B cell lineage commitment.

The 42nd Annual Conference of Japanese Society of Immunology, Chiba, Japan

3. Miyai T, Kawamoto H, Ikawa T. (2014) Genetic and epigenetic regulation during B cell lineage commitment process.

The 43rd Annual Conference of Japanese Society of Immunology, Kyoto, Japan

4. 宮井 智浩、縣 保年、河本 宏、伊川 友活. (2015) B 細胞系列への運命決定機構における転写制御ネットワークの解明

Kyoto T Cell Conference (KTCC2015), 京都.

[POSTER PRESENTATIONS]

1. Miyai T, Elazab M.F.A, Fukushima Y, Horiuchi H, Furusawa S. (2010) Induction of non-specific suppression in chicks by specific combination of maternal antibody and its related antigen.

The 14th International Congress of Immunology, Kobe, Japan

*2. Miyai T, Kawamura M, Ikawa T, Hojyo S, Koseki H, Hirano T, Fukada T. (2013) An essential role of zinc transporter ZIP10 in anti-apoptosis during the early development of B lymphocyte.

ZIBI International Summer School, Berlin, Germany

*3. 宮井 智浩、北條 慎太郎、伊川 友活、入江 太郎、美島 健二、深田 俊幸. (2014) 亜鉛トランスポーターSLC39A10/ZIP10 は B リンパ球前駆細胞の生存に必須である

第 9 回トランスポーター研究会年会, 名古屋.

*4. Miyai T, Kawamoto H, Ikawa T. (2015) Genetic and epigenetic regulation during B cell lineage commitment process.

Keystone Symposium on Hematopoiesis (B6), Denver, USA.

5. Miyai T, Agata Y, Kawamoto H, Ikawa T. (2015) Transcriptional network for proper fate devision into B cell lineage.

The 44th Annual Conference of Japanese Society of Immunology, Sapporo, Japan

AWARDS

1. **学生優秀発表賞**, メタルバイオサイエンス研究会, 静岡. September 2013

2. **優秀発表賞**, 第 9 回トランスポーター研究会年会, 名古屋. June 2014

3. **Tadamitsu Kishimoto International Travel Award**, Japanese Society for Immunology, for Keystone Symposium on Hematopoiesis (B6), Denver, USA. February 2015

SCHOLARSHIPS AND FELLOWSHIPS

1. **Scholarship for ZIBI Summer School**, RIKEN-ZIBI Exchange Program (2013)

2. **Junior Research Associate Program**, RIKEN (2013-15)